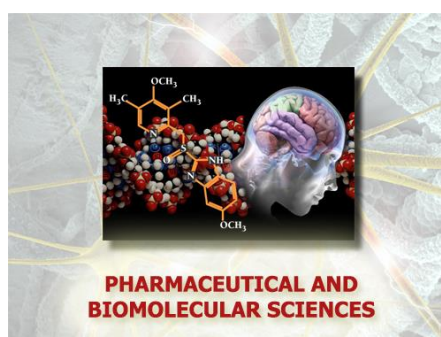


Università degli Studi di Torino



**Scuola di Dottorato in
Scienza della Natura e Technologie Innovative**

**Dottorato in
Scienze Farmaceutiche e Biomolecolari
(XXXV ciclo)**



TITOLO

**Characterization of the US12 protein of Human
cytomegalovirus: from functions to antiviral
intervention**

Candidato/a: Shree Madhu Bhat

Tutor(s): Prof. Giorgio Gribaudo

Università degli Studi di Torino



DIPARTIMENTO DI: Life science and Systems Biology

DOTTORATO DI RICERCA IN: Pharmaceutical and Biomolecular Science

CICLO: XXXV

TITOLO DELLA TESI: Characterization of the US12 protein of Human cytomegalovirus: from functions to antiviral intervention

TESI PRESENTATA DA: Shree Madhu Bhat

TUTOR(S): Prof. Giorgio Gribaudo

COORDINATORE DEL DOTTORATO: Prof. Roberta Cavalli

ANNI ACCADEMICI: 2019-2023

SETTORE SCIENTIFICO-DISCIPLINARE DI AFFERENZA: BIO-19

Contents

Abstract.....	1
Chapter 1- Introduction.....	3
1.1 Human Cytomegalovirus	4
1.2 Structure of the virus.....	4
1.2.1 Nucleocapsid	5
1.2.2 Tegument	5
1.2.3 Envelope.....	7
1.2.4 Types of viral particles.....	8
1.3 Virus genome	8
1.3.1 Organization and structure of viral genome.....	8
1.3.2 Clinical isolates and laboratory strains.....	9
1.3.3 Protein coding ORFs and their functions	10
1.4 HCMV replication	12
1.4.1 Virus attachment and entry	12
1.4.2 Post-fusion, pre-immediate early events	12
1.4.3 Regulation of the expression of viral genes.....	13
1.4.4. Characteristics and functions of the Immediate-Early proteins.....	14
1.4.5 Characteristics and functions of the Early proteins	15
1.4.6 Replication of viral DNA	15
1.4.7 Characteristics and functions of the Late proteins	16
1.4.8 Virion assembly, maturation and egress	16
1.5 Cytomegalovirus cell tropism	18
1.5.1 Target cells of HCMV <i>in vivo</i>	18
1.5.2 Target cells of HCMV <i>in vitro</i>	18
1.6 The US12 gene family	19
1.6.1 The US domain of HCMV genome	19
1.6.2 US12 gene family: general features.....	20
1.6.3 US12 family have homologs with cellular TMBIM proteins.....	22
1.6.4 Viroporins.....	25
1.6.5 US12 gene family characterization	25
Aim of the work	29
Chapter 2-Characterization of the expression of the US12 protein.....	31
2.1 Materials and Methods	32
2.1.1 Oligonucleotides	32
2.1.2 Bioinformatics	32
2.1.3 Cells and culture conditions	33
2.1.4 BAC recombineering.....	33
2.1.5 Recombinant viruses' preparation	35
2.1.6 Immunofluorescence.....	35
2.1.7 Immunoblotting	36
2.2 Results.....	37
2.2.1 The US12 gene encodes a 28 kDa protein expressed with an Early kinetics.....	37
2.2.2 pUS12 shows a time-dependent accumulation in the cytoplasm of HCMV--infected cells	38
2.2.3 Localization of pUS12HA within Golgi-derived structures.....	39
2.2.4 Localization of pUS12 within the cVAC of HCMV-infected cells	41
2.2.5 pUS12 is a 7 TMD protein with a cytoplasmic N-terminus and luminal C-terminus	43
2.3 Discussion.....	47

Chapter 3 – Functional characterization of the US12 protein of HCMV	49
3.1 Materials and Methods	50
3.1.1 Oligonucleotides	50
3.1.2 In silico protein modelling	51
3.1.3 Cells and culture conditions	51
3.1.4 Plasmids and generation of stable Tet-ON inducible cell lines	51
3.1.5 Generation of the TRUS12stop, TRUS12 D218N, and TRUS12 D246N BACs	53
3.1.6 Recombinant virus preparations and infections.....	54
3.1.7 Cytosolic Ca²⁺ measurement	55
3.1.8 Statistical Analysis	55
3.2 Results.....	56
3.2.1 Inactivation of the US12 gene affects efficient HCMV replication in epithelial and endothelial cells	56
3.2.2 US12 ORF shares sequence similarities with cellular proteins of the TMBIM family	57
3.2.3 Structural modelling of the US12 protein.....	60
3.2.4 pUS12 functions as a calcium leak channel	63
3.2.5 Mutation of aspartic acid residues of the putative US12 pore affects efficient HCMV replication in endothelial and epithelial cell lines	67
3.3 Discussion.....	69
Chapter 4 - Exploitation of the structures of US12 and US21 proteins for the identification of compounds with antiviral activity.....	73
4.1 Materials and Methods	74
4.1.1 Structure-based virtual screening	74
4.1.2 Cells and culture conditions	74
4.1.3 BAC recombineering and virus preparations.....	74
4.1.4 Preparation of stock solutions of the CCBs.....	76
4.1.5 Cell Cytotoxicity assay	76
4.1.6 Antiviral assay	76
4.1.7 Statistical analysis	77
4.2 Results.....	78
4.2.1 Structure-based virtual screening identifies CCB molecules that target the pUS12 and pUS21 predicted structures.....	78
4.2.2 Effect of selected CCB molecules on HCMV replication.....	83
4.3 Discussion.....	86
References	89
Acknowledgements.....	101

Abstract

The Human Cytomegalovirus (HCMV) is a β -herpesvirus which causes benign and persistent infections in healthy, immunocompetent individuals. Nevertheless, it is the leading viral cause of congenital infection. The HCMV genome of 235 kbp, is composed of two regions: the central – Unique long (UL) and terminal Unique short (US) regions. The UL region contains 50 core genes present in all herpesviruses and essential for HCMV replication *in vitro* in the standard cell culture system represented by primary fibroblasts. In contrast, the US region contains CMV-specific genes that are non-essential in *in vitro* replication in fibroblasts. The US ORFs, however, are thought to regulate the spread, persistence, reactivation, virulence and temperance in the host and to modulate host intrinsic, innate and adaptive immune responses. Among the US gene family, the US12 family genes is composed of a set of 10 tandemly arranged genes, US12 through US21, conserved in CMV specific to higher primates and predicted to encode 7TMDs membrane proteins. The functional characterization of all the US12 family members is yet to be completed.

The aim of this thesis work was the functional characterization of a member the US12 gene family, the same US12 gene.

First, by a combination of bioinformatic tools and experimental validation, the expression pattern, the cellular localization, and the topology of the US12 protein, the protein encoded by the US12 gene, were defined. The US12 protein with a molecular weight of 28 kDa was characterized as an Early viral protein, showing a time-dependent localization in infected fibroblasts, with a diffuse cytoplasmic distribution in the first phases of infection and then with an accumulation in Golgi-derived vesicles at late stages. Moreover, the accumulation of pUS12 late in infection produced a characteristic ring-like pattern at the periphery of the cytoplasmic Virion Assembly Complex (cVAC), a compartment in the cytoplasm of HCMV-infected cells in which virions acquire the final tegument and envelope. The US12 protein was then experimentally verified as a 7 transmembrane protein (7TMDs) with its N-terminal located in the cytosol and C-terminal within the Golgi-derived membranes.

Then, the importance of the US12 gene in the context of HCMV replication in different cell types was analyzed by means of different recombinant HCMV bearing deletion or inactivation of the US12 ORF. A defective growth phenotype was observed only in endothelial and epithelial cells infected with genetically US12-deficient viruses, thus suggesting a requirement of the US12 gene for efficient viral replication in these relevant cell types.

To get more insights in the putative US12 function(s), further bioinformatic analysis were performed by comparing the US12 ORF with some mammalian TMBIM proteins, and the bacterial TMBIM homolog, BsYetJ. Appreciable levels of identity were found between pUS12 and the TMBIM human Golgi Anti-Apoptotic Protein (hGAAP) (14.9%). TMBIM proteins are 7TMDs cellular “stress sentinels” that exert functions in the cell response to stress conditions by contributing to apoptosis, ER stress signaling, Ca^{2+} homeostasis, adhesion and migration. Little was known about the structure of TMBIM proteins, until the 3-D structure of BsYetJ, the bacterial TMBIM homolog and a 7TMDs protein was solved, thus allowing to identify its function as Ca^{2+} channel and the critical amino residues required for BsYetJ Ca^{2+} conducting activity. In this regard, all the six human TMBIM

proteins have been shown to exert a Ca^{2+} channel activity.

Multiple sequence alignment indeed revealed the conservation in pUS12 of two C-terminal TMBIM-conserved aspartic acid residues that are responsible for Ca^{2+} channel activity in BsYetJ. This prompted us to perform an *in silico* molecular modelling of pUS12 based on the crystal structure of BsYetJ through a fold-recognition approach. The structural model of pUS12 model allowed to predict the presence of a pore in the protein whose opening and closing could be regulated, as in BsYetJ, by the formation or the disruption of salt bridges between the negative di-aspartyl residues (Asp-218 in TMD6 and the Asp-246 in TMD7) and the positively charged Arg-109 in TMD2.

The predicted Ca^{2+} conducting activity of pUS12 was then verified experimentally through quantitative Ca^{2+} imaging experiments. TReX-293 cells in which a tetracycline-inducible expression of pUS12 was engineered, showed a decrease in the Ca^{2+} content of intracellular stores (ER and Golgi) as compared to the cells that were not induced to express pUS12, thus confirming that pUS12 exert a Ca^{2+} leaking activity. Furthermore, when the two aspartic acid residues likely involved in the viroporin activity of pUS12, were mutated in the context of infectious recombinant HCMV, their mutation impacted on the efficiency of viral replication in both endothelial and epithelial cells, thus suggesting a role in pUS12 function(s).

Moreover, since both the pUS12 and pUS21 (Luganini et al., 2018) show a viroporin activity, their protein structures were exploited as potential drug-targets to identify molecules that can interfere with the Ca^{2+} conducting activity and therefore may exert an antiviral effect. Through a structure-based virtual screening, a library of Calcium channel blockers (CCB) therefore was screened against the predicted structures of pUS12 and pUS21 to identify the best binding molecules. CCBs are antihypertensive drugs that block the flow of Ca^{2+} ions through cellular Ca^{2+} channels. Four CCBs molecules, namely efonidipine, lercanidipine, azelnidipine, and niguldipine were selected based on their favorable binding energy and dissociation constant. Then, these four CCBs were tested *in vitro* for antiviral activity against HCMV. All the selected molecules exerted a potent antiviral activity against the wild type virus (HCMV TRwt) with a low micromolar Effective Concentration 50 (EC_{50}) range. Interestingly, a significant difference in EC_{50} values was observed for all the four CCBs between the TRWT and a recombinant HCMV in which the US12 gene was deleted and the US21 gene was inactivated at the same time (TRAUS12-US21 stop). This finding suggested that the selected CCBs could interfere with the viroporin activity of US12 and US21, and this interference may contribute to their overall anti-HCMV activity. These molecules could thus represent possible candidates for repurposing CCBs drugs against HCMV.

In conclusion, the results of this thesis work indicate that the US12 gene of HCMV encodes a 7TMD Early protein that localizes within the cVAC in HCMV-infected cells and contributes to the efficient viral replication in cell types relevant for the spread and replication of HCMV in the natural host. pUS12 is a functional HCMV-encoded calcium conducting viroporin whose structure can be exploited as a novel drug target to identify antiviral agents.

Chapter 1- Introduction

Introduction

1.1 Human Cytomegalovirus

The Human cytomegalovirus (HCMV) is a widespread pathogen belonging to the family of beta-Herpesviruses, with a worldwide seroprevalence of 20-100% (Boeckh et al., 2011).

The primary HCMV infection is usually asymptomatic in immunocompetent hosts, with the virus establishing a life-long latency within the individual and causing some periodical asymptomatic or mild reactivations. On the contrary, it can cause life-threatening diseases when the cellular immune responses are compromised or not fully developed, such as in transplant recipients or AIDS patients, and in newborns (causing birth defects), respectively. HCMV can be transmitted from mother to infant during pregnancy as well as through breastfeeding during neonatal period. In adult life sexual transmission is one of the routes through which HCMV infection can occur, as well as with blood transfusions and organs transplant. Its impact, therefore, has increased in recent decades due to the rise in organ allografting, immunosuppressive treatments, and human immunodeficiency virus (HIV)-infected patients (Seitz., 2010; Mocarski., 2013).

To date, no vaccine against HCMV infection is available. Currently, anti-HCMV therapy relies only on a five FDA-approved drugs targeting the viral DNA polymerase (targeted by ganciclovir and its prodrug valganciclovir, acyclovir and its prodrug valacyclovir, foscarnet, and cidofovir) and the viral terminase complex (targeted by letermovir, the latest in order of license)(Britt and Prichard 2018). The use of DNA polymerase inhibitors is however limited in some relevant clinical settings, including infections with drug-resistant, and congenital and pediatric infections (Meesing and Razonable 2018). Moreover, the use of letermovir is restricted to adult HCMV- seropositive stem cell transplant recipients and has been associated to emergence of drug-resistant strains (Gerna et al. 2019).

1.2 Structure of the virus

The virion of HCMV consists of a 230-kbp linear double-stranded viral DNA surrounded by an icosahedral capsid, a complex proteinaceous layer defined as the tegument or matrix, which is enclosed by a lipid bilayer containing a large number of viral glycoproteins (**Figure 1**). The mature virion particle is 150 - 200 nm in diameter (Landolfo et al., 2003).

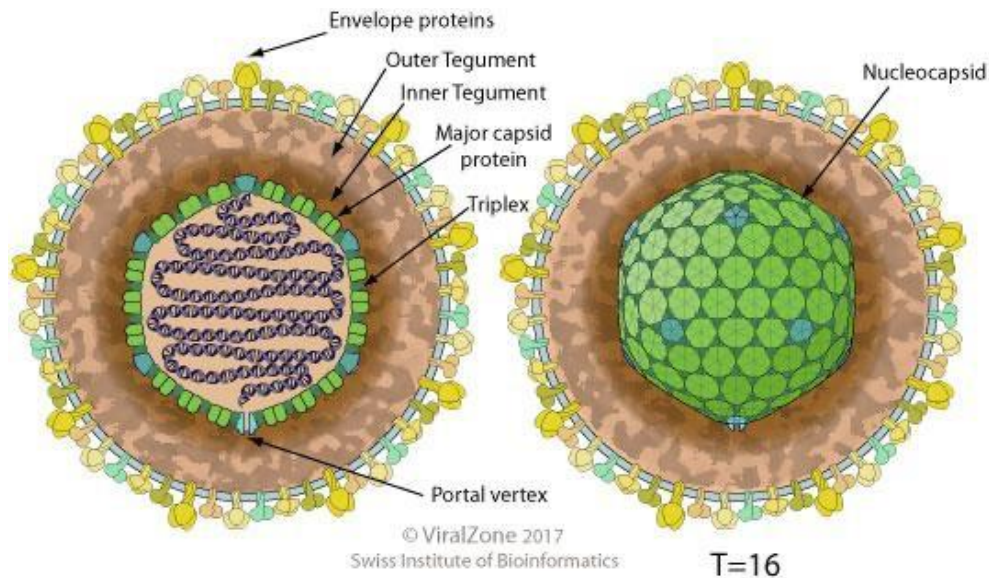


Figure 1. Human Cytomegalovirus mature virion. *Schematic representation of HCMV mature virion (from Swiss Institute of Bioinformatics).*

1.2.1 Nucleocapsid

The capsid of HCMV is characterized by a specific type of symmetry, icosahedric, with T=16 geometry: it comprises a total number of 162 capsomers divided in 12 pentamers and 150 hexamers. The capsid comprises four main proteins: i) the protein product of gene UL86, namely major capsid protein MCP; ii) the protein product of gene UL85, namely minor capsid protein mCP; iii) the protein product of the gene UL46, that is mCP binding protein mC-BP; iv) and lastly, the smallest capsid protein SCP, which is the protein product of gene UL48.5.

12 pentons constitute the vertices of the icosahedron: 11 out of 12 are composed of five mCP, the remaining one is built out of 12 molecules of a portal protein (PORT, protein product of UL104) which contributes to encapsidation phase of viral DNA.

Lastly, mCP and mC-BP are arranged in a complex, displaying a stoichiometry ratio of 2:1, to form triplexes located between adjacent hexons and pentons (Butcher et al., 1998).

1.2.2 Tegument

Surrounding the protein capsid, enclosed by the lipidic envelope, there is a proteinaceous layer that is called matrix or tegument. The proteins of viral tegument have an important role in the support of the stability of capsid structure and in directing the acquisition of viral envelope. The process of tegumentation is characterized by the first phases being carried on in the nucleus and then be continued in the cytoplasm, in a specialized structure which is the cVAC (cytoplasmic virion assembly complex), where both the remaining tegument as well as the envelope are acquired (Tandon et al., 2012).

The number of viral proteins found to be component of the tegument is 38, about one half of the total number of proteins which are observed in infectious virions. These proteins appear to be generally phosphorylated and the importance of this modification step to their activity is broadly unexplored yet, but it is presumed that the phosphorylation, together with the cellular localization

to the site where assembly occurs, association with capsid or envelope proteins, could all be events facilitating the incorporation of the proteins in HCMV tegument (Kalejta., 2008).

Not only viral proteins, but also proteins of cellular origin were observed in the HCMV virion, likely associated to the tegument, together with cellular RNAs as well (Kalejta., 2008).

Among the several tegument proteins, the most abundant one is pp65 phosphoprotein, the product of ppUL83. This protein is delivered to the nucleus at the beginning of a lytic cycle and constitutes a target for both humoral and cellular immunity. This protein was found capable of mediating phosphorylation process of viral IE proteins, thus blocking the presentation of such peptides by class I of major histocompatibility complex (MHC) molecules; it could also stimulate the HLA-DR alpha chain degradation through the mediation of an agglomeration, in the lysosome, of HLA class II molecules. Furthermore, pp65 performs a protection of infected cells from innate immunity through the inhibition of NK cell cytotoxicity thanks to an association with the activating receptor NKp30 (Kalejta., 2008). During the later stages of infection, pp65 translocates in the virion assembly compartment (VAC) (Tandon et al., 2012), and also its detection in white blood cells is the parameter to consider when the decision whether to begin or not an antiviral treatment must be taken (Mocarski., 2013).

Among the most abundant tegument proteins, immediately after pp65 we find pp150, encoded by UL32 gene. This protein carries a phosphorylation in a not mapped site, and a modification through a O-linked N-acetylglucosamine on the residues of serine number 921 and 952. This protein is present in a number of approximately 1500 copies per virion, which interact with performed capsid through their N terminal domain. The interaction of pp150 with the capsid, regardless of the region where it takes place, consists of one of the earliest steps in tegument assembly. Studies performed on mutant viruses lacking pp150 proved the fundamental role of this protein for a successful HCMV replication (R. F. Kalejta 2008). pp150 localizes to the nucleus in the early phases of virus maturation, then proceeds to translocate in the cytoplasm where it associates with the cytoplasmic viral assembly compartment (cVAC). Functional studies led to the conclusion that pp150 gives stability to the virus particles when they translocate to the cytoplasm from the nucleus, and also the close cooperation of pp150 with viral nucleocapsids and several cytoplasmic phases involved in the maturation opens the probability that pp150 has a role in the later steps of viral maturation as well (Tandon et al., 2012).

Further major tegument proteins to mention are pp71 and VPK. pp71, which was originally termed VP8, being the eighth largest viral protein, is the protein product of UL82 gene. It is an early late 71-kDa phosphoprotein, localizing in the nucleus. This protein was the first known HCMV transactivator, increasing the infectivity of viral genomic DNA after its transfection. This protein is necessary for an efficient replication of the virus, as shown by the severe growth defect observed in replication studies performed on a null mutant. pp71 is able to counter balance the repressive activity of the cellular protein Daxx, which is capable of binding histone deacetylases and eventually to initiate transcriptional repression: pp71 binding to Daxx and the stimulation of its proteasomal degradation is a fundamental step for the successful expression of viral IE genes (Kalejta., 2008).

Another fundamental tegument protein, produced with early late kinetics, is a kinase, the protein product of the gene UL97, namely ppUL97. This protein can phosphorylate and, consequently activate, the antiviral drug ganciclovir as well as other proteins.

The presence of three putative Rb-binding motifs on UL97 allow for its direct phosphorylation of Rb

protein, which leads to the stimulation of cell cycle progression thanks to its cyclin dependent kinase like activity. The absence of ppUL97 was associated with both mild and moderate defects, respectively to a reduction ranging from 5 to 20-fold of the replication of viral DNA and a defect in assembly and egress, as well as in packaging of DNA, exit of capsids from the nucleus and mis localization of tegument proteins (Kalejta., 2008).

1.2.3 Envelope

Surrounding the mature viral particles there is a lipidic bilayer which derives from the ERGIC (Endoplasmic Reticulum Golgi Intermediate Compartment) of the host cell: the envelope. It accommodates more than 20 viral glycoproteins, including virally encoded gB (gpUL55); gN (gpUL73); gO (gpUL47); gH (gpUL75); gM (UL100) and gL (gpUL115), with important functions during the phases of attachment to the host cell, viral entry, virion maturation and spread from cell to cell (Tandon., 2012).

From the envelope of HCMV virions three distinct families of disulfide linked glycoproteins could be extracted on the basis of their immunoprecipitations with monoclonal antibodies: i) gC1, ii) gCII, iii) gCIII, inclusive of gB, gM:gN, and gH:gL, respectively. These glycoprotein complexes are almost surely a target of immune response to HCMV infection, being recognized by monoclonal antibodies able to neutralize HCMV infectivity (Gretch et al., 1988).

The gB protein, product of UL55, is a type 1 integral membrane protein that is capable of undergoing a conformational change as to ensure that the envelope of the virus and the cell membrane can fuse together thanks to its association with heparan sulfate proteoglycans.

After the initial binding to these molecules, gB is involved in the entry at plasma membrane in fibroblasts, which is pH-independent, or through endocytosis as in the case of endothelial as well as epithelial cells (Mocarski et al., 2013).

GcII, the second glycoprotein complex of the envelope, is formed by gM (UL100 gene product) together with gN (UL73 gene product) (Kari et al. 1994). gM is a type II membrane protein characterized by the presence of eight membrane spanning domains, while gN is a type I membrane protein: together they form a heterodimer capable of binding heparan sulfate thus contributing to the early events of infection (Kari et al., 1994).

Among the envelope glycoprotein we find a third complex which consists of gH, the protein product of UL75; gL, the protein product of UL115, which form a complex that can associate with gB protein in order to initiate the fusion activity and virus entry (Mocarski., 2013).

The complex of gH and gL can additionally bind other proteins that can determine viral tropism, as an example we find gO, the protein product of UL74, with which they form a trimeric complex (gH:gL:gO) (Zhou et al., 2015) or UL128, UL130 and UL131A products, originating a pentameric gH:gL complex which increases infection in epithelial and endothelial cells but also virus interactions with dendritic cells, neutrophils and several other types of cells (Mocarski et al., 2013). Several HCMV envelope glycoproteins, which do not have a direct involvement in the processes of entry or egress, display instead an immunomodulatory function: some of the viral glycoproteins are capable of binding to IgG and also to secreted glycoproteins, one example being constituted by the protein product of UL22A, which has an impact on the response of the host to the infection (Mocarski et al., 2013).

1.2.4 Types of viral particles

Inside the nucleus of cells which HCMV can infect, there are three different types of viral capsid types which have been observed (**Figure 2, left**): i) capsids of type A that seem to be empty, devoid of packaged viral DNA, whose accumulation comes as a consequence of abortive attempts to package viral genome; ii) capsids of type B that lack DNA too, although they contain viral structural as well as assembly proteins, are seen as the result of abortive capsid formation; iii) type C capsids represent the fully mature nucleocapsids, they contain viral DNA with no scaffold, and display a particular preference for the egress from nucleus in the course of HCMV infection (Tandon et al., 2012).

In the cytoplasm of HCMV infected cells three types of virus particles can be detected as well: (**Figure 2, right**): i) dense bodies (DB) are enveloped particles that do not possess any assembled nucleocapsid nor viral DNA, they instead contain many tegument proteins, pp65 being the most abundant among them; ii) Non-Infectious Enveloped Particles (NIEP) constituted of B-capsid surrounded by an envelope but lacking viral DNA; iii) completely mature virions which are constituted by entirely mature type C nucleocapsids.

DB as well as NIEP can enhance the ratio particle/PFU (plaque forming unit) of the viral stocks, furthermore the high quantity of NIEP produced suggests a possible role they have in overwhelming host immune surveillance.

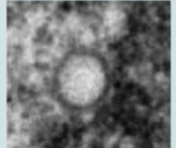
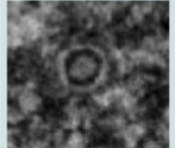
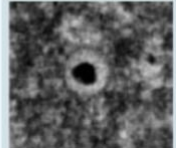
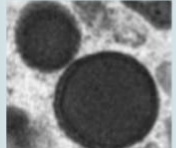
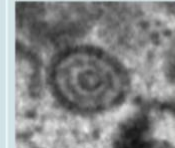
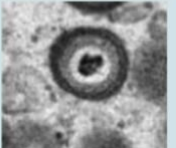
Nuclear			Cytoplasmic		
A capsids	B capsids	C capsids	Dense bodies	NIEP	Virion
Lack scaffold as well as viral DNA and are believed to result from abortive viral DNA encapsidation	Contain scaffold but lack viral DNA: likely to result from abortive capsid formation or DNA encapsidation	Contain viral DNA and lack scaffold; probably representing nucleocapsids in the process of maturation	Noninfectious capsidless particles that carry pp65 tegument protein as the main constituent	Noninfectious enveloped particles (NIEP) produced when B capsids mature	Infectious virus particles produced when C capsids mature, containing encapsidated viral DNA.
					

Figure 2. HCMV viral particles. *Viral particles generated in the course of a HCMV infection (Tandon and Mocarski, 2012).*

1.3 Virus genome

1.3.1 Organization and structure of viral genome

HCMV virions are characterized by a linear, double stranded, approximately 230kbp long DNA genome characterized by a high G+C content (Pass et al., 2001).

The genome shows an arrangement consisting of unique long (UL) and unique short (US) regions, each of which can be oriented in either direction, thus giving origin to four different genome isomers in the progeny of the virus (structure of Class E) (**Figure 3**). The genome is divided in two components, both composed of unique sequences flanked by unrelated pairs of inverted repeats. Adjacent to the (UL) unique long and (US) unique short regions there are terminal repeats to be

written as ab-UL-b'a'c'-US-ca (Figure 3) (Landolfo et al., 2003).

The replication of the DNA occurs through a rolling circle kind of mechanism which gives origin to several tandemly linked copies of the genome of the virus. During the packaging phase, a cleavage of the DNA ensures the production of unit length molecules which can circularize thanks to the presence of unpaired base at each end.

Cytomegalovirus genomes include cis-acting elements with a fundamental role in directing the replication of DNA, its packaging and transcription: *a* regions contain multiple repetition of *a* sequences, they also include two packaging elements that are *cis*-acting, namely *pac1* and *pac2*. The cleavage of sequences which lie adjacent to *pac1* and *pac2* regions produces a single 3' protruding base which allows the circularization of viral genome (Murphy et al., 2008).

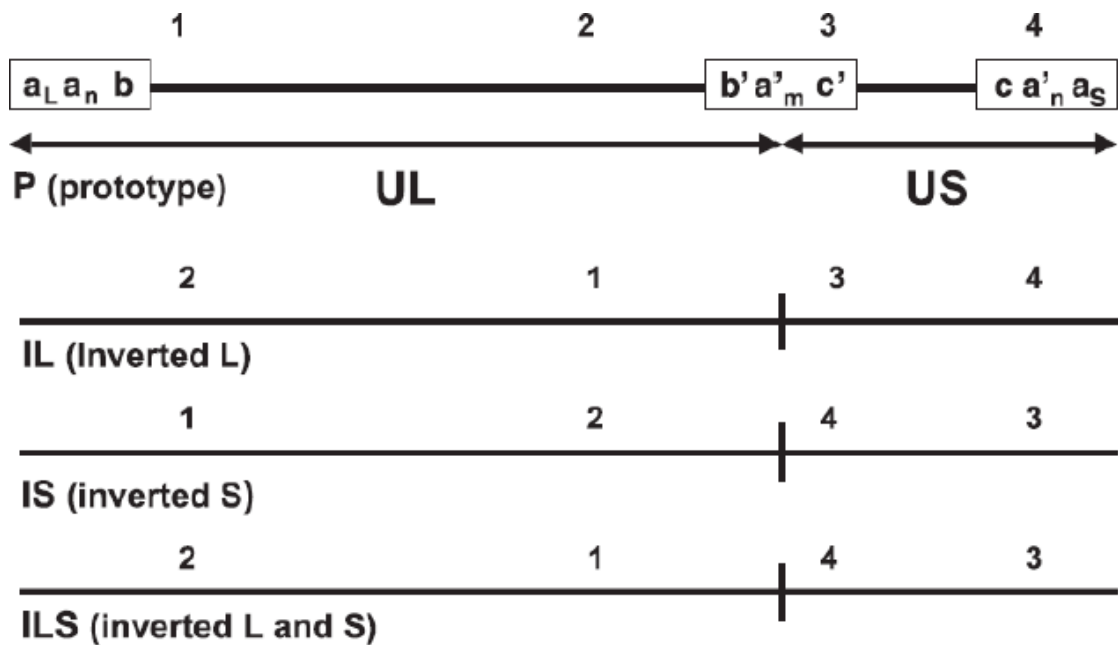


Figure 3. Representation of the structure of the four genome isomers of HCMV. Schematic illustration of the structure of Human Cytomegalovirus isomers (from Landolfo et al., 2003).

1.3.2 Clinical isolates and laboratory strains

The sequences of four HCMV clinical isolates (FIX, TR, PH and Toledo) as well as one primary virus (Merlin) result available: while the four clinical isolates were first cultured in fibroblasts, successively cloned as BAC (Bacterial Artificial Chromosomes) and then sequenced (Murphy et al., 2008). Merlin strain underwent in fibroblasts three serial passages preceding its sequencing as not cloned DNA (Dolan et al., 2004).

In an attempt to produce a vaccine, some HCMV clinical isolates were used to perform serial passages in cultured fibroblasts: the rapid replication occurring in fibroblasts coincided with the loss of the capability for the virus to successfully enter and replicate in various types of cells susceptible to the original virus, as a result from the onset of mutation in the open reading frame of a complex of glycoproteins (composed of gH, gL, pUL128, pUL130, pUL131) (Wang et al., 2005) located in the viral envelope. Eventually such viruses did fail as vaccine candidates, nevertheless, due to their ability to grow faster, give origin to more cell free virus and produce

higher quantity in fibroblasts if compared to clinical strains, they are now widely studied and termed laboratory strains (Murphy et al., 2008).

The observable changes in the genome of these viruses include large deletions as well as duplications. The laboratory strains AD169 and Towne are both characterized by the loss of a multigene region and the gain of a repeated multigene region of similar dimension. The recombination events, leading to the disruption of gH, gL, pUL128, pUL130, pUL131 complex ORF, result as the effect of evolutionary pressure to get rid of it for a successful replication cycle in fibroblasts (Murphy et al., 2008).

1.3.3 Protein coding ORFs and their functions

An initial estimation of the number of functional ORFs to be found in HCMV genome was provided by the sequence of AD169 strain, which predicted 208 coding ORFs, including several repeated ones, of 100 amino acids or more. The subsequent discovery of 19 additional ORFs in Toledo HCMV strain raised the original number up to 227 ORFs. Later, other HCMV clinical strains sequences were obtained, changing the estimated ORFs number to a range of maximum 252 to a lowest of 165, which are conserved among the clinical isolates of HCMV and CCMV (Davison et al., 2003).

The comparison of the aminoacidic sequences between HCMV AD169 strain and herpesvirus genomes showed that more than 40 ORFs protein products present a consistent value of similarity with proteins that are encoded both by alpha and gamma herpesviruses (Chee et al., 1990; Karlin et al., 1994), underlying an origin which is in common among the subfamilies.

Among the ORFs which result conserved, about a quarter of them encodes functionalities which are linked to the metabolism and replication of the viral genome, while the other 75% are involved in maturation and organization of the structure of the virions.

The UL ORFs, whose protein products have a role in the metabolism of nucleotides and DNA or in viral structure, are arranged in blocks of seven genes, conserved among herpesviruses and whose order is specific for the distinct subfamilies, suggesting that the functions are conserved. US ORFs are located in the repeated regions of HCMV and show a lower degree of conservation (Chee et al., 1990).

The creation of a map containing all of HCMV ORFs allowed the distinction between genes which are considered to be essential (red), augmenting (yellow), or yet nonessential for in fibroblast replication (green) (**Figure 4**) (Dunn et al., 2003).

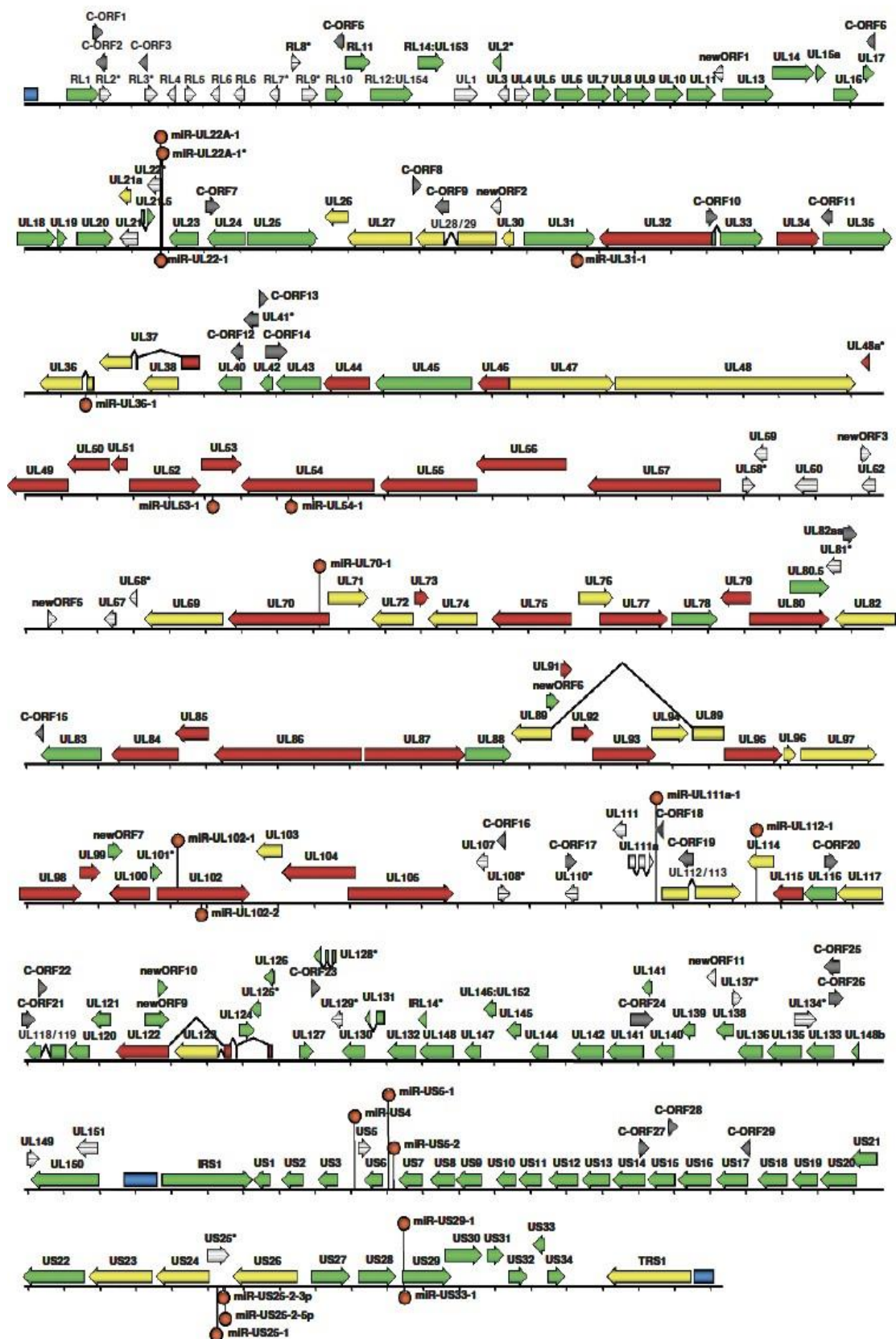


Figure 4. Arrangement of the genome of clinical strains of HCMV. ORFs are depicted as arrows indicating their orientation. The different colors highlight ORFs which are essential (in red), augmenting (in yellow) or non-essential (in green) for the viral replication in cultured fibroblasts. The

arrows that are grey show ORFs which, up to these days, have not been tested for their function. ORFs enriched with an asterisk do not include an AUG \geq 80 codons from a stop codon. The three dark blue rectangles represent the repeat regions located at the ends of unique long and unique short regions (Murphy et al., 2008).

1.4 HCMV replication

1.4.1 Virus attachment and entry

Human Cytomegalovirus shows an extended cellular tropism which is associated to the possibility to manifest the disease in many tissues and organs of the human host: this capability is the consequence of the presence of a high number of cellular receptors.

The first phase of HCMV entry requires the tethering to heparan sulfate proteoglycans (HSPGs) coordinated by gB and gM, a step which stabilizes the virion until the involvement of other receptors allowing a more stable docking (Isaacson et al., 2009). It has been reported the interaction of gB with both integrin heterodimers and epidermal growth factor receptors to mediate the entry of the virus. Eventually, cellular and viral membranes fuse together, thus releasing the tegument proteins as well as the capsid in the cytoplasm: this fusion step requires gB and gH/gL complex presence.

Wild type HCMV possesses two complexes of gH/gL: gH/gL/gO, that improves the infection of fibroblasts, a cell type into which HCMV enters through a fusion process occurring at plasma membrane at a neutral value of pH; and also, gH/gL/UL128-131, which promotes the entry step into endothelial and epithelial cells, cell types in which HCMV entry requires an endocytosis process and a fusion step, occurring at low pH values, with the endosomes (Wille et al., 2010).

1.4.2 Post-fusion, pre-immediate early events

After the interaction of the glycoproteins of the envelope with those cellular receptors present on fibroblasts, the fusion of the membranes is the step allowing the release of the viral capsid, as well as the tegument proteins, in the cytoplasm; for what concerns epithelial and endothelial cells instead, the entry happens through a mechanism of endocytosis at low pH value. Once the fusion step occurred, the possible destiny for tegument proteins are three: they can either remain in the cytoplasm, either migrate to the nucleus in an independent way, as pp65 and pp71 or remain strongly linked with the capsid coordinating its delivery through microtubules to the NPC (nuclear pore complex) (Compton., 2004).

The transport of HCMV capsids through the cytoplasm to the nucleus is possible thanks to the presence of the organized network of microtubules extending in the cell: a complex of tegument associated protein composed of pp150, pUL47 and pUL48 allows this movement.

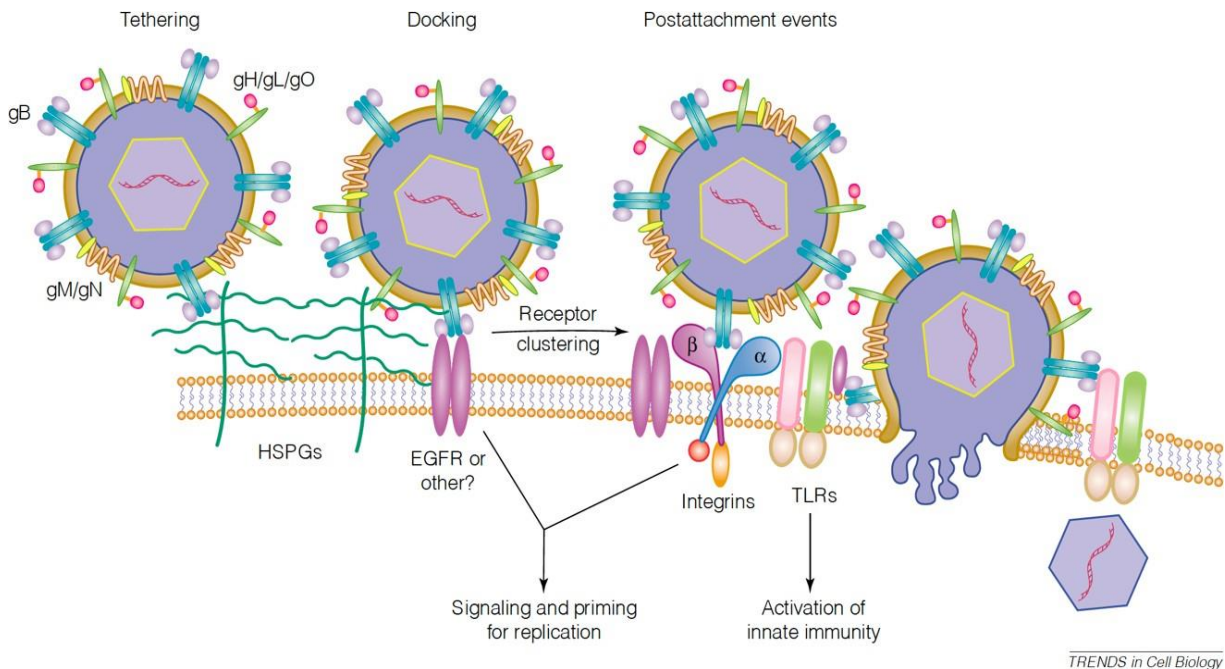


Figure 5. Scheme of HCMV attachment and entry phases into cells (Compton, 2004).

Upon entering the nucleus, viral DNA rapidly gets packaged into chromatin through histone association. A subset of viral genomes associates with PML nuclear bodies, subnuclear structures near to which HCMV seems to be transcribed, validating the hypothesis according to which PML-NB constitute a preferential localization for expression of viral genes. This hypothesis was questioned though, since many of the proteins localizing to PML-NBs work as transcriptional repressors: among them there is Daxx protein, which associates to histone deacetylases and is then recruited to promoters, eventually giving origin to transcriptional repression. HCMV tegument protein pp71 can bind to Daxx thanks to the presence of two DID (Daxx interaction domains) and induce its proteasomal degradation, thus counteracting Daxx effect on HDAC activity (Kalejta., 2008; Kalejta., 2008).

1.4.3 Regulation of the expression of viral genes

The expression of HCMV genes, in the course of a productive infection, occurs in a series of transcriptional events which are temporally coordinated and regulated through cascading events and which eventually lead to the production of three different categories of viral proteins termed as IE (immediate-early) or α , E (early) or β , and L (late) or γ (Landolfo et al., 2003).

The regulation of the expression of viral genes is given by two main mechanisms: (i) viral factors together with cellular factors that influence directly the machinery of transcription, with an association to promoter or enhancer regions in a direct manner (transcription factors) or by binding to other adaptor proteins; (ii) viral factors that can have an impact on the process of chromatin remodeling by acting on the antagonistic activities of HATs (histone acetyl transferases) acting in sync with demethylases, (HDACs) histone deacetylases and methylases.

Inadequacy during the expression of early genes and the following replication of viral DNA (more than attachment or penetration) could possibly represent the events which, in non-permissive cells,

are defined restrictive (Landolfo et al., 2003).

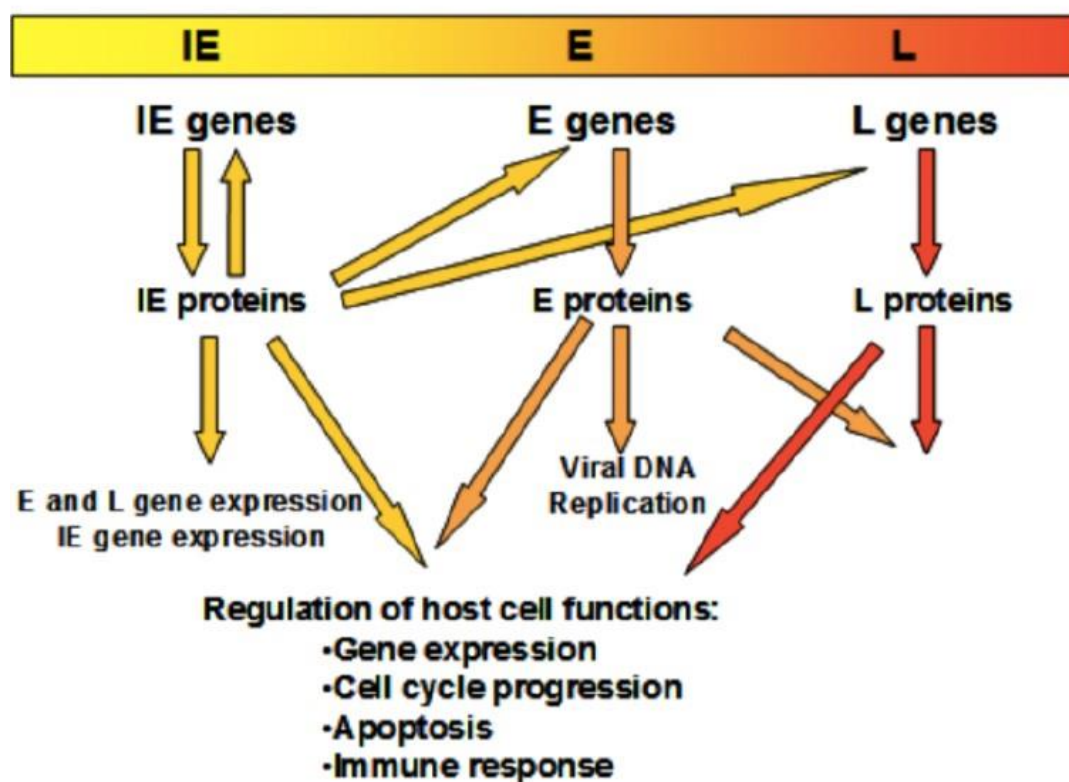


Figure 6. HCMV gene expression and gene product functions during a productive infection (Landolfo et al., 2003).

1.4.4. Characteristics and functions of the Immediate-Early proteins

The first HCMV genes to be transcribed as soon as one h p.i. are the immediate early (IE or α) genes, whose expressions does not require the previous synthesis of *de novo* viral proteins and that peaks between 4 and 8 h p.i.

The genes to be included in the IE group are several: major Intermediate Early (MIE), codified by genes UL122 and UL123 (IE1 and IE2) but also auxiliary genes, for example UL36, UL37 and UL38, UL115, UL116, UL117, UL118 and UL119, IRS1 and TRS1 and finally US3.

Major Intermediate early proteins, either by themselves or in coaction with others, are necessary for the following gene expression due to their role as auto stimulators and transactivators of viral genes (Landolfo et al., 2003).

The impact these proteins have on the physiology of host cell is deep, since they are involved in the regulation of the expression of a high number of cell genes (Fortunato et al., 1999).

The expression of these ie1/ie2 genes is coordinated by a complex enhancer-modulator element that acts in way that is both a tissue specific and cell type specific (Nelson et al., 1990; Meier et al., 1996).

The different starting point and splicing for MIE region transcripts give origin to four different proteins: IE1491aa and IE2579aa, that are the most abundant ones, and which also share the same N-terminal region which is 85 amino acid long; IE2 isoform (IE2425aa), which is less available and

that is encoded by a spliced transcript carrying a deletion within *UL122* and, lastly, a 40-kDa polypeptide (IE2338aa), which is a true late protein.

The other IE genes functions are diversified: IRS and TRS1 work together with IE1-72 and IE2-86 in order to transactivate the promoters of E genes. US3 protein product is a glycoprotein with a role in the immune evasion in cells which are infected: these proteins, which are located on the endoplasmic reticulum, are able to avert the movement of the major histocompatibility complex (MHC) Class I to the Golgi from the endoplasmic reticulum and, in this way, to down regulate MHC Class I antigen presentation (Stasiak et al., 1992; Jones et al., 1996).

On the other side, the region from UL36 to UL38 includes proteins like UL36 and UL37, which present antiapoptotic activity and which act at various steps during the caspase cascade (Skaletskaya et al., 2001; Arnoult et al., 2004).

UL36 and UL37, US3 and IRS1 all are not necessary for HCMV replication in *in vitro*.

1.4.5 Characteristics and functions of the Early proteins

Oppositely to IE genes, which do not need *de novo* protein synthesis, early (E or β) genes expression relies on the previous synthesis of IE gene products to occur (Fortunato and Spector 1999). The class of Early genes comprises two subgroups, β 1 (E) and β 2 (E-L) which differ for the time at which their expression occurs: 4-8 hours p.i for β 1 genes, 8-24 hours p.i for β 2 genes.

The type of proteins encoded by E genes include mainly nonstructural proteins such as viral DNA replication factors, repairing enzymes and also proteins which display a role in immune editing (Mocarski., 2013).

E genes are diffuse inside the genome of HCMV: dissimilarly to UL region genes, many US genes exhibit E class expression features. There are though many E genes, including UL4 and UL44, UL112, UL113 and UL54, that are transcribed during the late phase of the infection by various systems, such as the activation of a promoter which is different and independent from the promoter which is transcriptionally active in E times; then also through the start of the transcription at a different start site together with the modification of the pattern of splicing (Fortunato., 1999; Mocarski., 2013).

E genes transcription is thought to be enhanced by IE2-86 (acting by itself or cooperating with IE1-72), by the transactivation of the corresponding promoters in a TATA box dependent way, requiring host transcription initiation complex as well as specific transcription factors (Fortunato et al., 1999). The roles for UL112/113 include functional roles such as DNA-binding, while many other E proteins show a role in establishing immune evasion in infected cells, where US2 and US11 encoded glycoproteins stimulate the proteasomal driven deterioration of heavy chains of MHC class I (Shamu et al., 1999; Story et al., 1999).

Another E class protein with a role in immune evasion is US28, which is a receptor for CC chemokines, sequestering them from the extracellular milieu, thus avoiding the elimination of HCMV infected cells (Gao et al., 1994; Bodaghi et al., 1998).

1.4.6 Replication of viral DNA

Soon after 16 h p.i., the process of synthesis of viral DNA, which requires both specific viral and cellular proteins, begins in the nuclei of infected cells (Mocarski et al., 2013).

Lacking genes coding for deoxyribonucleotides biosynthesis enzymes, HCMV relies on the host cell supply of dNTPs in order to accomplish its genome replication: thus, it stimulates cellular transcription and translation through various strategies, all aiming at the enhancement of biochemical pathways which are implicated in the biosynthetic process of precursors of DNA, such as the intensification in expression of cellular enzymes including, among the others, thymidine kinase, topoisomerase II and ornithine decarboxylase.

This HCMV feature, that is the stimulation of expression of enzymes from the host cell which are required for DNA precursor biosynthesis, is fundamental for the replication of the virus in quiescent as well as differentiated cells which do no longer activate the expression of these enzymes.

Among the six conserved ORFs which encode the core replication proteins we find: (i) ppUL57, preventing the reannealing of the DNA once unwinded by the helicase-primase; (ii) helicase-primase complex, composed of UL70, UL105 and UL102, encoded subunits and DNA polymerase (Griffiths., 2000; Mocarski., 2013).

More viral proteins are involved, for example UL84, functioning as an initiation factor origin specific, stimulating viral origin dependent synthesis of DNA and UL112/113, which localize to limited intranuclear regions considered the precursors of the replication centers, where they recruit fundamental replication enzymes and proteins (Penfold et al., 1997; Ahn et al., 1999).

At 4 h p.i. the circularization of the input genome determines the start of the DNA replication of HCMV genome, which begins from a single origin through a bidirectional mechanism, to then change into a form of DNA replication which is defined as “rolling circle”. This is a modality through which the largest part of viral DNA is produced. The replication of DNA in this phase occurs in the form of long concatemers, which are then cleaved in order to be encapsulated. Before their packaging, new viral DNAs are inverted, cleaved, and packed thanks to the highly conserved packaging signals *pac1* and *pac2* (Mocarski., 2013).

1.4.7 Characteristics and functions of the Late proteins

The vast majority of HCMV genes belongs to the L class, the last class of genes expressed in the course of HCMV infection, which present primarily structural roles and cooperate to the assembly of the virion (Chambers et al., 1999).

These genes are divided in two classes, according to their time of transcription: L proteins $\gamma 1$ (leaky late), transcribed between 24h and 36 h p.i. and $\gamma 2$ (true late), transcribed at 24-48 h p.i. and whose transcription depends on DNA replication (Mocarski., 2013).

The promoter of leaky and true late L genes are simple promoters defined by the region surrounding the TATA box, but many show multiple transcription start sites (Gatherer et al., 2011). During the 1990s, three loci were characterized as late gene loci: (i) UL94 locus, comprising ORFs from UL93 to UL99; (ii) UL99 gene, encoding tegument protein pp28; (iii) UL75, encoding envelope gH protein.

1.4.8 Virion assembly, maturation and egress

In a way analogous to other herpesviruses, Human Cytomegalovirus replication cycle involves both nuclear and cytoplasmic phases: the assembly of viral capsids, the synthesis of viral DNA and its encapsidation, together with the initial tegumentation steps, all take place in the nucleus of the host

cells. After nucleocapsid formation, the newly formed nucleocapsids exploit the nuclear egress complex (NEC), to translocate from the nucleus to the cytoplasm, where they are then accepted by the cVAC or cytoplasmic Virus Assembly Compartment, the site in which tegument and viral envelope are finally acquired (Tandon et al., 2012).

The formation of the capsid, composed of pUL86, pUL46, pUL85 and pUL48A, is mediated by a pUL80 based scaffold, which organizes the capsid shell and additional proteins that associate with the capsid, such as PORT protein and specific capsid vertex components pUL77 and pUL93. The encapsidation occurs through the recognition of packaging signals *pac1* and *pac2*.

The nuclear egress complex subsequently favors the dissolving of nuclear lamina allowing the egress of virus particles moving to the cytoplasm: this process is favored by a complex of pUL50-pUL53-like NEC, which interfaces viral and cellular kinases able to phosphorylate nuclear laminas, thus opening laminar network (Tandon et al., 2012).

The initial budding through the inner nuclear membrane and the second budding through the outer nuclear membrane are events leading to a de-envelopment followed by a re-envelopment model, in which the capsid first collects the primary envelope from the inner nuclear membrane, which is subsequently lost once they undergo fusion with the outer layer of the nuclear membrane or the endoplasmic reticulum membrane, juxtaposed to it, and move into the cytoplasm.

Once in the cytoplasm, virions undergo the final maturation steps in a specialized cytoplasmic compartment that is the VAC (Virion assembly compartment), cylindrical structures present one per infected cell, with one side showing perinuclear localization that leads to the bending of the nucleus in a kidney like shape. The cVAC consists of a series of concentric enclosed cylinders, and each of the cylinders is made of a specific type of vesicle deriving from the several cell compartments (Golgi, TGN, early endosomes).

It has been observed that the early endosomes, which belong to the secretory apparatus, considered normally as intermediaries between trans Golgi network and the surface of the cell, are localized in the center of the AC which is surrounded by ER to Golgi intermediate area.

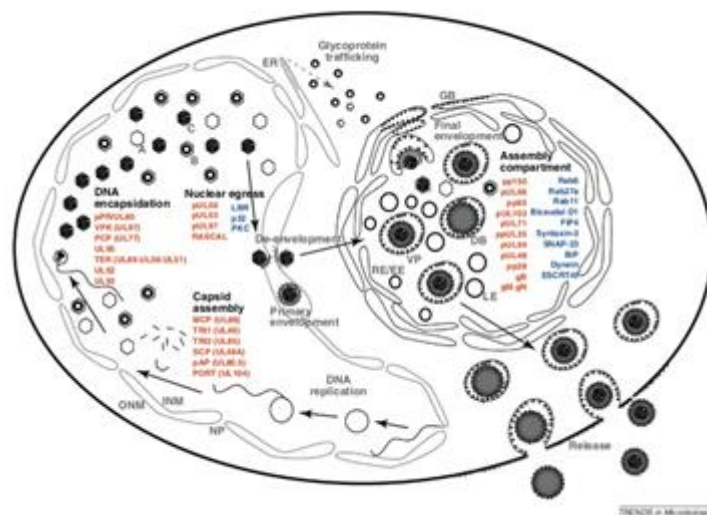


Figure 7. HCMV assembly, maturation and egress. Illustration representing HCMV assembly and maturation phases. The model represents the events occurring in the nucleus and the cytoplasm during the maturation of HCMV, together with the main players participating in this process. The

proteins depicted in red belong to the virus. Abbreviations used are: VP, virus particle; DB, dense body; EE/RE, early endosome/recycling endosome; LE, late endosome; GB, Golgi body; ER, endoplasmic reticulum; NP, nuclear pore; ONM, outer nuclear membrane; INM, inner nuclear membrane; A, B, C, kind of nuclear capsids (from Tandon et al., 2012).

1.5 Cytomegalovirus cell tropism

Human Cytomegalovirus is able to infect a noticeably wide range of cells in its host, comprising cells from parenchymal tissue and cells from connective tissue of potentially any organ; it can also infect several hematopoietic cell types. Epithelial and endothelial cells, together with fibroblasts and smooth muscle cells as well, are the prevailing targets for replication of the virus.

This consistent range of target cells that can possibly be infected by HCMV is what determines the pathogenesis of HCMV infections.

Infection of epithelial cells likely impacts on inter host transmission of the virus; infection of both endothelial as well as hematopoietic cells promotes systemic dissemination in the host, while the infection which concerns ubiquitous cell types, like smooth muscle cells and fibroblasts, contributes with the platform for a successful viral proliferation (Sinzger et al., 2008).

Various HCMV strains, as a result of the alterations occurring in the gene region going from UL128 to UL131, display a different tropism for macrophages, dendritic and endothelial cells (Sinzger et al., 2008).

1.5.1 Target cells of HCMV *in vivo*

HCMV is firmly confined to humans for what concerns the host level, but in the human host it is able to diffuse to potentially any tissue thanks to a particularly wide range of target cell types.

The type of cell HCMV can infect has been studied in several tissues through the years with the double staining of cell markers and viral antigens as well as DNA, and the results showed three features of HCMV tropism *in vivo*: (i) cell types which are ubiquitously distributed, like epithelial and endothelial cells, also fibroblasts, are the main targets of HCMV infections; (ii) leukocytes that circulate in the peripheral blood are prone to be a viral target; (iii) specialized cells from parenchymal tissue, like neurons both in the brain and retina, muscle cells of gastrointestinal tract and liver cells can undergo an infection potentially giving rise to cytopathogenicity.

Another kind of cells usually infected by HCMV is endothelial cells, which could have a role in the spread of the virus and fibroblasts, noticed to be a common target for HCMV *in vivo* in the past: cells from connective tissue are in fact an optimal target for multiplication of the virus as they are commonly diffused in the stroma of multiple organ systems (Sinzger et al., 2008).

1.5.2 Target cells of HCMV *in vitro*

A growing number of models of cell culture represents, in a very precise manner, the *in vivo* situation regarding various cell types susceptibility.

The list of primary cell kinds which can support the whole viral replication process, obtain a cytomegalic aspect and be eventually lysed, is consistent, and comprises fibroblasts from smooth muscle cells, from vessels, epithelial cells of retina pigment, hepatocytes and placental trophoblast

(Sinzger et al., 2008).

Furthermore, a reduced replication can be obtained in a series of immortalized cell lines, including glioblastoma and teratocarcinoma cell lines, but also monocytic cell lines. Despite this aspect though, a certain degree of differentiation is regularly required to make these cell lines capable of supporting of a whole replication cycle (Shelbourn et al., 1989).

If, on one hand, *in vivo* studies were preferred to identify the types of cells susceptible of infection by HCMV in its natural host; on the other hand, cell culture models could make it possible to investigate quantitative features concerning susceptibility as well as productivity, thus revealing important distinctions among cells with a different origin. Fibroblast from skin or lungs have always been considered the regular cell type suitable for both isolation and propagation of HCMV derived from samples obtained from different patients and are nowadays still the most successful producer cell line, independently of which is the virus strain considered (Mocarski., 2013).

1.6 The US12 gene family

1.6.1 The US domain of HCMV genome

Among the eight species of human herpesviruses, HCMV is considered a complex virus which shows the largest of the viral genomes and, due to this feature, it is not easy to define which are the functions encoded by the genome because, in addition, the lack of an animal model for HCMV infections has to be taken in account as well.

The genome of HCMV presents about 50 core genes that are evolutionally conserved, ORFs common among herpesviruses which encode the basic functionalities necessary for the replication of viral genome and the subsequent assembly into viral particles. The location of these 50 genes, which result to be mandatory for viral replication *in vitro* in primary fibroblasts, is the UL domain (Yu et al., 2003).

On the contrary, the genes located in US region of the genome of Human Cytomegalovirus, which are cytomegalovirus or beta herpesvirus specific, resulted being non-essential for viral replication in fibroblasts cell culture: this region of the genome thus, does not encode for functions mandatory for the replicative cycle, but it is however strongly conserved between the clinical strains and thought to have a role in the regulation of many phases of HCMV infection, such as host immunoregulation, modulation of the cellular innate response and determination of cellular tropism, aiding in this way pathogenesis of the virus (Mocarski., 2004).

For the majority, the genes defined as non-essential, found in the US region, are distributed in six families of homologous ORFs that do not present any degree of homology with other known human herpesviruses ORFs, with the exception of the family of G protein-coupled receptor (GPCR) (Weston et al., 1986).

Each of the family contains from 2 up to 13 ORFs that occur not only as tandem arrays (US2, US6, US12 families) but that are also dispersed in the US regions (US1, US22 and GPCR families) (**Figure 8**).

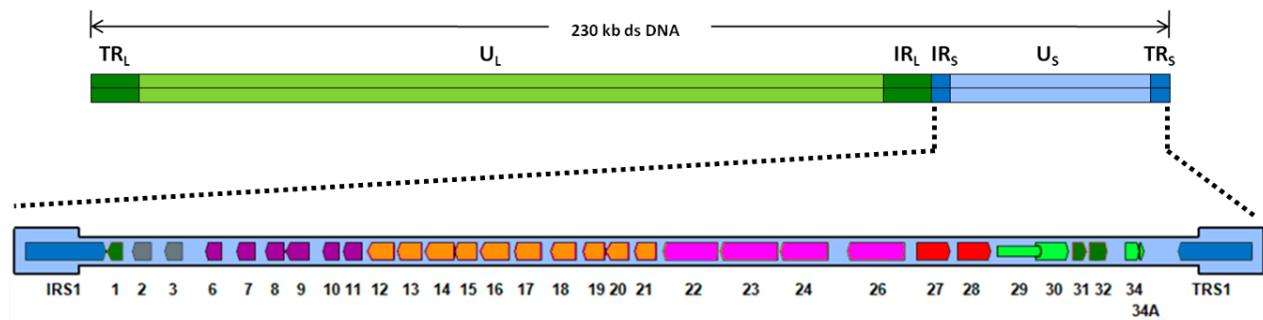


Figure 8. Gene families of the US region. The picture shows in detail the organization of the US ORFs in the different gene families. Color code: dark green, US1 family; grey, US2 family; violet, US6 family; orange, US12 family; pink, US22 family; red, GPCR family.

The family of US2 comprises US2 and US3 ORFs, which produce a group of abundant ImmediateEarly (IE) transcripts, that encode for some glycoproteins which are supposedly associated to membranes (Weston., 1988).

The family of US6 is made of six genes, spanning from US6 to US11, that encode a series of Early transcripts (among which there are also two bicistronic mRNAs) for several glycoprotein complexes associated to viral envelope.

The US22 family comprises 12 members, of which just four, namely US22, US23, US24 and US26, are found inside the US region: these genes encode for some Early viral proteins characterized by the presence of glycosylation sites located at their N-terminal and charged residues in their C-terminal region, but that lack an evident transmembrane, hydrophobic region. Last, the GPCR family gives rise to membrane spanning glycoproteins that share a certain degree of homology, in their sequence, with cellular receptors belonging to the opsin family (Chee et al., 1990).

Up to date, only little information is available regarding the remaining two large families, US1 and US12: among them, US12 family is the one which is likely to show potential for high importance from the biological point of view.

1.6.2 US12 gene family: general features

Between the families US6 and US22 of the US region of HCMV genome we find the gene family of US12 (Weston and Barrell 1986): this family includes 10 tandemly disposed genes going from US12 to US21, which are categorized as non-essential (**Figure 9**).

The US12 gene family is not present in the genome of CMVs infecting non primates, whereas it was observed to be conserved among those CMVs infecting higher primates, including Chimpanzee, Rhesus and Cynomolgus: this feature suggests that this family underwent an evolutionary emergence only in recent times (Lesniewski et al., 2006; Stern-Ginossar et al., 2012; Van Damme et al., 2014).

The members of US12 family show a high level of conservation in the clinical isolates as well as in the laboratory strains of HCMV (Murphy et al., 2003), a finding that suggests that these proteins possess a fundamental biological role still to be enlightened.

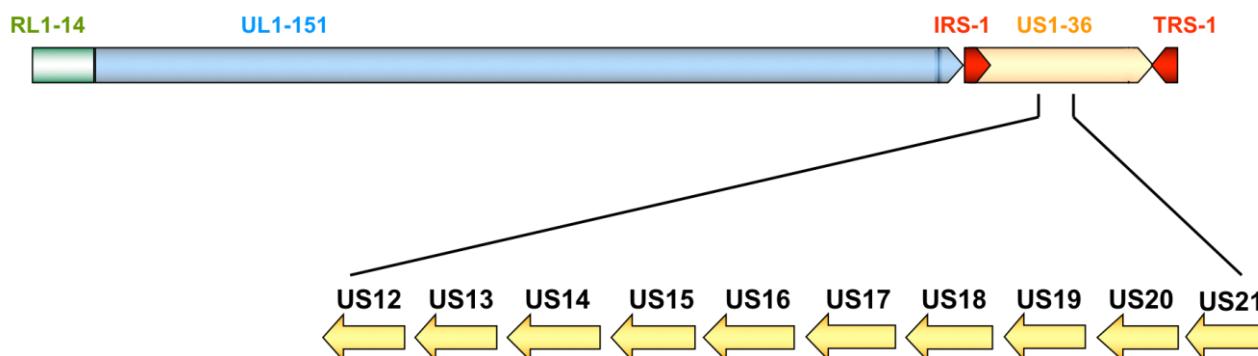


Figure 9. The disposition of US12 gene family located in the US domain of HCMV genome: Representation of the US12 gene family in HCMV genome, illustrating the arrangement of the ten genes from US12 to US21.

When some members among US12 family are deleted, the consequence on viral replication in cell culture is only modest, even though it can vary depending on the cell type, (Dunn et al., 2003; Yu et al., 2003) and no precise roles have been discovered.

These proteins possess several hydrophobic segments and seem to belong to the superfamily of proteins characterized by the presence of seven transmembrane segments. Unfortunately, there is very poor knowledge regarding the function of these proteins. In previous studies, similarity was highlighted comparing members of US12 family and seven transmembrane domain proteins, like G-protein-coupled receptors, and an inhibitor of Fas regulated apoptotic process (Holzerlandt et al., 2002; Rigoutsos et al., 2003).

The general role of GPCRs is transmembrane signal transduction, through the activation of signaling cascades in the cytoplasm as response to the binding of a ligand. In order for some proteins to be included in the superfamily of GPCR, two requirements must be fulfilled: i) presence of seven hydrophobic spans approximately 25 to 35 amino acids long; ii) ability to interact with G proteins. Lately, this definition was extended as to take into account also several related proteins capable of signaling in a manner which does not rely on the action of G proteins.

Despite the fact that protein products of the US12 family are not required for viral replication in cell cultures, due to their homology to proteins which possess a significant roles in regulation of metabolism of the cell, like GPCR, and due to their conservation, there is the possibility for members of US12 family to have an important roles in HCMV biology, or it would have been otherwise implausible that the virus would devote such a huge proportion of its genetic content on genes with functions that are not important (Lesniewski et al., 2006).

In order to explain the global relationships within the members of US12 family and between them and their relatives of other higher primates Cytomegaloviruses, across the entire locus an intra , but also an inter species comparison, were performed: the first important conclusion obtained was that the original events of duplication and divergence, which led to the modern version of the US12 family, happened before the occurrence of the divergence of both the rhesus lineage and the hominoid lineage.

With the creation of a phylogenetic tree that resulted from the analysis, it was observed that proteins from US12 family gather in a clade which differs from any of those that had been formerly described. These discoveries led to the formulation of the hypothesis that multiple families of

duplicated genes, and of diverged genes, underwent an evolutionary process in order to gain advantage from structural scaffolds, functionally flexible, that are able to accommodate various functional domains.

For what concerns US12 family, the structure with seven transmembrane domains gives a structural scaffold which will be linked with membranes of the cell, and its precise localization on those membranes is determined by rather little sets of amino acid sequences which often reside in the C-terminal domain. Modifications in even little residues residing in the cytoplasmic loops can alter the precision of the association with cytoplasmic proteins like G proteins; in a similar way, little alterations occurring in intramembrane sequences, but also in the extracellular domains, would change the interactions occurring with other proteins membrane associated or with extracellular ligands, respectively.

Thus, the evolutionary onset of important alteration in function can be obtained by relatively small changes in the sequence (Lesniewski et al., 2006).

1.6.3 US12 family have homologs with cellular TMBIM proteins

The proteins of US12 family are characterized by the presence of seven transmembrane hydrophobic domains and by a significant level of homology with two known TMBIM (Transmembrane BAX Inhibitor motif-containing) proteins, namely BI (BAX inhibitor 1) and hGAAP (human Golgi anti apoptotic protein), two cellular proteins with a confirmed role in conservation of homeostasis of intercellular calcium, apoptotic process, endoplasmic reticulum stress, migration and adhesion processes of infected cells (Carrara et al., 2015; Liu., 2017). The TMBIM containing proteins are family of proteins that maintain Ca^{2+} homeostasis by the flux of Ca^{2+} across membranes. These cellular proteins are highly conserved in mammals, and homologs with fish, insects, plants, yeasts and viruses. The TMBIM proteins are composed of six well conserved members showing inhibitory activity in different setting of programmed cell death (Chang et al., 2014). The TMBIM proteins take part in maintaining the calcium homeostasis of the intracellular cells, apoptosis process, endoplasmic reticulum stress, migration and adhesion process of infected cell (Carrara et al., 2017; Rost et al., 2014). TMBIM family members are anti-apoptotic with seven transmembrane domain (Carrara et al., 2012).

Bax Inhibitor-1 (BI-1) is also the TMBIM6 which plays as an integral membrane protein that is in the ER and interacts with the BCL-2 and BCL-XL playing an anti-apoptotic role. In mammals, its cryoprotective properties are most evident in paradigms of endoplasmic reticulum stress. Lack of BI-1 therefore leads to defective unfolded protein response and increased susceptibility to ER stress (Lisak et al. 2015). BI-1 is also a Ca^{2+} leak channel protein and it has been suggested to regulate intra-ER Ca^{2+} concentrations ($[Ca^{2+}]_{ER}$) via its interaction with IP3R (Hu et al., 2009; Reimers et al., 2008), thus maintaining Ca^{2+} homeostasis.

These studies are supported by the three dimensional structure and pH sensitive Ca^{2+} flux properties of bacterial homologue of BI-1, BsYetJ (Chang et al., 2014). BsYetJ possesses the di-aspartyl pH sensor in its C-terminal pore domain (Asp171- Asp 195) which corresponds with the two aspartate residues present in BI-1 (Asp 188-Asp213). A homology model of BI-1 and BsYetJ shows an opening of a pore in neutral pH and closing of the pore in acidic pH depending on the cytosolic pH (Bultynck et al., 2014).

TMBIM1 (also known as LFG3) is a 35kDa protein predicted to have a seven transmembrane domain located in endosomal/ lysosomal membranes (Lisak et al., 2015). TMBIM1 protects Fas-mediated apoptosis by reducing the Fas expression on the cell surface. TMBIM2 (also known as LFG) is located in the ER and in Golgi apparatus and in the lipid raft microdomains of the plasma membrane (Fernández et al., 2007; Somia et al., 1999). TMBIM3 (also known as LFG1) is upregulated during ER stress and protects against ER stress – mediated cell death via mechanism that involves TMBIM6 and IP₃Rs (Rojas-Rivera et al., 2012). All these TMBIM family members are predicted to have seven transmembrane domains.

TMBIM4 also called GAAP is a highly conserved hydrophobic protein present throughout eukaryotes and Pox viruses. It is a 27 kDa protein that is localized in the membranes of ER and Golgi apparatus (Lisak et al., 2015). The function mainly resembles of that of TMBIM6; the overexpression of hGAAP inhibits the trigger of apoptosis by intrinsic and extrinsic stimuli (Gubser et al., 2007) and it releases the Histamine – induced Ca²⁺ release from intercellular stores by lowering the Ca²⁺ content within the stores and decreasing the efficacy of IP₃ (De Mattia et al., 2009). TMBIM5 (also known as GHITM) is a 37 kDa protein predicted to have eight transmembrane domains. The tMBIM5 is expressed in most tissues and appears to reside in the inner mitochondrial membrane (Lisak et al., 2015). TMBIM5 downregulates the induction of the rapid release of pro-apoptotic proteins from the mitochondria during apoptosis. Overexpression of TMBIM6 results in the stabilization of cytochrome c at the inner membrane, irrespective of the permeabilization of the outer membrane (Oka et al., 2008).

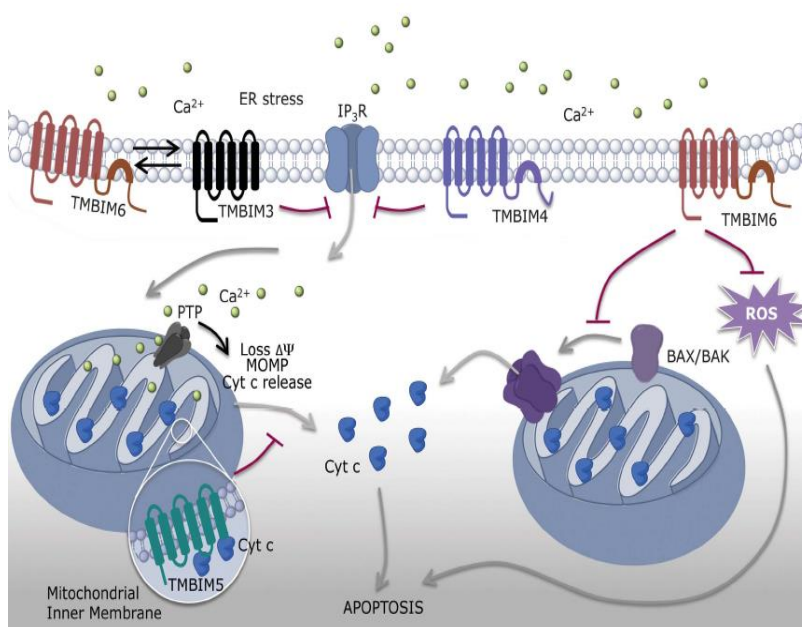


Figure 10: The TMBIM family proteins and the control of intrinsic protein. *The TMBIM family have several adaptive responses of cells to environmental changes like apoptosis, ER stress signaling, Autophagy, mitochondrial bioenergetics, lysosomal function and calcium homeostasis (Rojas-Rivera and Hetz., 2015).*

The first GAAP to be characterized was from the camelpox virus (CMLV). The viral GAAP described was in cowpox virus (CPXV) and in vaccinia strains (VACV). A GAAP human orthologue was

identified during the human genome project. Since the discovery, the hGAAP mRNA has been expressed ubiquitously in all human tissues and proposed to be a housekeeping protein. Both the vGAAP and the hGAAP localize within the Golgi apparatus and have resistance to a broad range of pro-apoptotic stimuli of both intrinsic and extrinsic stimuli. hGAAP regulates the Ca^{2+} content and fluxes from intercellular Ca^{2+} stores like the ER and Golgi. In addition to this, hGAAP also promotes cell adhesion and migration by activating the store operated Ca^{2+} entry (SOCE) from the extracellular space. vGAAP from VACV and CMLV were also shown to form cation-selective ion channels.

Bioinformatics analysis of hGAAP, vGAAP and BI-1 predicted that each protein has either six or seven Transmembrane domains (TMDs). The experimental validation for this prediction was performed by using antibody accessibility to specific protein tags. The results indicated with both the N and C terminals to be cytosolic thus being consistent with six TMDs topology. Further analysis showed that the seventh TMD might form as a re-entrant loop near the C-terminal.

A little was known about then TMBIM family as we do not have any structural representation of animal model for TMBIM protein, we use the bacterial homolog of TMBIM protein, *Bacillus subtilis*, known as the BsYetJ to understand some of the structural insights on the function of the proteins in the calcium channel (Chang et al., 2014; G. Guo et al., 2019). The BsYetJ also has a seven transmembrane helix fold and is characterized by a presence of a pore whose opening and closing is driven by pH. When there is a decrease of pH from pH 8 to pH 6, the di-aspartyl bond Asp 171 and Asp 195 present on the transmembrane helix 6 and 7 respectively, is broken with the Arg 60 and there is lateral shift in the movement in the transmembrane helix 2 resulting in the opening of the pore and Ca^{2+} flux across membranes. Thus, BsYetJ is characterized with a functional viroporin activity (**Figure 11**).

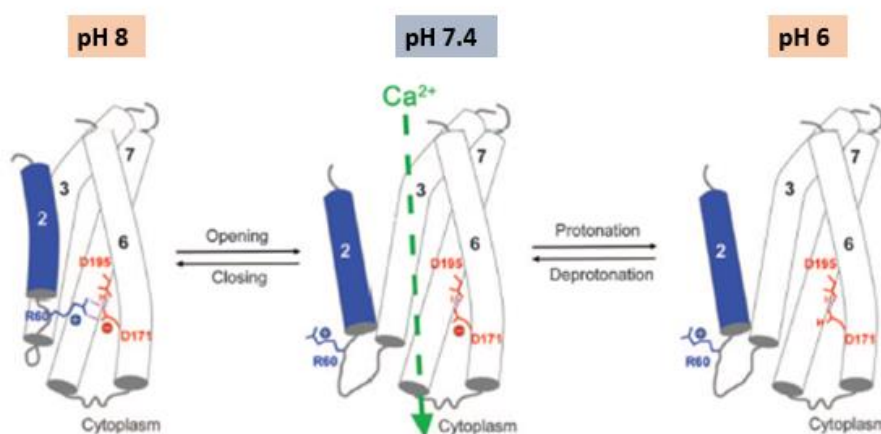


Figure 11: A model of BsYetJ showing a pH sensitive calcium leak. At higher pH 8, Asp 195 is protonated and Asp 171 is deprotonated. Asp 171 also forms a H-bonds with positively charged Arg 60 and the Arg 60 and Asp 171 latch closes the pore. Neutral pH 7, Asp 171 equilibrates between the protonated and deprotonated states. Calcium passage only occurs if Asp 171 is transiently deprotonated. At pH 6, there is a complete protonation of Asp 171 disfavoring calcium passage to pore neutralization (Chang et al., 2014).

1.6.4 Viroporins

Eukaryotic cells have evolved to have many ion channels, transporters, pumps to maintain and regulate the transmembrane ion gradients. Viruses have also similarly evolved to have ion channel proteins termed as the Viroporins (Hyser and Estes., 2015). Viroporins are small, hydrophobic integral membrane proteins that have a channel-forming activity (Scott and Griffin., 2015). The viroporins have an essential role in life cycles of RNA and DNA viruses; thus, making it a potential target for antiviral development. The viroporins disrupt the normal homeostasis of the ions to promote the viral replication and pathogenesis (Hyser and Estes., 2015).

The viroporins share some similarities which makes it easier for identification: A) viroporins are small integral membrane proteins of 100 amino acids or even lesser, B) Viroporins are generally hydrophobic and are predicted to be α -helical proteins that can oligomerize, C) Viroporins contain two motifs – an amphipathic α -helix that forms an aqueous channel and an adjacent cluster of positively charged residues (like the Arginine). These positively charged residue can hold the viroporin in the membrane by interacting with the negatively charged phosphate groups that are present in the lipids surrounding the membrane. These motifs are important as they form the pore through which the ions can cross the membrane (Fig 9). Mutation or deletion of these residues can stop the viroporin activity (Hyser and Estes., 2015).

The function of viroporins can be categorized into four groups, 1) virus entry, 2) virus morphogenesis and release, 3) modulation of apoptosis and 4) disruption in Ca^{2+} homeostasis (Hyser and Estes., 2015). Disruption of Ca^{2+} signaling can take place without involving the Ca^{2+} conducting viroporins. Since viroporins have important role in virus replication, these are ideal targets to use calcium blockers to use as antiviral candidate. The ubiquitous nature of Ca^{2+} signaling has led to the development of Ca^{2+} channel blockers that are used to treat neurological, cardiovascular, and autoimmune diseases. Repurposing these drugs offers less cost and a new area for drug development.

1.6.5 US12 gene family characterization

To date, due to the fact that very little information on expression, localization and function of US12 family members is available, several studies are being focused on the discovery of the features and roles of these protein in order to understand better how they fit in the modulation of the replicative cycle of Human Cytomegalovirus.

The existence of polyadenylation signals, to be found at each end of the US12 family locus, and the presence of supplementary shared polyadenylation signals inside the locus, implies that the US12 family locus constitutes an island which is transcriptionally isolated inside the US region, likely projected to ensure deeply coordinated expression of such genes (Lesniewski et al. 2006). Two transcripts were discovered to be expressed starting from the region encoding US18-US19-US20: an early tricistronic mRNA, 2.85 kb long together with a late 1.1 kb 3' co-terminal monocistronic mRNA that encodes US18. The expression of these three proteins was observed as early as only 18 hours after infection (Guo and Huang., 1993).

Recent studies proved that in correspondence of US18-US20 locus, at 5 hours post infection, there is one major transcript produced starting immediately upstream of US20, thus allowing the translation of US20. 24 hours post infection, another form of the transcript, shorter, is observed

just upstream US18, thus allowing its translation. A third novel transcript version, beginning within the coding sequence of US18, appears at 72 h.p.i., which results in the translation of a truncated US18 version (ORFS346C.1) (Stern-Ginossar et al., 2012).

Subsequently, another study analyzed the pattern of transcription of the gene region comprising genes from US12 to US17, finding a group of 3' coterminal, unspliced transcripts with different 5' transcriptional initiation sites during the late phases of HCMV clinical strain infection (Lu et al., 2016).

After conducting functional and localization studies about US12 family members, it was shown that these proteins are non-essential for the growth of the virus in cultured fibroblasts and their deletion had little impact on replication of the virus (Yu et al., 2003).

Other studies conducted on the effects of US12 family members deletion, in cells other than fibroblasts, such as human gingival tissues, reported the presence of growth defects, like the case of eight viral mutants, where the deletion at ORF of US18 was associated to an impairment in growth in oral tissues of humans (Hai et al., 2006).

Studies regarding the localization of US14, US17 and US18 gene products proved that the intracellular distribution of these proteins significantly changes during the course of viral infection: during the initial phases of the infection and preceding the development of viral assembly compartment (VAC), which is about 4 days post infection, US14 and US18 show a homogenous distribution all over the cytoplasm; in the late phase instead their localization coincides with markers of viral assembly compartment (VAC). In the cells where US14 associates with AC, it shows a strong colocalization with TGN and early endosomes.

For what concerns US17C, its main cytoplasmic colocalization was with TGN and early endosomes as well, also 54 hours post infection it was shown to transiently colocalize with GM130 (a marker for Golgi apparatus). Later was then shown a colocalization for US17C with a protein in the nucleus which is almost only associated with TGN (golgin-97).

US18 shows an early strong association (starting from 36 to 54 hours post infection) with GM130 while at later times its association with Golgi, TGN and early endosomes grows higher, ultimately strongly associating with the TGN at 144 hours post infection (Das and Pellett., 2007). The intracellular localization of US17 gene product has been deeply studied too: oppositely to pUS14 and pUS18, which are expressed in the cytoplasm only, pUS17 was found in high quantities in the cytoplasm as well as in the nucleus of infected cells.

Additional studies proved that this protein is expressed in a segmented way, with both its terminal domains being associated to the VAC: the N-terminal domain of the protein forms a ring-shaped structure at the periphery of cVAC while the C-terminal domain localizes in the inner zone of the compartment (Das and Pellett., 2007; Lesniewski et al., 2006). Further studies conducted on US17 showed how this protein has a fundamental role in the maturation of the virion: the generation of mutant viruses lacking US17 functional ORF led to an increased generation of non-infectious viral particles and to the delivery of increased amount of pp65 to newly infected cells, suggesting in this way a role for US17 in the modulation of host pathways to enable the production of virions, eliciting a balanced host immune response (Gurczynski et al., 2014). US17 was proven to have an important role in virion maturation and was deeply analyzed for the phenotype obtained as a result of viruses devoid of the functional ORF (Gurczynski et al., 2014). It was noticed that impairment of this gene expression resulted in an enhanced generation of noninfectious viral particles in producer

fibroblasts. These deficient virions, consecutively, deliver higher quantity of the tegument protein pp65, which has an immunomodulatory role, to newly infected cells, affecting in this way the modulation of not only the intrinsic but also the innate response of cells infected with the virus lacking US17 (Gurczynski et al., 2014). These data underline a role for US17 in the regulation of an adequate composition of the virus during its maturation (Gurczynski et al., 2014).

Concerning two other members of US12 family, namely US18 -US20, it was recently demonstrated how they can affect the expression of MICA, major histocompatibility complex class I (MHC-I) chain-related molecule, ligand of NKG2D induced by the infection (Fielding et al., 2014).

Another US12 family members, US20 protein product, was analyzed in its expression profile, leading to the discovery that the absence of this gene impacts significantly on HCMV ability of replicating successfully in endothelial cells, leading to the hypothesis of this protein having a significant involvement in virus dissemination, pathogenesis and the persistence in the host. US20 protein product, an early protein, localizes in the ER as confirmed by immunofluorescence studies in which an association with calreticulin-positive compartments was observable (Cavaletto et al., 2015). The membrane topology of this protein was predicted as well with several algorithms only to be confirmed with experimental investigation, showing that the N-terminus of this protein resides on the cytosolic side whereas the C-terminus locates on the luminal side (Cavaletto et al., 2015).

Concerning the remaining US12 family members, previously our laboratory demonstrated that pUS16 is characterized by a late expression kinetics and shows a colocalization with markers of the cVAC, including gB and pUL99 (Bronzini et al., 2012). The deletion of this gene from the BAC had no impact at all on the replication of the virus in fibroblasts, whereas US16 null viruses showed a growth impairment in microvascular endothelial cells as well as in retinal pigment epithelial cells. Furthermore, when the US16 ORF carries a mutation, the expression of IE, E and L viral protein is negatively impacted in infected endothelial cells, thus suggesting the presence of a defect in the replicative cycle attributable to an unsuccessful entry and/or post entry events (Bronzini et al., 2012). Our laboratory demonstrated how viral particles produced in fibroblasts previously infected with US16 devoid viruses are effective for the gH-gL-pUL128-pUL130- pUL131A complex, impacting in this way on the entry phase in endothelial and epithelial cells (Luganini et al., 2017).

Among the 10 genes of US12 family, US21 protein as a viroporin activity (Luganini et al., 2018). US21 protein has been observed to have few conserved features and it has a well diverged branch that separates it from the rest of the US12 genes of the family (Lesniewski et al., 2006). US21 gene can be a descendent from the TMBIM gene. US21 protein not only is a viral-encoded ion channel that regulates the Ca^{2+} homeostasis, but also protects the cells against apoptosis (Luganini et al., 2018). The deletion or inactivation of this protein had a severe impact on HCMV growth in endothelial and epithelial, which was observed to be reduced also in fibroblasts. The expression of US21 can reduce the Ca^{2+} content of the intracellular ER stores and consequently an increment in cell resistance to intrinsic apoptosis is noticed as a critical repercussion of modification of intracellular Ca^{2+} homeostasis (Luganini et al., 2018). On this regard, recently our laboratory demonstrated that pUS21 expression affects cytobiological consequences, such as cell adhesion and motility, that stem from perturbing intracellular Ca^{2+} homeostasis due to the presence of US21 in the cell (Luganini et al., 2022, submitted).

Except for the genes US14, US16, US17, US20 and US21, no study has been conducted on the other

genes of the US12 family, the kinetics of the expression of the proteins, the localization, or their role in the replicative cycle of the HCMV. This project will not only help in unveiling our understanding for the US12 protein and its expression but also help us to understand the function of US12 protein as a viroporin. Further this project also gives us inputs on the structure-based identification of molecules that can affect the viroporin activity for both pUS12 and pUS21.

Aim of the work

Aim of the work

The HCMV genome includes at least 165 canonical genes. Among them, the US12 gene family is composed of 10 tandemly arranged genes from US12 through US21. The US12 family genes are highly conserved with homologs identified only in CMV of higher primates like the Chimpanzee, Rhesus and *Cynomolgus* macaques (Lesniewski et al., 2006). The family likely originated from duplication events from an ancestor gene followed by divergence to generate 12 putative ORFs. The US12 genes are indeed conserved in clinical isolates and laboratory strains of HCMV (Murphy et al., 2008). This fact sustains that the US12 family genes may play important biological roles in HCMV biology. Studies on different US12 family genes also confirmed that they take part in different aspects of virus replication, modulating immune response, dissemination, and persistence of the virus within the host and regulating the infection in different cell types. US16 and US20 have been shown to affect HCMV replication in endothelial and epithelial cells (Bronzini et al., 2012; Cavaletto et al., 2015; Luganini et al., 2017); US18 and US20 have been observed to exert an immunoevasion function by reducing the expression of ligands for NK cells on the surface of HCMV-infected cells (Fielding et al., 2014; Charpak-Amikam et al., 2017). US17, on the other hand, seems to play a role in modulating innate and intrinsic immunity of infected cells.

The predicted US12 proteins show a common protein scaffold characterized by 7 hydrophobic trans-membrane segments and a low level of homology to the cellular TMBIM proteins. Like the cellular TMBIM proteins, recently, the US21 protein has been characterized to be endowed with as a Ca²⁺ channel function (Luganini et al., 2018). Further studies on pUS21 then showed its role in the protection of cells to apoptotic stimuli (Luganini et al., 2018) and in the regulation of cellular migration and adhesion (Luganini et al., 2022). Thus, these observations sustain pUS21 roles in contributing to the overall ability of HCMV to counteract apoptosis, and in facilitating the viral spread within the host. Together, these observations underline the importance of US12 family genes in HCMV pathogenesis.

Since to have a complete picture of the importance of the US12 family in the pathogenesis of HCMV, it is necessary to define the functions also of those family members not characterized so far, the aim of this work was to study the expression pattern and the function(s) of another member of the US12 family, the same US12 protein, and to investigate its feasibility as a new HCMV-specific druggable target to design and develop new anti-HCMV agents.

Chapter 2-Characterization of the expression of the US12 protein

2.1 Materials and Methods

2.1.1 Oligonucleotides

The complete list of oligonucleotides used for PCR amplification of the US12 ORFs are listed below in **table 1**. These were all purchased from Life technologies.

Table 1: *Oligonucleotides used for PCR sequencing*

Primer Name	Sequence 5'→3'
US12HA F	ACCACCCATCGTCCCCCTTCTC
US12HA R1	CTAAGCGTAGTCTGGGACGTCGTATGGGTATCCTCC TCCCTGAAAATACAGGTTTTCTCCTCTTATGAAAAAGCCAGTGCCGT
US12HA R2	GCGGGGGACAAAGGACAGTACGACAGATTAGGTGATAGAAACGTTTTTTCTAAGC GTAGTCTGGGACGTC
US12-NV5-F1	CGAGCACCCGTCATGGGTAAGCCAATCCCTAACCCGCTCTAGGTCTTGATTCTACG GTACAGATCCAGTTTCACCA
US12-NV5-F2	AAACTTGCCGGGTACCTAAAGCCCCGACGACTGTTTCGTCGACACCCGTCATGGGTA AG
US12F	TGCCGGGTACCTAAAGCCCCGACGACTGTTTCGTCGAGCACCCGTCGAAGTTCCTATA CTTTCTAGAGAATAGGAAGTTCCTGTTGACAATTAATCATCG
US12R	GGGACAAAGGACAGTACGACAGATTAGGTGATAGAAACGTTTTTTGAAGTTCCTA TTCTCTAGAAAGTATAGGAAGTTCCTCAGCAAAAGTTCGATTA

2.1.2 Bioinformatics

Sequence alignments were performed using TM-Coffee server. ExPaSy tool compute pI/Mw was used to calculate the predicted molecular weight of pUS12HA. The GenBank™ (<https://www.ncbi.nlm.nih.gov/genbank/>) accession numbers for the proteins analyzed by the bioinformatic tools were the following: TR BAC5 US12, US21 (AC146906.1) *H.sapiens* TMBIM6/BI-1 (NP_003208.2), *H.sapiens* TMBIM4/hGAAP (NP_001269535.1), CMLV TMBIM4/vGAAP (AAG37461.1), *Bacillus subtilis* YetJ (O31539).

To perform the different alignments of the sequences, the server used were Phyre2 (<http://www.sbg.bio.ic.ac.uk/phyre2/html/page.cgi?id=index>), TopPred 1.10 (<https://mybiosoftware.com/tag/topology>), TMHMM 2.0 (<https://services.healthtech.dtu.dk/service.php?TMHMM-2.0>), TMCoffee (<https://tcoffee.crg.eu/>) and MEMSAT_SVM (<http://bioinf.cs.ucl.ac.uk/psipred/>).

2.1.3 Cells and culture conditions

Low-passages human foreskin fibroblasts (HFFs) and human embryo lung fibroblasts (HELFs – passage 5-11) were grown as a monolayer in Dulbecco Modified Eagle's Medium (DMEM) (Euroclone), supplemented with 10% Fetal Bovine Serum (FBS) (Euroclone), 2 mM glutamine, 1 mM sodium pyruvate, 100 U/ ml penicillin and 100 µg/ ml streptomycin sulphate.

2.1.4 BAC recombineering

The HCMV TR BAC was used to generate US12-mutant viruses. The TR strain was derived from an ocular specimen (Smith et al., 1998), and after few passages in fibroblasts, a Bacterial Artificial Chromosome (BAC) was generated by substituting the US2-US5 region of the TR strain with the BAC plasmid (Murphy et al., 2003).

To obtain the desired mutations of the US12 gene of interest, TR recombinant viruses carrying mutations in the US12 or US21 ORFs were generated with a two-step's replacement strategy using the BAC recombineering methods as described (Warming., 2005) and as applied by Luganini et al., 2018.

To generate the TRΔUS12 BAC (**Figure 12**), the galK-kan ORF was amplified from pgalk-kan (Warming., 2005) by PCR using the primer sets, US12F and US12R. The 3' end of the forward and reverse primers are specific to sequence that amplify the galK-kan cassette and 50 bps at their 5' end tail are homologous to the sequences flanking the different US12 gene (primer F homology arm from 6536 to 6581 bp, primer R homology arm from 5645 to 5690 bp) (**Table 1**).

Following the PCR, 2378 bp galK-kan cassette was digested with DpnI to remove any plasmid (Warming 2005) template and fractionated by agarose gel electrophoresis. The band of 2378 bp was then purified with Nucleospin extraction II kit (Macherey-Nagel) and quantified.

To generate the TRΔUS12 BAC derivative (**Figure 12**), 100 ng of the galK-kan cassette was electroporated in *E. coli* SW102 cells containing the TR BAC. Since *E. coli* SW102 express γ -red encoded recombination protein (exo, bet, gamma) upon temperature shifting, bacteria were grown at 32° C and then incubated at 42° C for 15 minutes before electroporation to induce the expression of recombination machinery. After electroporation, cells are recovered for 1 h at 32° C and then plated on LB agar plates containing 15 µg/ml Chloramphenicol (Caf) and 25 µg/ ml kanamycin (Kan) for 24-48 h.

The colonies that appeared on the plates were re-streaked on MacConkey agar plates containing 0.2% galactose and 15 µg/ ml Caf. Several single Gal-positive TRΔUS12 clones that produced bright red colour colonies were further characterized for US12 replacement by PCR. Recombinant TRΔUS12 BAC was then purified from SW102 cells with NucleoBond Xtra BAC (Macherey-Nagel) according to the manufacturer instructions.

To generate TRUS12HA BAC and TRUS12NV5-CHA BAC, (**Figure 12**), the galactokinase-kanamycin (galK-kan) cassette in TRΔUS12 BAC was replaced with the appropriate US12 ORF-modified cassette (generated with the primer sets shown in **table 1**).

For the TRUS12HA BAC, the US12HA cassette was amplified by PCR from TR BAC using the US12HA primer set in a two-step PCR. In the first step (primers US12HA F and US12HA R1, (Table 1) the HA

epitope, inserted in the reverse primer sequence was added at C-terminal end of US12 ORF. In the second step (primers US12HA F and US12HA R2, **table 1**) the 3' homology arm used in the first selection step was added to the 3' end of the US12HA sequence.

The resulting TRUS12HA BAC was then used to generate the TRUS12 NV5-CHA BAC and the TRUS12HA stop BAC. The corresponding US12 ORF-modified gene cassettes were thus amplified by using US12 NV5-CHA primer sets and the US12HA stop primer sets (**table 1**). For the generation of the US12 NV5-CHA cassette, in the first step using the primers US21NV5 F1 and US12HA R2 (**table 1**), the V5 epitope was added at the N-terminal of the US12 ORF between the first and the second codon. In the second step, with the primers US21NV5 F2 and US12HA R2 (**table 1**), the 5' homology arm used in the first selection step was added to the 5' end of US12HA NV5 segment. The US12HA R2 primer was used as a reverse primer to maintain the HA epitope at the 3' end of the US12 ORF.

Following PCR, the US12HA and US12HA NV5-CHA were gel purified and extracted using NucleoSpin Extract II kit (Macherey-Nagel). 200 ng of the cassettes were electroporated into SW102 cells harbouring TRΔUS12 BAC clone. Bacteria were then plated on M63 plates containing 0.2% 2-deoxygalactose (DOG), 15 µg/ml of Caf and glycerol as their sole carbon source. Gal-negative colonies were further selected by their inability to grow in the presence of Kan by streaking them both on LB+ Caf 15 µg/ml and LB +Caf 15 µg/ml + Kan 25 µg/ml plates. They were screened for the replacement of galK/kan with the modified versions of US12 ORF by PCR screening and sequencing. Two independent TRUS12HA and TRUS12NV5-CHA clones were selected and characterized to ensure that their phenotypes did not result from an off-target mutation.

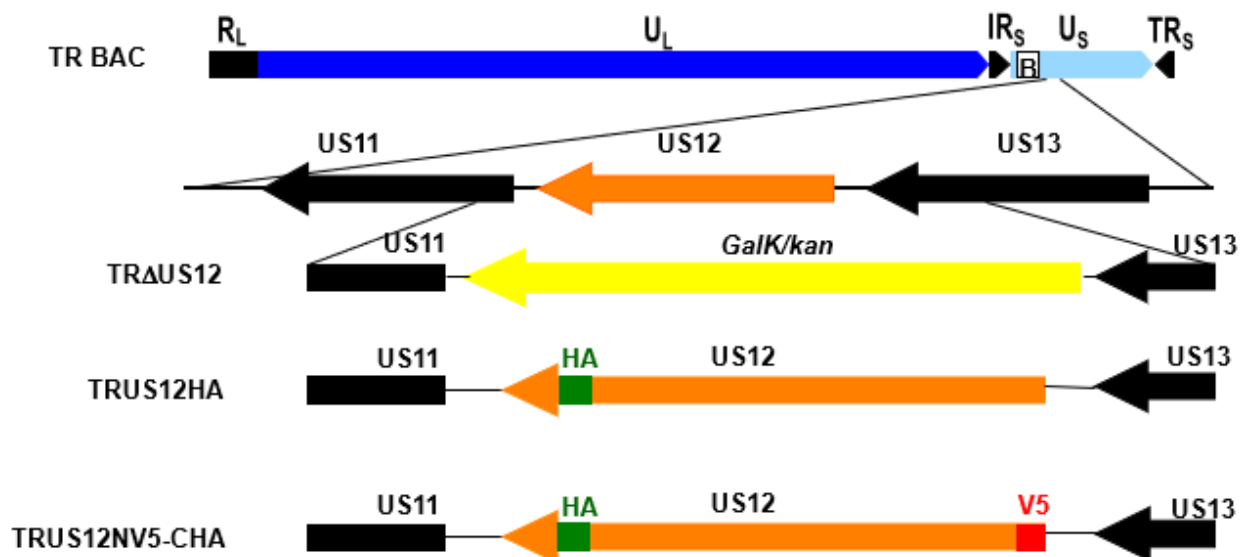


Figure 12. Schematic representation of the HCMV US12 gene region and the modification of the US12 ORF introduced in different BACs. In TRΔUS12, the US12 ORF was replaced by GalK/Kan. TRUS12HA, a HA tag was added at the C-terminal end of the US12 ORF. A double tagged BAC TRUS12NV5 CHA was generated with a HA tag at the C-terminal end and a V5 tag at the N-terminal end of the ORF.

2.1.5 Recombinant viruses' preparation

Infectious recombinant HCMV viruses TRUS12HA and TRUS12NV5-CHA were reconstituted in HELFs by co-transfection of the correspondent recombinant BAC and a plasmid expressing HCMV pp71 (a gift from T. Shenk) using SuperFect transfection reagent (Qiagen), according to the manufacturer instructions. Transfected HELFs were then cultured until a marked cytopathic effect were observed. Viral stocks were then prepared by infecting HFF cells at a virus-to-cell ratio of 0.01. Cells were supplemented with 5% heat inactivated FBS and cultured until a marked cytopathic effect was observed. Recombinant HCMV viruses were titrated by an indirect immunoperoxidase staining procedure on HFF cells using an anti-IEA (IE1 plus IE2) (clone E13, Argene Biosoft Mab) as previously described (Cavaletto et al., 2015; Luginini et al., 2017).

2.1.6 Immunofluorescence

Two distinct protocols were followed for the immunofluorescence (IF) experiments which were aimed at investigating both the intracellular localization of pUS12 protein, and the topology of the US12 protein. The topology was determined by the orientation of the US12 protein C- terminal and the N-terminal ends at either the luminal or the cytoplasmic side of internal membranes (Cavaletto et al., 2015).

In the first IF protocol, to determine the intracellular localization of US12 protein by IF, HFF cells were seeded onto coverslips in a 24-well multi-dishes and grown in DMEM supplemented with 10% FBS. The infection of the cells with TRUS12HA was performed at an MOI of 1 pfu/cell for 2 hours at 37° C. Following the adsorption step, the viral inoculum was removed, and cells were cultured in DMEM + 10% FBS. At different time points post infection (p.i.), cells were then fixed with 1% paraformaldehyde (PAF) for 15 minutes at room temperature. In the next phase, samples were quenched from autofluorescence by incubating them in 50 mM ammonium chloride for 15 minutes at room temperature. The cells were then washed with PBS 1X three times, and then permeabilized with 0.2% Triton X-100 in blocking buffer for 15 minutes in oscillation at room temperature. The blocking buffer contained 10% HCMV negative human serum+ 5% glycine in PBS 1X. Both the primary and the secondary antibodies for IF were added to the permeabilized cells after the blocking and incubated for 2 hours and 1 hour at 37° C, respectively.

To investigate whether pUS12 localizes in the Endoplasmic reticulum (ER), HFF cells were infected with TRUS12HA with an MOI 1. At 48 h p.i., the cells were stained with 1:2000 diluted ER tracker (Life technologies, E34250) (ER tracker diluted in prewarmed HBSS [H8264]) for 15 minutes at 37° C, washed three times with HBSS, and then fixed with 1% PAF for 10 minutes at room temperature. In the second IF protocol to determine the topology of the US12 protein, HFF cells were seeded on the coverslips and the following day were infected with TRUS12 NV5-CHA virus at MOI – 1 for 2 hours at 37° C. At 48 hours and 120 hours p.i., the cells were washed with cold KHM buffer, which is a combination of Potassium acetate 110 mM, HEPES pH 7 20 mM, MgCl₂ 2 mM in PBS 1X. The cells were then fixed or not with 1% paraformaldehyde for 15 minutes at 4° C. All the coverslips were then washed with KHM buffer and non-fixed coverslips were selectively permeabilized with 12 µM digitonin (Sigma) in KHM buffer for 4° C on ice. While the remaining fixed cells where either

permeabilized with 0.1% triton X-100 or not permeabilized at all. Blocking and addition of primary antibody were according to the procedure described by Cavaletto et al., 2015). In the end, the coverslips permeabilized with digitonin were fixed with 1% PAF for 15 minutes at 4° C and secondary antibody is added to all the coverslips for 1 hour at 37° C.

The primary antibodies that were employed for IF experiments were: the rat mAb anti-HA (Roche, 11867423001), the mouse mAb anti-GM130 (Millipore, 04581), the mouse mAb anti-EEA1 (Biosciences, BD610457), the mouse mAb anti-CD63 (Santa Cruz, SC_5275), the mouse mAb anti-gB (Virusys, P1201), and the mouse mAb anti-gH (Santa Cruz, SC_58113). The binding of the primary antibodies was detected by the addition of the secondary antibodies Alexa Fluor488-conjugated goat anti-rat IgG antibody (ThermoFisher A11006), or the Alexa Fluor 594-conjugated anti-mouse IgG antibody (Sigma, SAB4600121). Confocal laser microscopy was performed with a Leica TCS SP8 confocal system (Leica Microsystems) equipped with a HCX PL APO 63x/1.4 NA oil immersion objective. Images were analysed using the ImageJ software.

2.1.7 Immunoblotting

HFF cells were infected with TRUS12 NV5-CHA at an MOI of 2 PFU/cell and at 12, 24, 48, 72, 96 indicated times p.i., whole-cell protein extracts were prepared by resuspending pelleted cells in Laemmli sample buffer (50mM Tris-Cl, pH 6.8, 100mM dithiothreitol [DTT], 2% SDS, 10% glycerol, 1 protease inhibitor cocktail (Sigma P8340)). After boiling at 95°C for 5 min, soluble proteins were collected by centrifugation at 15,000 g for 10 min. Supernatants were analyzed for protein concentrations with a Bio-Rad Dc protein assay kit (Bio-Rad Laboratories) and stored at 80°C.

Proteins were then separated by 15% SDS-polyacrylamide gel electrophoresis (50 µg of protein per lane) and then transferred to TransBlot Turbo mini-size PVDF membranes (BioRad). The filters were blocked in a solution of 5% nonfat dry milk, 10mM Tris-Cl (pH 7.5), 100mM NaCl, and 0.1% Tween 20.

Immunostaining of HCMV proteins was carried out with the following antibodies: mouse MAbs against IEA (IE1 plus IE2) (clone E13, Argene Biosoft); UL44 (clone CH16, Virusys); UL99 (pp28) (clone CH19, Virusys); and the rat anti-HA mAb conjugated to horseradish peroxidase (clone 3F10, Roche). Immunodetection of tubulin with a mouse mAb (clone TUB 2.1, Sigma) was used as a control for cellular protein loading. Immunocomplexes were detected with goat anti-mouse immunoglobulin antibodies conjugated to horseradish peroxidase (Life Technologies) and visualized by enhanced chemiluminescence (Western blotting Luminol reagent; Santa Cruz).

2.2 Results

2.2.1 The US12 gene encodes a 28 kDa protein expressed with an Early kinetics

Due to the lack of anti-US12 antibodies, first we generated a recombinant HCMV containing a modified US12 ORF with a double tag: a HA tag was added at the C-terminal and a V5 tag was added at N-terminal end of the protein. This TR derivative was called TRUS12NV5-CHA (**Figure 12**).

With the availability of TRUS12NV5-CHA recombinant virus, the expression kinetics of the putative US12 protein was assessed via immunoblotting analysis of whole-cell protein extracts prepared at different times post infection (p.i.) from the HFF cells infected with the TRUS12NV5-CHA. A mouse mAb against the V5 epitope was used for the detection of the US12NV5-CHA protein.

As shown in **Figure 13**, a single band of about 28 kDa was detected by the V5 mAb. The MW of the detected protein is consistent with the theoretical molecular weight of pUS12 (33.6 kDa) computed by ExPasy. The expression of pUS12 was not detected at 12 h p.i. as for the Immediate-Early proteins (IEA), and observed starting from 24 h p.i. even if barely detectable, and then it gradually increased as the HCMV infection progressed into 48, 72 and 96 h p.i.. In addition to this, pUS12 expression was still observed in infected HFFs when treated with foscarnet (PFA), an anti-HCMV drug that inhibits viral DNA replication. We could observe that, although the expression of pUS12HA is slightly decreased by PFA, it is not completely abolished as for the UL99 (a true Late HCMV protein). To the contrary, the expression pattern of pUS12 in the presence of PFA was more similar to that of UL44 (an Early protein). This observation thus suggested that pUS12 was expressed as an Early kinetics.

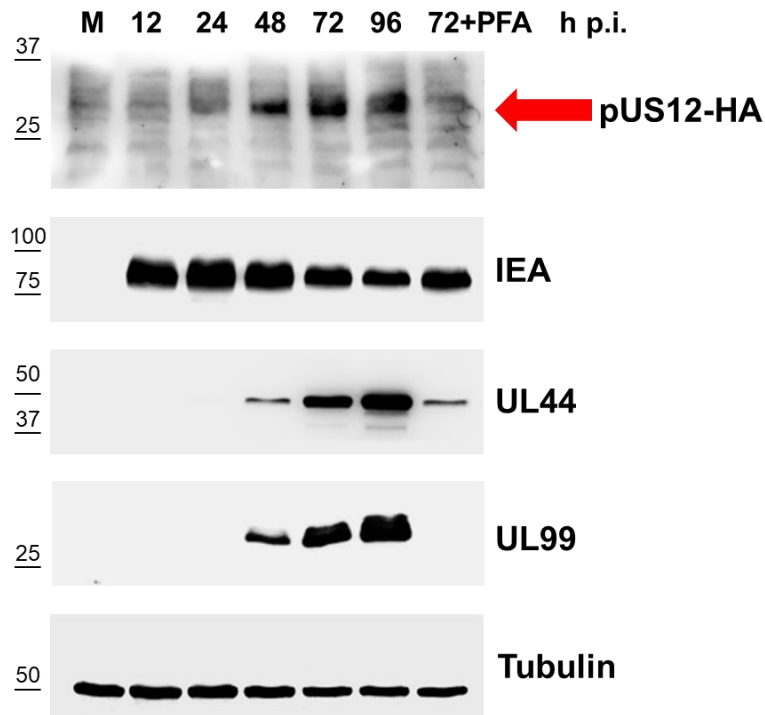


Figure 13. The expression kinetics of pUS12 during HCMV infection. HFFs were infected with TRUS12NV5-CHA at an MOI of 2 PFU/cell. Whole cell protein extracts were prepared at the indicated time points p.i. Then 50 μ g/lane of proteins were fractionated through a 15% SDS-PAGE and analysed by immunoblotting with anti-V5, anti-IEA, anti-UL44, anti-UL99 mAbs. The immunodetection of tubulin was performed as an internal control. Cell extracts were from mock infected HFFs cells (M), and HFFs infected for 12, 24, 48, 72 and 96 h p.i., and cells infected- and treated with PFA (200 μ g/ml) for 72 h p.i.

2.2.2 pUS12 shows a time-dependent accumulation in the cytoplasm of HCMV--infected cells

The localization of pUS12HA in HFF cells infected by another recombinant HCMV, the TRUS12HA in which the US12 ORF was modified by the addition of HA tag at the C-terminal (**Figure 12**), was then analysed by immunofluorescence at different time points using an α -HA mAb.

The expression of pUS12HA was detectable starting from 24 h p.i., (**Figure 14**). The intracellular localization of pUS12HA showed a diffuse pattern throughout the cytoplasm until 48 h p.i., As the infection progressed to 72 h p.i., the pUS12HA started to accumulate mainly in a characteristic perinuclear ring-shaped structure which became clearly obvious at 96 h p.i., At 120 h p.i., the HA staining revealed an almost complete accumulation of pUS12 within these perinuclear ring-shaped structures.

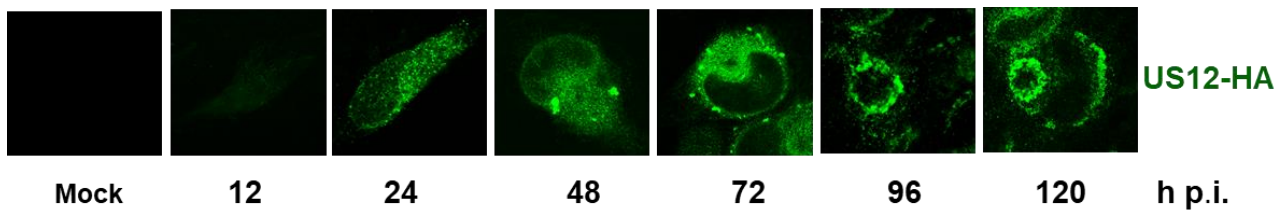


Figure 14. Cytoplasmic localization of US12HA protein in HFF cell line. *HFFs were infected with TRUS12HA at an MOI of 1 PFU/cell. At different time points p.i., cells were fixed and then and immune-stained with an anti-HA mAb.*

2.2.3 Localization of pUS12HA within Golgi-derived structures

Since the US12 protein was observed to accumulate in ring-shaped structures at late stages of HCMV infection (**Figure 14**), and this ring-shape structure resembles the appearance of Golgi-derived membranes in HCMV infected cells (Das and Pellett 2007., 2011), we investigated whether pUS12 associated with the Golgi apparatus in HCMV-infected cells. To this end, IF experiments were performed in HFF cells infected with TRUS12HA to localize the pUS12HA and the GM130, a cis-medial Golgi protein marker (Luganini et al., 2017).

As depicted in **Figure 15**, at 12 h p.i., the GM130 marker showed a typical diffuse pattern like that observed in mock-infected cells (**Figure 15**). However, starting from 24 h p.i., the GM130 marker started to accumulate in structures located in the perinuclear region that later showed the characteristic ring-shape appearance. The ring-shape pattern of GM130 was clearly visible from 72 h p.i., This ring like-shape aspect of cis-medial Golgi is the result of the HCMV-induced remodelling of GM130-containing Golgi stacks within the cytoplasm of infected cells and corresponds to the peripheral cylinder structure of the cVAC (Das and Pellett 2007., 2011b). As for US12HA, it accumulated mainly in ring like-shape structures at late times of infection that were stained also by the GM130 mAb, (**Figure 15**), thus indicating a co-localization of pUS12HA and GM130-containing membranes in HCMV-infected cells. This results points towards a localization of pUS12 into Golgi-derived vesicles at late times of the HCMV replication cycle. However, we did not observe the accumulation of pUS12HA within ER-derived vesicles (**Figure 16**).

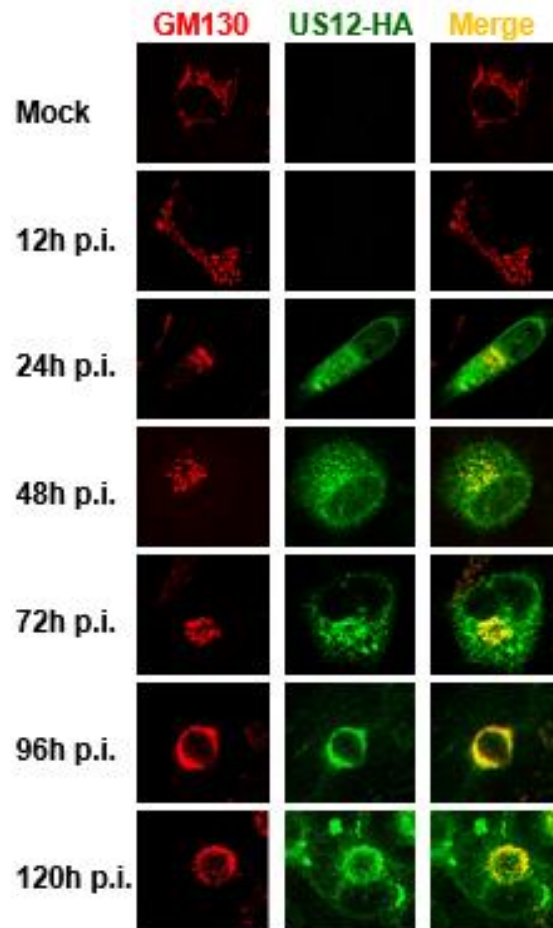


Figure 15. Localization of pUS12 within Golgi-derived vesicles in infected HFF cells. *HFF cells were infected with TRUS12HA at an MOI of 1PFU/cell. Infected cells were then fixed at different time points p.i. and then subjected to IF staining with both anti-HA (for the US12HA protein, green) and anti-GM130 mAbs (cis-Golgi marker, red).*

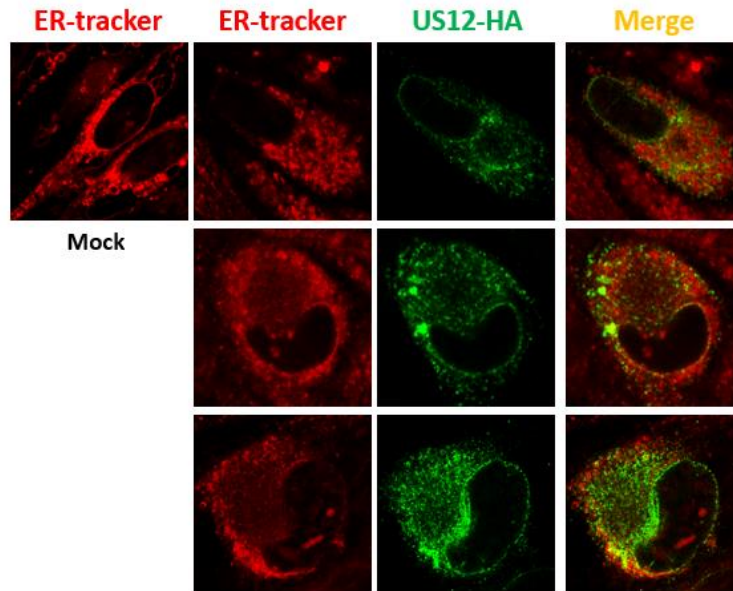


Figure 16. pUS12 does not accumulate within ER in HCMV-infected HFF cells. *HFFs were infected with TRUS12HA at an MOI of 1PFU/cell. At 48 h p.i., infected cells were stained with the ER tracker (red). IF staining was performed with anti-HA mAb (for US12HA protein, green).*

2.2.4 Localization of pUS12 within the cVAC of HCMV-infected cells

During HCMV replication, a specialized compartment called the Virion Assembly Complex (cVAC) (Figure 17) is formed in the late stages of infection within the cytoplasm of infected cells. This structure results from modifications and rearrangements of host cytoplasmic organelles, such as the Golgi apparatus, Trans-Golgi network, and various endosomal vesicles. In the cVAC, HCMV virions undergo maturation by acquiring the final tegument layer and the final envelopment before egressing from infected cell (Das and Pellett 2007., 2011b; Tandon et al., 2012).

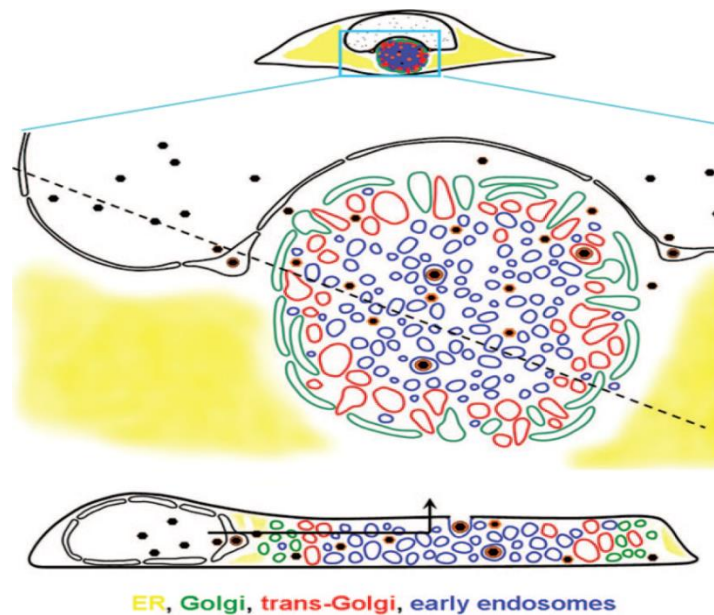


Figure 17. The cytoplasmic Virion Assembly Complex (cVAC). *The cVAC is a specialized compartment observed in the HCMV-infected cells during the later stages of infection (Das and Pellet., 2011).*

Several US12 family members have been observed to co-localize within the cVAC, such as the US14, US16, US17 and US18 proteins (Das and Pellett 2007; Luganini et al., 2017). Since we observed the localization of pUS12 within Golgi-derived vesicles (**Figure 15**), next we wanted to verify whether pUS12 localizes within the cVAC in HCMV-infected cells.

To this end, we investigated the co-localization of pUS12HA with markers of three different cytoplasmic organelles that are known to be reorganized by HCMV infection in the cVAC. The markers were: GM130, a cis-medial Golgi marker; EEA1 as an early endosomal marker; and CD63 as a late endosomal marker. These three cellular markers localizes within the cVAC in the periphery and in the centre, respectively (Das and Pellett 2007., 2011b) (**Figure 18**). As shown in **Figure 18**, at 120 h p.i., when the cVAC is completely formed in TRUS12HA-infected HFF cells, the pUS12HA showed, as expected, the characteristic ring-shaped structure that overlapped with the GM130 staining pattern, thus indicating the accumulation of pUS12 in the periphery of cVAC. Moreover, pUS12HA partially overlapped with the cellular EEA1 and CD63 markers, and with the HCMV glycoprotein gB used as a viral marker (**Figure 18**). Since these endosomal and viral markers are known to localize within the centre of cVAC (Tandon et al., 2012; Sanchez et al., 2000), the observed staining pattern of pUS12HA (**Figure 18**) sustains its localization in the periphery of cVAC within Golgi-derived membranes at late stages of HCMV infection.

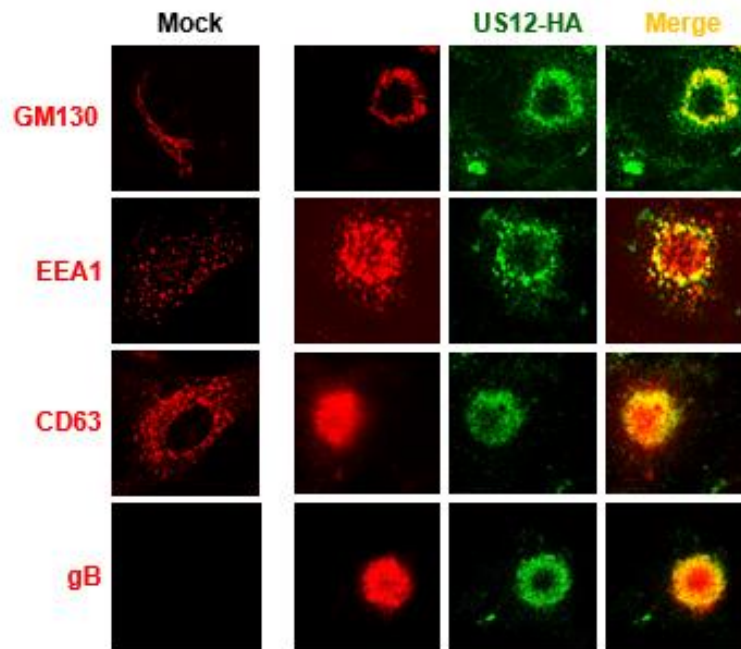


Figure 18. pUS12HA localizes within the cVAC of HCMV-infected cells. HFFs were infected with TRUS12HA at an MOI 1 PFU/cell. Cells were fixed at 120 h p.i., and immunostained for pUS12HA (stained in green), and for cellular markers, such as GM130 (a cis-Golgi marker, red), or EEA1 (an early endosomal marker, red), or CD63 (a late endosomal marker, red), or for gB (the HCMV glycoprotein B, red) that accumulate within the cVAC.

2.2.5 pUS12 is a 7 TMD protein with a cytoplasmic N-terminus and luminal C-terminus

To predict the membrane topology of pUS12, four different membrane topology prediction algorithms: Phyre 2 (Kelley et al., 2015), TopPred 1.10 (Claros and Heijne., 1994), MEMSAT_SVM (Nugent and Jones 2009) and TMHMM 2.0 (Krogh et al. 2001) were employed. All the algorithms predicted a 7 transmembrane domain (TMDs) architecture of pUS12, with a cytoplasmic N-terminus and a predicted C terminus located on the luminal side of an internal membrane (**Table 2**).

Table 2: Bioinformatics predictions of pUS12 membrane topology. pUS12 ORF sequence was used to predict the hydrophobic regions of the protein and its orientation using four different algorithms.

Software	n° TM	N terminal	C terminal
Phyre2	7	Cytosol	Lumen
TopPred 1.10	7	Cytosol	Lumen
MEMSAT SVM	7	Cytosol	Lumen
TMHMM	7	Cytosol	Lumen

To experimentally confirm this prediction, we used the TR derivative, TRUS12NV5-CHA. Thus, an immunofluorescence epitope accessibility assay following selective permeabilization (Carrara et al., 2012) was performed to determine whether the N- and C-terminal epitopes of pUS12NV5-CHA

were cytosolic or luminal, To this end, HFFs infected with TRUS12HA NV5 for 120 h were permeabilized either with 12.5 μ M digitonin for 4 min, to permeabilize the plasma membrane only (while leaving internal membranes, such as the Golgi apparatus and the ER, intact), or with 0.1% Triton X-100 for 5 min, which allowed complete permeabilization and allowed antibodies to access epitope tags regardless of their orientation on the membrane (Carrara et al., 2012). Viral protein markers, such as the luminal glycoproteins gB and gH, and the cytoplasmic tegument pp65 protein were used to validate the selective permeabilization assay (**Figure 19**). Following the treatment with digitonin, pp65, but not gB and gH, was immune-stained (**Figure 19**), thus validating these experimental conditions for the detection of membrane-associated epitopes with a cytosolic or luminal orientation.

Then, the orientation of both the N and C termini of pUS12 was determined by immunostaining HFFs infected with TRUS120NV5-CHA with anti- V5 and anti-HA mAbs. Both digitonin treatment and Triton X-100 treatment allowed the anti-V5 mAb to access the N terminus of pUS12, with positive immunostaining results seen at both 48 and 120 h p.i. (**Figure 20**). These results thus confirmed the cytosolic location of the N terminus of pUS12 as predicted by bioinformatics (**Table 2**). In contrast, only complete cell permeabilization by Triton X-100 allowed immunostaining of the C-terminal HA tag of pUS12 (**Figure 20**), thus demonstrating that the C terminus of the protein was located within the lumen of a Golgi-derived vesicle, and thus confirming the predicted 7TMD topology of pUS12.

Taken together, the results shown in this section indicate that the HCMV US12 gene encodes a 7TMD protein (**Figure 21**) that accumulates late in infection within cytoplasmic structures derived from the Golgi compartment and localized within the cVAC of HCMV-infected cells.

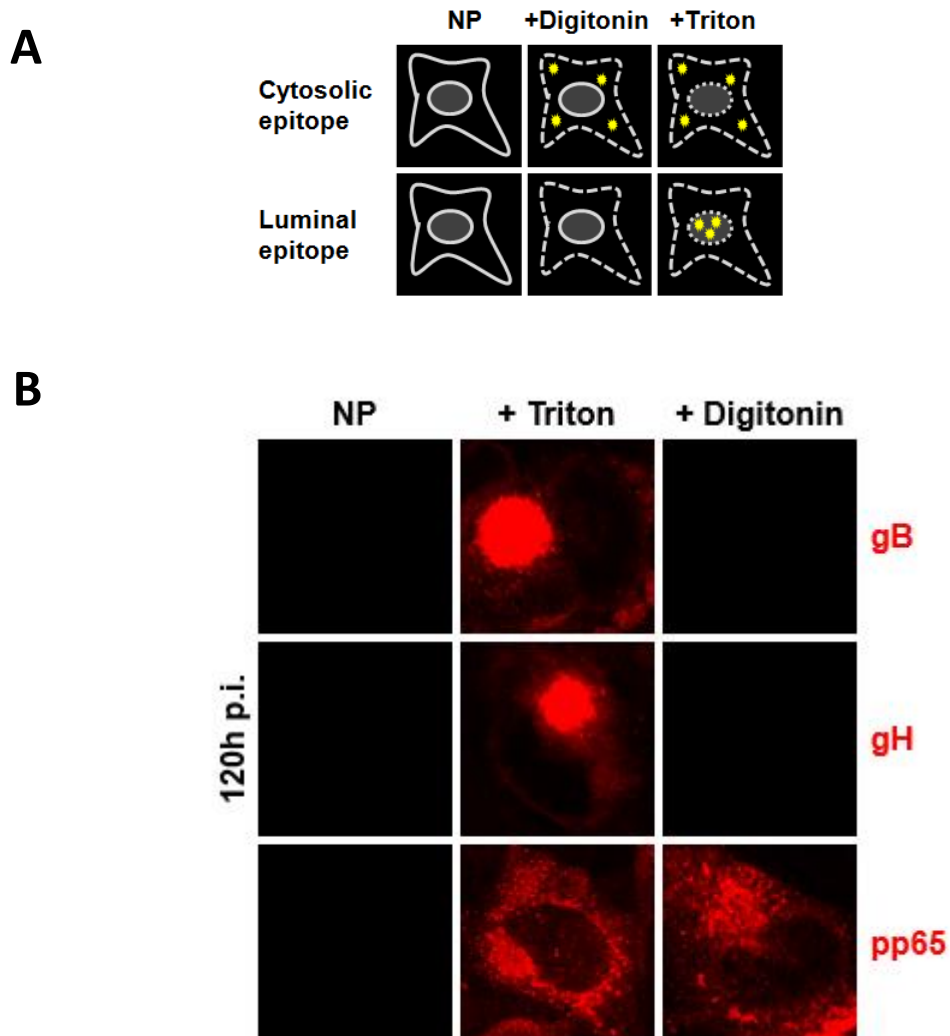


Figure 19. Validation of the immunofluorescence epitope accessibility assay. **A)** Scheme of the epitope accessibility assay that depicts how the selective permeabilization with Digitonin (+Digitonin) or Triton X-100 (+Triton) allow cytosolic or luminal epitopes with different orientation to interact with respective antibodies (Carrara et al., 2012) **B)** Validation of the selective permeabilization assay through viral markers with known orientation. HFFs were infected with TRUS12NV5-CHA at an MOI 1 PFU/cell, and at 120 h p.i., cells were fixed with 1% PAF and were or not permeabilized (NP), or selectively permeabilized with Digitonin (+Digitonin) or completely permeabilized with Triton X-100 (+Triton). Cells were then stained with gB, gH (luminal markers) and pp65 (cytoplasmic marker) mAbs. The images are representative of three independent experiments.

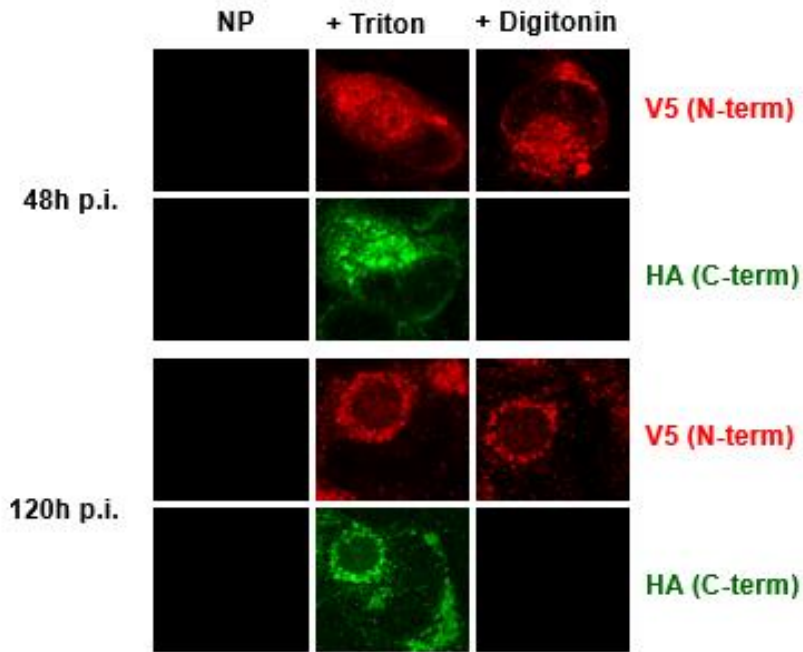


Figure 20. Membrane topology of pUS12. HFFs were infected with TRUS12NV5-CHA at an MOI 1 PFU/cell. At 48 and 120 h p.i., cells were fixed with 1% PAF and not permeabilized (NP), or selectively permeabilized with Digitonin (+Digitonin) or completely permeabilized with Triton X-100 (+Triton). The N-terminus and C-terminus of pUS12NV5-CHA were then immune-stained with anti-V5 and anti-HA mAb, respectively. Images shown are representative from three different experiments.

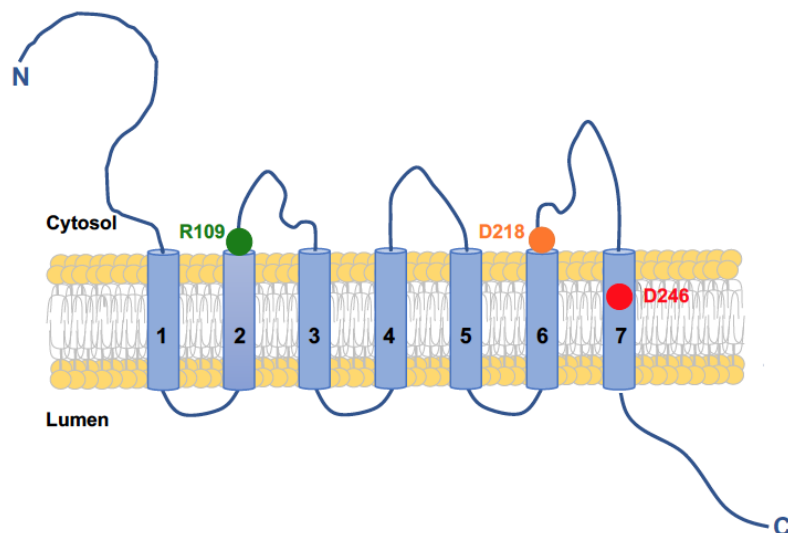


Figure 21. Schematic representation of the 7TMD architecture of the US12 protein. The illustration depicts the membrane topology of pUS12 with a cytosolic localization of the N-terminus and luminal localization of the C-terminus as demonstrated by immunofluorescence epitope accessibility assay.

2.3 Discussion

In this chapter of the thesis work, we have characterized the pattern of protein expression, the intracellular localization, and the membrane topology of the US12 gene product. These investigations were aimed at characterizing the fundamental US12 protein features and pave way for a subsequent functional characterization.

First, we characterized the pattern of US12 protein expression. pUS12 showed an apparent molecular weight of 28 kDa in SDS-PAGE (**Figure 13**). Theoretically, the US12 ORF may produce a polypeptide of a molecular weight of 33.6 kDa as computed by ExPasy; thus, the observed MW of 28 kDa is enough in agreement with the expected molecular mass of the protein. The US12 protein was slightly detectable already at 24 h p.i., and then increased up to 96 h p.i. (**Figure 13**). Its accumulation was partially reduced, albeit not completely prevented, by the treatment with Foscarnet (PFA) which is an anti-HCMV drug that inhibits the viral DNA synthesis and consequently, the transcription of viral Late genes. We could observe that although the expression of pUS12HA was decreased by it, is not completely abolished as in the case of UL99 (true Late protein) (**Figure 13**). Thus, we could suggest that the US12 gene is expressed with an Early gene kinetics.

The US12 ORF sequence contains a dileucine motif DXXLL sequence (DGDLL, amino acid position 233-237). The dileucine motifs of the sequence 'DXXLL' type have been found to be critical in the transport of the cellular TMEM192 protein to late endosome/lysosomes. TMEM192 or Transmembrane protein 192 is a constituent of late endosomal/lysosomal membranes (Behnke et al., 2011). Similarly, the packaging of mannose-6 phosphate receptors (MPR) hydrolase complex into clathrin-coated endosomal transport is dependent on the DXXLL signal (Braulke et al., 2009). The aspartate residue located three positions to the left to the first leucine is also critical for the signaling. Because of these requirements, these amino acid motifs are also called as minimal motif, DXXLL (where, X can be any amino acid) (Braulke et al., 2009). The occurrence of this amino acid motif within the US12 ORF may impact on its stability by facilitating its export in late endosomal/lysosomal vesicles and its degradation. This may be the reason for the low content of US12HA as detected by immunoblotting analysis.

To the contrary, a clear pUS12HA expression pattern was detected at the cellular level by immunofluorescence assays. In fact, analysis of the immunofluorescence staining pattern of pUS12 produced by TRUS12HA infection of HFFs, revealed further insights on the expression kinetics of pUS12 which was consistent with the immunoblotting results (**Figure 14**). Indeed, at 12 h p.i., pUS12HA immunostaining was not observed. pUS12HA expression began to be detected at 24 h p.i., which confirmed the US12 protein being an Early protein, like pUS20 which also showed a similar profile (Cavaletto et al., 2015). Other US12 family members like US14, US16, US17, US18 and US21 are all characterized by a Late gene expression kinetics (Bronzini et al., 2012; Lesniewski et al., 2006; Das and Pellett., 2007; Luganini et al., 2018).

The Eukaryotic linear motif website (The eukaryotic Linear Motif resource: 2022 release) (PMID:34718738) then predicted the localization of pUS12 within the Golgi-derived membranes due to the presence in the ORFs of RRVTV (positions 31-35), RRRL (positions 109-112) and LLYMD

(positions 242-246) amino acid sequences. Indeed, we observed that pUS12HA accumulated in a ring-like structure that overlapped completely with GM130, a cellular marker of Golgi apparatus. Thus, it was concluded that pUS12 localizes within vesicles derived from the cis-medial Golgi compartment. Furthermore, pUS12 was observed to co-localize with cellular and viral markers of cVAC, thus suggesting that it may be involved in the final maturation of HCMV, as observed for some other members of the US12 family, like US14, US16, and US17 (Das and Pellett., 2007; Bronzini et al., 2012). In fact, in cells infected with the recombinant HCMV TRUS16HA, the pUS16HA showed a cytoplasmic staining pattern and co-localized with GM130, gB and UL99 virion tegument protein, suggesting that pUS16 accumulates within the cVAC complex in infected cells (Bronzini et al., 2012; Lukanini et al., 2017). Interestingly, the pUS21 does not accumulate within the cVAC (Lukanini et al., 2018) suggesting that unlike the rest of the proteins in US12 family, pUS21 is not likely involved in final maturation step in HCMV virions.

We also predicted the topology of the pUS12 using different algorithms. All the results pointed us towards pUS12 being a seven transmembrane domain protein (7TMDs). These *in silico* predictions were then experimentally confirmed by taking advantage the TR-derived double-tagged virus, TRUS12NV5-CHA. Indeed, we observed that the N-terminus of pUS12 was placed in the cytosol whereas, the C-terminus was present within the luminal side of a Golgi-derived membrane vesicle. These findings are in agreement with some previous general bioinformatics studies which had proposed US12 family members to share a potential 7TMDs architecture (Lesniewski et al. 2006; Bronzini et al. 2012; Lukanini et al. 2018). pUS16 was predicted to have six TMD (TMHMM) and seven TMD (Phyre v2, MEMSAT3, MEMSAT_SVM and TopPred v0.01). After performing an epitope accessibility assay with the recombinant virus TRUS16HA-UL130V5-infected HFFs, the pUS16HA was confirmed to have seven TMDs, with the C-terminal at the luminal side of cVAC (Lukanini et al., 2017).

In conclusion, this chapter gave out the detailed characterization of pUS12 protein expression as a 7TMD protein that is expressed with an Early gene kinetics, and which localizes in Golgi-derived membranes within the cVAC of HCMV-infected cells. Due to the localization of pUS12 in the cVAC, we can speculate a role in final maturation and egress of HCMV virions from infected cell.

Chapter 3 – Functional characterization of the US12 protein of HCMV

3.1 Materials and Methods

3.1.1 Oligonucleotides

The complete list of oligonucleotides used for the PCR and mutagenesis of the US12 ORF are listed below in **Table 3**. These were all purchased by Life Technologies.

Table 3: *Oligonucleotides used for PCR and mutagenesis*

Primer name	Sequence 5' → 3'
US12HA_E coRI_For	TGTGACGAATTCATGGTACAGATCCAGTTTCAC
US12HA_X baI_Rev	TGTGACTCTAGACTAAGCGTAGTCTGGGACGTCGTATGGGTATCCTCCTTTATGAA AAAGCCAGTGTG
US18HA_H indIII_For	TGTGAACAAGCTTATGGGCGACACCGCCTCGG
US18HA_X BaI_Rev	TGTGAACTCTAGACTAAGCGTAGTCTGGGACGTCGTATGGGTATCCTCCCAACAA GCTGAGGAGACTCACGC
US12- D246N-F	CTATGCTGCTATACATGAACCAAGTTATTATGTTT
US12- DN246R	AAACATAATAACTTGGTTCATGTATAGCAGCATAG
US12- D218N-F	AGATCGTGCTTATCCGCAACACATTAACGGTGCTT
US12- D218N-R	AAGCAGCGTTAATCAGTTGCGGATAAGCACGATC
US12F	TGCCGGGTACCTAAAGCCCCGACGACTGTTTCGTGAGCACCCGTCGAAGTTCCTA TACTTTCTAGAGAATAGGAACTTCCCTGTTGACAATTAATCATCG
US12R	GGGACAAAGGACAGTACGACAGATTAGGTGATAGAAACGTTTTTTTTGAAGTTCCT ATTCTCTAGAAAGTATAGGAACTTCCCTCAGCAAAGTTCGATTTA
US12 stop	AAACTTGCCGGGTACCTAAAGCCCCGACGACTGTTTCGTGAGCACCCGTCATGGTA CAGATCUAGATTCACCAAGGC
US12F1	AAACTTGCCGGGTACCTAAAGCCCCGACGACTGTTTCGTGAGCACCCGTCATGGT ACAGATCCAGTTTCAC

3.1.2 In silico protein modelling

For US12 protein modelling, the Phyre2 (Kelley et al. 2015) server was used for fold recognition-based modeling of pUS12. This analysis identified BsYetJ structures (Chang et al., 2014) as the templates for producing US12 models with the highest level of confidence (100%). The crystal structures of BsYetJ in the open [Protein Data Bank (PDB) ID code 4PGS] and closed (PDB ID code 4PGR) conformations were thus selected as templates to generate refined models of pUS12. The Phyre2 predictions were then imported into the Chimera software and 3D modelling of the protein was prepared.

The GenBank (<https://www.ncbi.nlm.nih.gov/Genbank>) accession numbers for the proteins analyzed were the following: HCMV TR Genome (AC146906.1); H. sapiens TMBIM6/ BI-1 (NP_003208.2); H. sapiens TMBIM4/hGAAP (NP_001269535.1); CMLV TMBIM4/vGAAP (AAG37461.1); and B. subtilis YetJ (O31539).

3.1.3 Cells and culture conditions

T-REx-293 cell line (Life Technologies) that stably express the Tetracycline repressor (Tet R) encoded by the pcDNA6/TR plasmid (Life Technologies) was grown in DMEM (Euroclone) supplemented with 10% tetracycline reduced FBS, 100 U/ ml penicillin, 100 µg/ ml streptomycin sulphate and 5 µg/ ml blasticidin (Life technologies).

Retinal epithelial cell line (APRE-19 – ATCC CRL-2302) were grown as a monolayer in Dulbecco Modified Eagle's Medium (DMEM) (Euroclone) supplemented with 10% Fetal Bovine Serum (FBS) (Euroclone), 2 mM glutamine, 1 mM sodium pyruvate, 100 U/ ml penicillin and 100 µg/ ml streptomycin sulphate.

Human microvascular endothelial cells (HMVECs – CC-2543) were obtained from Clonetics (San Diego, CA), and cultured in Endothelial Growth Medium (EGM) (Clonetics) corresponding to Endothelial Basal Medium (EBM) (Clonetics) containing 2% FBS, human recombinant vascular endothelial growth factor (VEGF), basic growth factor (bFGF), human epidermal growth factor (hEGF), insulin growth factor – 1 (IGF-1), hydrocortisone, ascorbic acid, heparin, gentamycin, and amphotericin B as previously described (Cavaletto et al. 2015; Lukanini et al. 2017). The cells were seeded onto culture dishes coated with 0.2% gelatin. Experiments were performed using HMVEC cells at passage from 4-8.

3.1.4 Plasmids and generation of stable Tet-ON inducible cell lines

To generate the pcDNA4/TO-US12HA plasmid, the full length US12HA ORF was amplified by PCR from TRUS12-HA BAC, adding EcoRI and XbaI restriction sites at the 5' and 3' of the ORF, respectively (primers US12_EcoRI_for and US12_XbaI_rev, **Table 3**). US12HA_XbaI_Rev primer, in addition to XbaI restriction site, also contained the HA sequence to maintain the HA epitope at the C-terminus of the ORF. The cassette was then cloned in the inducible expression vector pcDNA4/TO (Life Technologies) using EcoRI and XbaI as restriction sites. The pcDNA4/TO-US18HA was

constructed in a similar fashion by adding HindIII and XbaI restriction sites at the 5' and 3' end, respectively (**Table 3**). The HA tag was also added to the 3' end of the US18 ORF.

The pcDNA4/TO expression vector allows for efficient tetracycline-inducible expression (Tet ON) of the protein of interest in the T-REx system implanted in different mammalian cell lines. The pcDNA4/ TO vector in fact contains two tetracycline operator 2 (Tet O₂) sequence sites located between the TATA box and the transcriptional start site of the HCMV Immediate-Early gene promoter region, thus allowing a tetracycline-regulated expression of the gene of interest. In uninduced T-REx cells that stably express Tet R, the Tet O₂ operators are repressed by two Tet R homodimers, and gene transcription is repressed. However, on the addition of tetracycline, the antibiotic binds to the Tet R homodimers and cause a conformational change that leads to the dissociation of the Tet R molecules along with the bound tetracycline from the Tet O₂ sequence, thus allowing the transcription of the gene of interest (**Figure 22**).

The pcDNA4/TO-US12HA or pcDNA4/TO-US18HA were transfected into T-REx-293 cells using Lipofectamine 3000 (Invitrogen) according to manufacturer instructions. After 48 h post transfection, stably transfected T-REx-293-US12HA and T-REx-293-US18HA cells were selected by their resistance to 350 µg/ ml zeocin (Life technologies) and 5 µg / ml blasticidin.

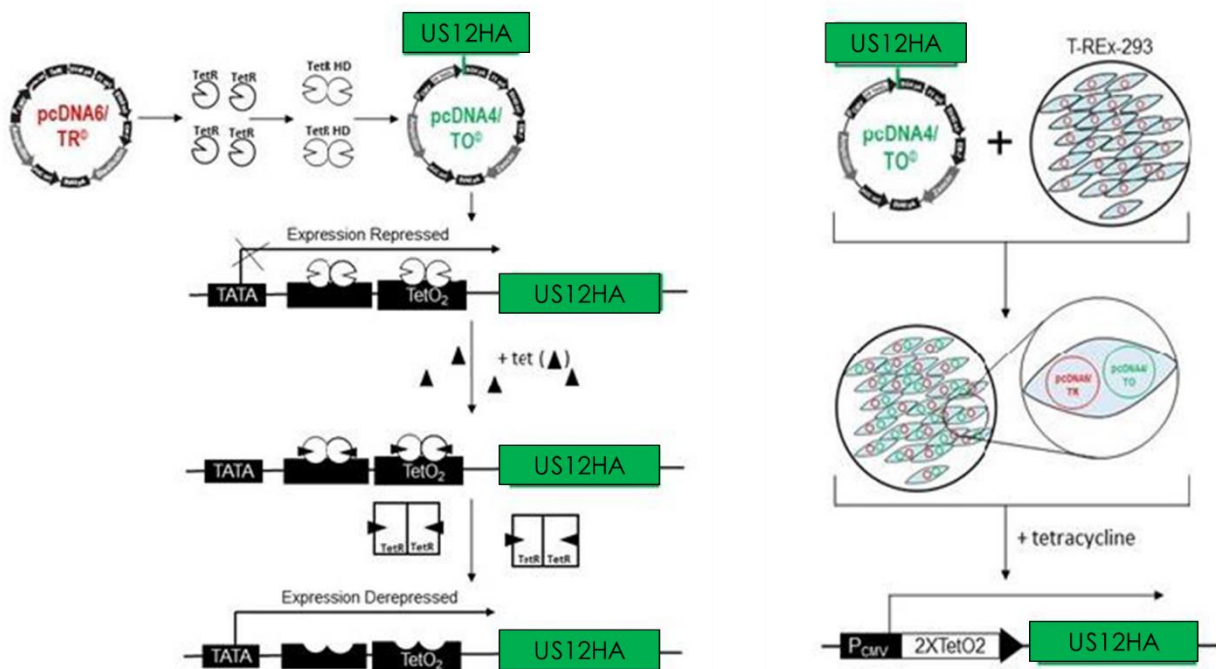


Figure 22: Schematic representation of the T-REx system tetracycline-inducible expression of pUS12HA. Components and working principles of the T-REx system are shown. Tet repressor (Tet R) is provided by pcDNA6/TR expression vector that is stably transfected in T-REx-293 cells. Tet R homodimers bind to the Tet O₂ sequences and thus the expression of the US12HA ORF is repressed. With the addition of tetracycline, it binds to the Tet R homodimers resulting in conformational change and their dissociation from the Tet O₂ sequences, thus allowing the expression of the US12HA ORF.

3.1.5 Generation of the TRUS12stop, TRUS12 D218N, and TRUS12 D246N BACs

The generation of TRΔUS12 BAC and TRUS12-HA BACs has been described in Chapter 2.

To generate the US12stop, first a US12stop stop cassette was produced by a PCR amplification performed using the F-US12 stop and US12HA R2 primer set (**Table 3**) with TRUS12HA BAC used as a template. The PCR product was then digested with DpnI for 2 hours at 37° C to remove any traces of DNA plasmid template.

Then, 200 ng of the TRUS12stop cassette was electroporated into SW102 cells harbouring the TRΔUS12 BAC clone. Bacteria were then plated on M63 plates containing 0.2% 2-deoxygalactose (DOG), 15 µg/ml of Caf and glycerol as their sole carbon source. Gal-negative colonies were further selected by their inability to grow in the presence of Kan by streaking them both on LB+ Caf 15 µg/ml and LB +Caf 15 µg/ml + Kan 25 µg/ml plates. They were screened for the replacement of galK/kan with the modified versions of US12 ORF by PCR. Two independent TRUS12stop BAC clones were selected and characterized to ensure that their phenotypes did not result from an off-target mutation. Recombinant TRUS12stop BAC was then purified from SW102 cells with NucleoBond Xtra BAC (Macherey-Nagel) according to the manufacturer instructions.

To generate the TRUS12HA D218N and TRUS12HA D246N BACs, starting from the pcDNA4/TO-US12HA plasmid as a template, two other plasmids pcDNA4/TO-US12HA D218N and pcDNA4/TO-US12HA D246N were first created using the Quick-change II site directed mutagenesis kit (Stratagene Agilent), using the specific primer set described in **Table 3**. The PCR products were then digested using DpnI for 1 hour at 37° C to remove the traces of template DNA and then transformed into XL1-Blue bacteria. Bacteria were then plated in LB plates with ampicillin at a concentration of 100 µg/ml. The resulting colonies on LB plates were then screened by PCR and sequenced to confirm the accuracy of introduced mutations. The resulted pcDNA4/TO-US12HA D218N and pcDNA4/TO-US12HA D246N plasmids had a mutation from aspartic acid (D) to asparagine (N) at 218 or at 246 positions of the US12 ORF, respectively. Starting from pcDNA4/TO-US12HA D218N and pcDNA4/TO-US12HA D246N, to generate the US12HA D218N and US12HA D246 N cassettes, PCR amplifications were performed using the primers US12HA F and US12HA R2 (**Table 1**). Then, 200 ng of the TRUS12HA D218N or TRUS12HA D246N cassettes were electroporated into SW102 cells harbouring TRΔUS12 BAC clone. Bacteria were then plated and selected as described above for TRUS12stop BAC. Recombinant TRUS12HA D218N and TRUS12HA D246N BACs were then purified from SW102 cells with NucleoBond Xtra BAC (Macherey-Nagel) according to the manufacturer instructions.

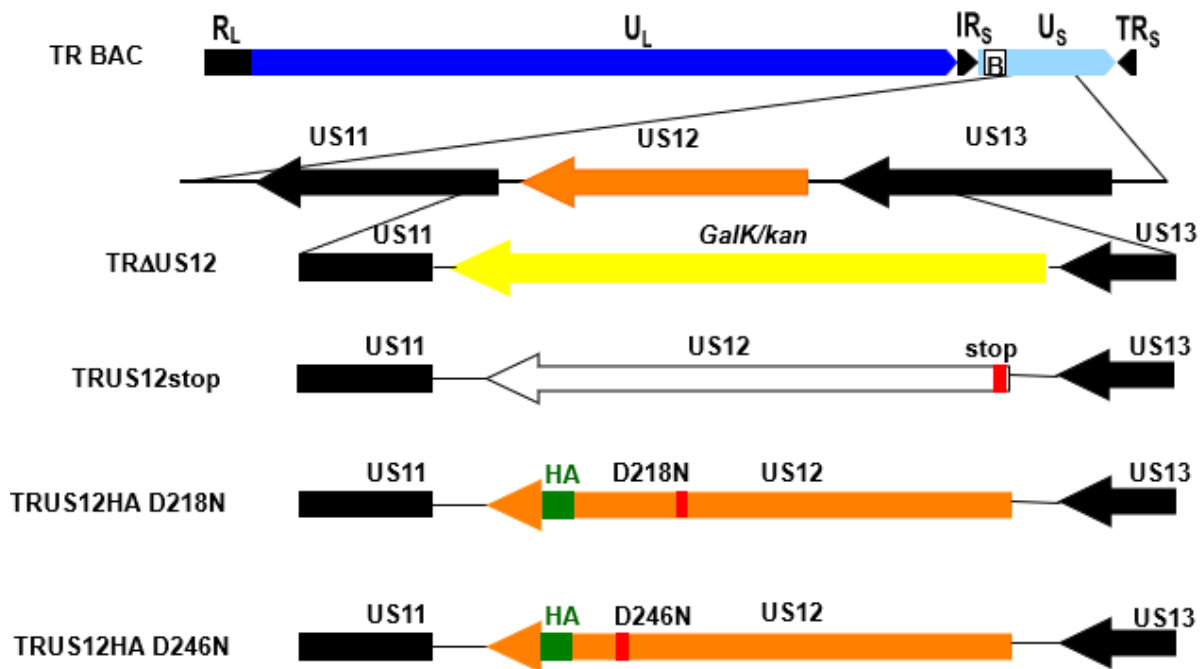


Figure 23: Schematic representation of the HCMV US12 gene region and the modification of the US12 ORF introduced in the TRUS12stop, TRUS12HA D218N, TRUS12HA D246N derivatives. *The GalK-Kan cassette replaced the US12 ORF in the TRΔUS12. In TRUS12 stop, a stop codon was added at the 5' end of US12 ORF, such that, the translation of the US12 ORF was interrupted by a stop codon inserted after 4 aa at the N-terminal end. In TRUS12HA D218N or TRUS12HA D246N, a point mutation was performed where the aspartic acid residue was mutated to an asparagine residue at the 218 or 246 aa positions of US12 ORF.*

3.1.6 Recombinant virus preparations and infections

The infectious TR recombinant viruses (TRΔUS12, TRUS12-HA, TRUS12stop, TRUS12 D218N and TRUS12 D246N) were reconstituted in HELFs by co-transfection of the correspondent recombinant BAC and a plasmid expressing HCMV pp71 (a gift from T. Shenk) using SuperFect transfection reagent (Qiagen). Transfected HELFs were then cultured until a marked cytopathic effect were observed. Subsequent TR virus stocks were prepared by infecting HFF cells at a virus-to-cell ratio 0.01.

To determine the kinetics of viral replication, HFFs, ARPE-19 or HMVEC cells were infected with TR derivative viruses at an MOI of 0.1 PFU/cell. Virus adsorptions were carried out for 2 h at 37° C. For all the experiments, the time zero is the time at which the virus is added to the cells. Both cells and supernatants were harvested at different times post infection (p.i.).

HCMV virus titration was performed by an indirect immunoperoxidase staining procedure on infected HFF cells at 96 h p.i., using an anti-IEA (IE1 plus IE2) (clone E13, Argene Biosoft mAb as previously described (Cavaletto et al., 2015; Luganini et al., 2017)).

3.1.7 Cytosolic Ca²⁺ measurement

Cytosolic calcium quantification was determined as previously described (Pla et al., 2012; Luganini et al., 2018). Briefly, T-REx-293-US12HA, T-REx-293-US18HA, T-REx-293-US21HA (Luganini et al., 2018) cells were seeded at a density 5,000 cells/coverslip and treated or not treated with 1 µg/ml of tetracycline for 48 hours. Cells were subsequently loaded with 2 µM Fura-2 AM (Invitrogen) for 45 minutes at 37°C, and then ratiometric analysis for cytoplasmic Ca²⁺ was performed as described previously (Fiorio Pla et al., 2010; Fiorio Pla et al., 2012).

Briefly, for fluorescence measurement, the cells were excited at 340 nm and 380 nm alternatively to acquire the fluorescence by Nikon Eclipse TE-2000S (Minato, Tokyo, Japan) inverted microscope and MetaFluor Imaging System (Molecular Devices, Sunnyvale, CA, USA). During the experiments, cells were maintained in standard extracellular solution: 145 mM NaCl, 5 mM KCl, 2 mM CaCl₂, 1 mM MgCl₂, 10 mM N-(2-hydroxyethyl)-piperazine-N'-ethane sulfonic acid (HEPES), 10 mM glucose (NaOH pH 7.35). Ca²⁺ free extracellular solution was also provided so that the Ca²⁺ influx from the extracellular environment was prevented, such that, the Ca²⁺ in the cytosol was solely produced from intracellular stores. The extracellular Ca²⁺ buffer was: 145 mM NaCl, 5 mM KCl, 2 mM ethylene glycol-bis (β-aminoethyl ether) – N, N, N', N' – tetra acetic acid (EGTA), 1 mM MgCl₂, 10 mM N-(2-hydroxyethyl)-piperazine-N'-ethane sulfonic acid (HEPES), 10 mM glucose (NaOH pH 7.35).

To assess the intracellular store Ca²⁺ content in T-REx-293 US12-HA (NI or I cells), the intracellular Ca²⁺ pools were depleted with thapsigargin (TG, 2 µM) and ionomycin (IONO, 5 µM), in absence of extracellular Ca²⁺ (0 Ca²⁺), and compared the following [Ca²⁺]_c increase.

Ratiometric cytosolic Ca²⁺ ([Ca²⁺]_c) measurement was expressed as a ratio (R) of emitted fluorescence at 510 nm corresponding to two excitation wavelengths. For each condition, at least 50 regions of interest (ROIs) were selected, each corresponding to a single cell in the chosen image field, and images were acquired every 3 seconds. Real time back-subtraction was applied in order to limit noise. Each fluorescent trace (340/380 nm ratio) represented one region of interest corresponding to the cells in the chosen field. Peak amplitude (510 nm) was determined by the difference between the maximum and the minimum values of fluorescence intensity before reaching the peak itself.

Ca²⁺ imaging analysis was performed by peak amplitude quantification using Clampfit 11.1 (Axon pClamp, Molecular Devices, San Jose, CA, USA). Peak amplitude was calculated as the highest value of R within 300 seconds following the treatment, only considering response with ΔR_{340/380} > 0.05.

3.1.8 Statistical Analysis

All data are presented as means ± standard deviation (SD). The data were analysed for significance using a paired t-test, and were considered statistically significant at P value of < 0.05. All statistical tests were performed using GraphPad Prism version 5.01 for windows (GraphPad Prism software).

3.2 Results

3.2.1 Inactivation of the US12 gene affects efficient HCMV replication in epithelial and endothelial cells

To investigate the requirement for the US12 gene during the HCMV replication in cell types known to be relevant for the virus's replication and dissemination in the host, such as epithelial and endothelial cells, we generated different US12-deficient viruses from the TR clinical isolate (Smith et al. 1998). Ryckman et al., (2006) previously demonstrated that infectious viruses reconstituted from the TRwt BAC clone could successfully replicate in both epithelial and endothelial cells.

For the derivative Δ US12, the entire ORF was replaced by the Gal/Kan cassette; for TRUS12 stop, a stop codon was inserted near at the 5' end of the US12 gene (at the start of US12 ORF), resulting in an inactivated US12 ORF (**Figure 23**).

To determine their growth kinetics, HFFs, HMVECs, and ARPE-19 cells were infected at an MOI of 0.1 PFU/ cell with TRwt, TR Δ US12, TRUS12 stop, or the revertant TRUS12HA viruses. Their replication was then assessed at different days p.i.

In HFF fibroblasts, there was no difference between the growth rates of the US12-deficient viruses in comparison to TRwt or TRUS12HA, thus indicating that the US12 gene is not required for the successful replication in this cell type (**Figure 24**).

In contrast, the growth kinetics of the US12-null viruses in the epithelial ARPE-19 cell line showed a 3-log titer reduction at days 4, 6, 10 and 12 as compared with the TRwt or TRUS12HA (**Figure 24**). Similarly, in endothelial HMVEC cells, the US12-null viruses showed a 4-log reduction at days 6, 8, 10 and 12 in comparison with the TRwt or TRUS12HA (**Figure 24**).

Importantly, the replication kinetics of the US12 revertant virus (TRUS12HA) in HMVECs and ARPE-19 cells was similar to that of TRwt (**Figure 24**), thus indicating that the defective growth phenotype of the US12-deficient viruses in endothelial and epithelial cells was indeed due to a specific inactivation of the US12 coding sequence, since the TRUS12HA virus was obtained from the TR Δ US12 BAC by re-implanting a functional US12HA ORF.

Taken together, these results suggested that the US12 gene of HCMV encodes a protein whose function(s) contributes to the efficient infection and productive replication in both endothelial and epithelial cells.

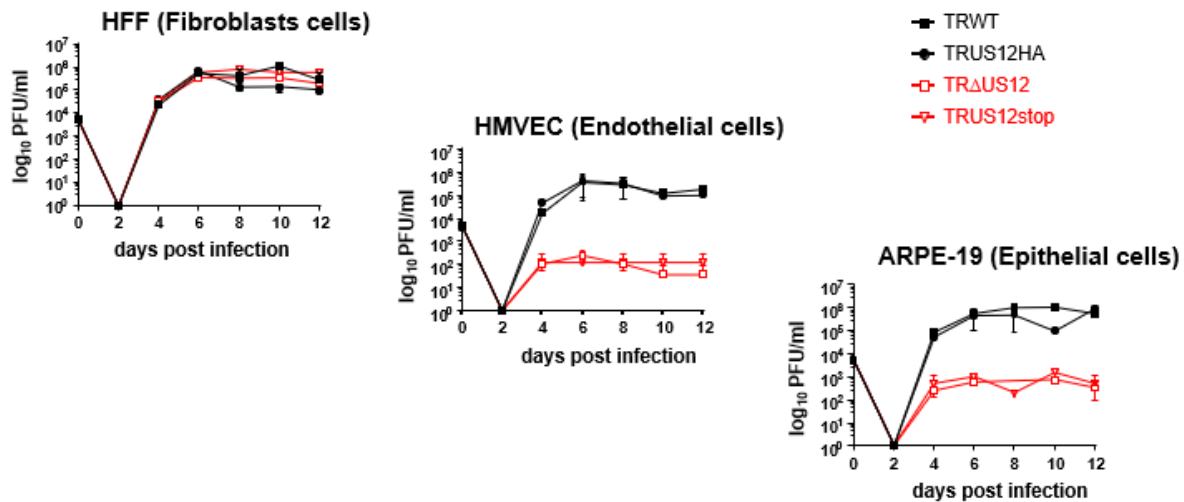


Figure 24. Inactivation of the US12 ORF affects HCMV replication in epithelial and endothelial cells. HFFs, ARPE-19, and HMVECs cells were infected with TRwt, TRΔUS12, TRUS12stop, or TRUS12HA at an MOI of 0.1 PFU/ cell. The extent of the virus replication at different times p.i was then determined by titrating the infectivity of the supernatants of the cell suspensions on HFFs and quantifying infectious viruses by IEA immunostaining. The data shown are the average of the results of two independent experiments \pm SD, performed in triplicate.

3.2.2 US12 ORF shares sequence similarities with cellular proteins of the TMBIM family

To get further insights into the US12 function(s), the US12 ORF sequence was aligned against some members of the TMBIM (TransMembrane BAX Inhibitor Motif containing) protein family members using the TM-COFFEE server. The US12 protein showed a sequence identity of 11.9% with BI-1 (Bax inhibitor-1) and 14.9% identity with hGAAP (human Golgi-Anti Apoptotic Protein), of 18.8% with camel pox virus GAAP (CMP GAAP), and 17% with the bacterial TMBIM homolog BsYetJ (Chang et al., 2014) (**Figure 25**).

Given that the absence of crystal structures for any of the mammalian TMBIM proteins, the availability of high-resolution structures of the *Bacillus subtilis* BI-1 homolog BsYetJ, has provided structural insights into TMBIM functions. BsYetJ is in fact a seven-TMD Ca^{2+} channel characterized by a the pH driven mechanism of opening and closing of the Ca^{2+} channel determined by a “di-aspartyl pH sensor” which consists of Asp171/Asp195 residues that establish interactions with the positive Arg60 residue (Chang et al., 2014). The two aspartic acid residues which are located in TMD6 and TMD7 respectively, and they can form or resolve a hydrogen bond with Arginine 60 located in the loop between TMD2 and TMD3, thus causing a movement or shifting of TMD2 that, in turn, results in the opening or closing of the pore (Chang et al., 2014). The opening and closing of the pore are driven by pH. In fact, depending on the pH, the aspartic acid residues undergo to protonation or deprotonation which results in the formation or prevention of the hydrogen bond with the Arg 60 residue (Chang et al., 2014).

Importantly, the two aspartic residues are indeed conserved among the TMBIM family members hBI-1 (Asp 188/Asp 213), hGAAP (Asp 196/Asp 219), CMLV_GAAP (Asp 196/Asp 219). Moreover, they are conserved in the pUS21 viroporin (Asp 178/Asp 201) (Luganini et al., 2018), and also

conserved in the US12 ORF as Asp 218 and Asp 246. By contrast they are not present in the pUS18 ORF (**Table 4**).

The BsYetJ latch partner Arg 60, on the other hand, is conserved in hGAAP (Arg 91) and CMVL_GAAP (Arg 90). But it not in hBI-1 and in US21. In hBI-1, the His 78 residue has been proposed to form an alternative latch by forming a hydrogen bond to Asp 209 (Chang et al., 2014; Bultynck et al., 2014). In pUS21, the latch partner Arg 69 has been predicted to interact with Asp 178 and Asp 201 (Luganini et al., 2018). Whereas, for pUS12, the Arg 109 aligns perfectly with the Arg60 of BsYetJ, and thus it can be predicted that it may interact with the putative US12 di-aspartyl pH sensor Asp 218-Asp 246 (**Figure 25**).

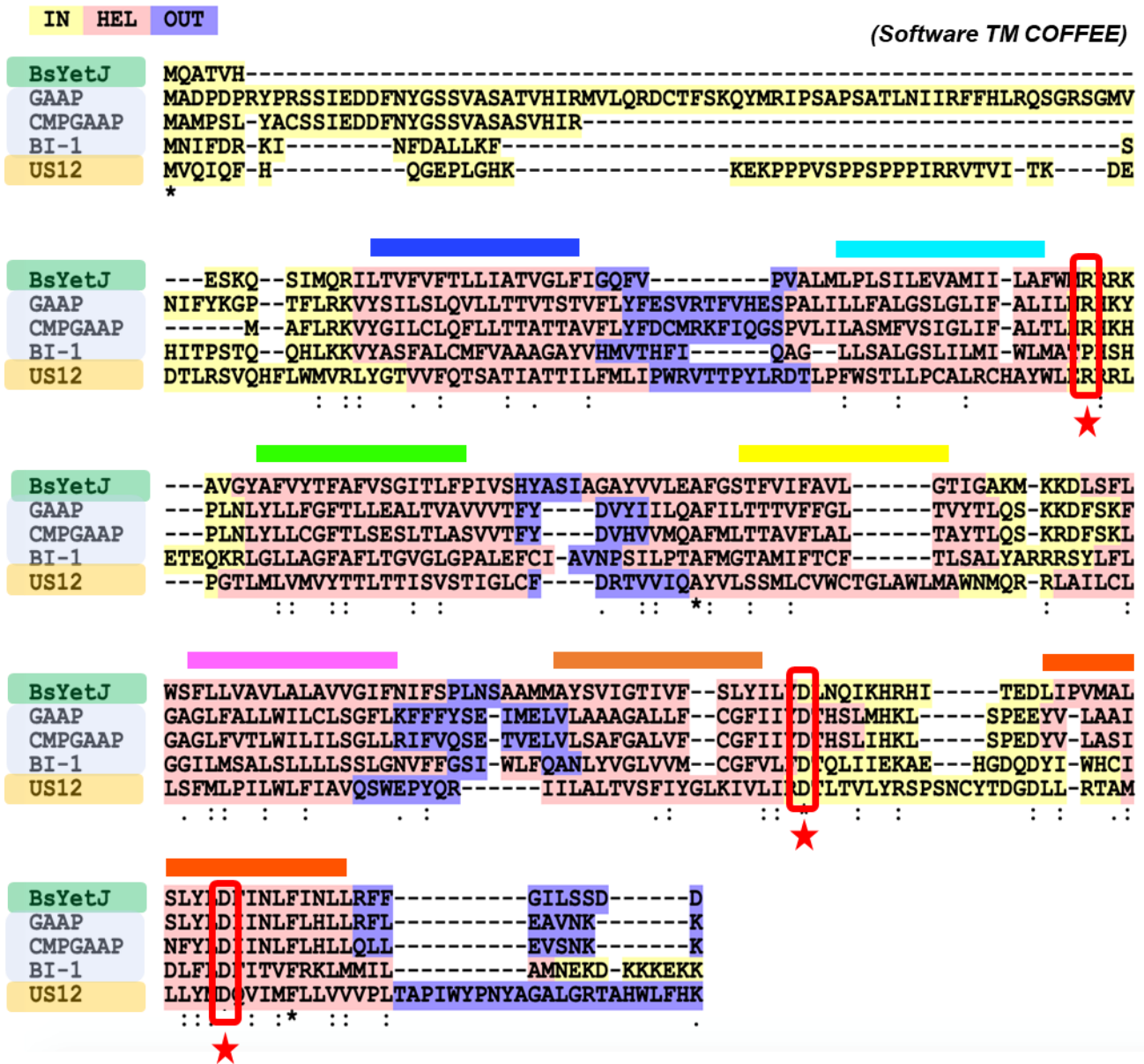


Figure 25: TM-Coffee Multiple sequence alignment of the US12 ORF with BsYetJ, hBI-1, hGAAP, CMP-GAAP. A multiple sequence alignment between US12 with BsYetJ, hBI-1, hGAAP, CMP-GAAP was performed to identify similarities, identities and differences between the proteins. TM-Coffee software also highlights which part of the protein sequence are predicted to face the cytoplasmic side (yellow), the extracellular luminal (Blue) and the transmembrane domain (pink). The location of the seven TMDs is indicated by various bar color codes – TMD1 (Dark blue), TMD2 (Light blue), TMD3 (Green), TMD4 (Yellow), TMD5 (Pink), TMD6 (Brown) and TMD7 (Orange). Red stars with the rectangular box highlight the aspartate residues and the arginine latch partners conserved among all the proteins.

Table 4: Table depicting the occurrence of the di-aspartyl pH sensor residues and their latches partners in BsYetJ, TMBIM proteins, pUS21, and pUS12.

	Di-Aspartyl pH sensor		Latch
BsYetJ	Asp171 (D171)	Asp195 (D195)	Arg60 (R60)
hBI-1	Asp188 (D188)	Asp213 (D213)	His78 (H78)
hGAAP	Asp196 (D196)	Asp219 (D219)	Arg90 (R90)
pUS18	Glu210 (E210)	Ile235 (I235)	Glu45 (E45)
pUS21	Asp 178 (D178)	Asp 201 (D201)	Arg 69 (R69)
pUS12	Asp 218 (D218)	Asp 246 (D246)	Arg 109 (R109)

3.2.3 Structural modelling of the US12 protein

pUS12 shares the similarities with TMBIM family proteins, with BsYetJ and with pUS21, such as the conservation of aspartic acid and arginine key residues and the 7TMD topology. Thus, a protein fold recognition approach was applied for pUS12, starting from the crystal structures of BsYetJ in closed (PDB ID 4PGR) and open (PDB ID 4PGS) conformations (Chang et al., 2014) as templates to generate structural models of pUS12 in the closed and open conformations.

Interestingly, these models predicted a pore within pUS12 spanning the membrane and opening at the shift of TMD2 helix. In pUS12, Asp 218 and Asp246 are located near the cytosolic end of TMD6 and at the centre of TMD7, respectively. In the **closed state** of pUS12 (**Figure 26 A**), Arg 109 which is located at the cytosolic end of TMD2, is oriented towards the inside of the putative pore, and towards the two Asp acid residues with the TMD2 located at the core of the structure (**Figure 26 A**).

For comparison, in BsYetJ, in the **closed state**, the two Asp acid residues located in the pore region, namely Asp 171 and Asp 195 (which align with Asp 218 and Asp 246 of pUS12, respectively) form salt bridges with each other, and Asp 171 forms additional salt bridge with Arg 60 residue. In BsYetJ, these interactions stabilize the **closed state** (Chang et al., 2014). Protonation of the two aspartates (Asp 171 and Asp 191) disrupt these interactions, leading to the displacement of TMD2 and thus opening the pore (Chang et al., 2014).

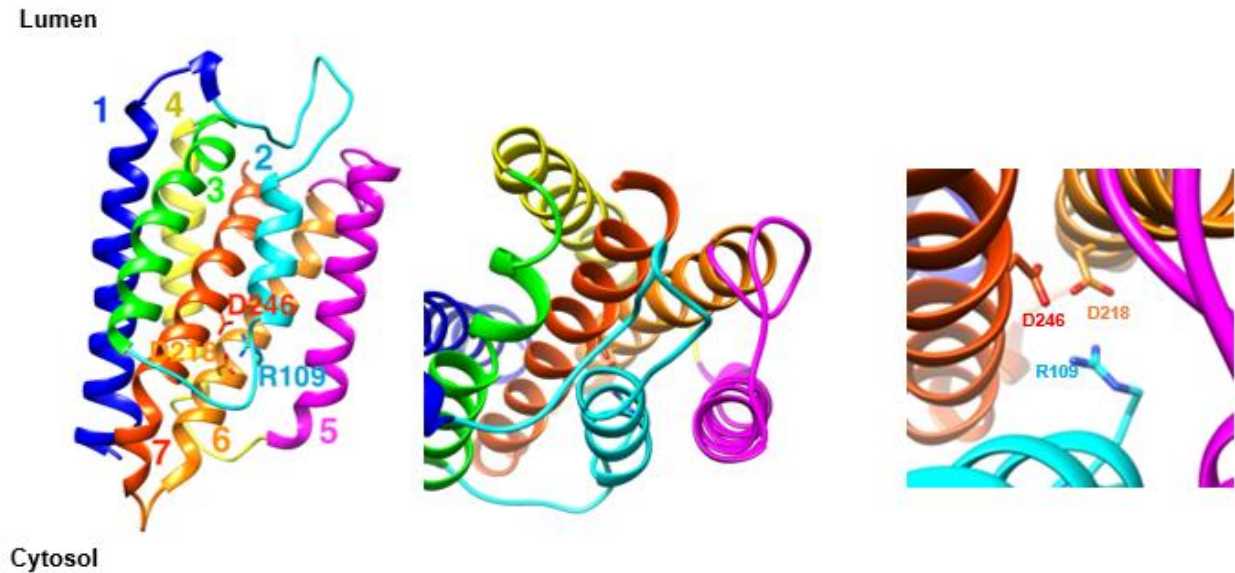
In the **open state** of pUS12 (**Figure 26 B**), the TMD2 is predicted to shift from the core region towards the external part of the protein. Due to the displacement of the helix, the orientation of the Arg 109 changes and it moves further away from the Asp residues in the pore, as in its position in the closed state, thus preventing the interaction with Asp residues. This shift of TMD2 results in the opening of the pore of pUS12 (**Figure 26 B**).

Figure 26 C summarizes the prediction of the closed and open states of pUS12, and shows the

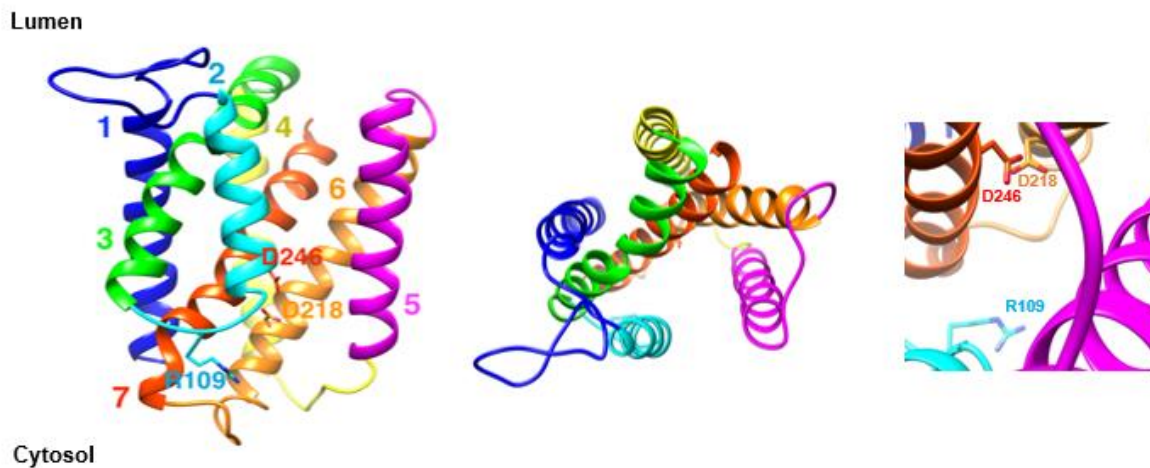
location of the predicted continuous protein pore across the membrane viewed from the luminal side.

Figure 27 is a representation of the distances between the Asp 218, Asp 246 and Arg 109 of pUS12 in the **closed (Figure 27 A)** and **open (Figure 27 B)** states. We can observe that the distance between the three amino acids increased in open state as compared to the closed state.

A



B



C

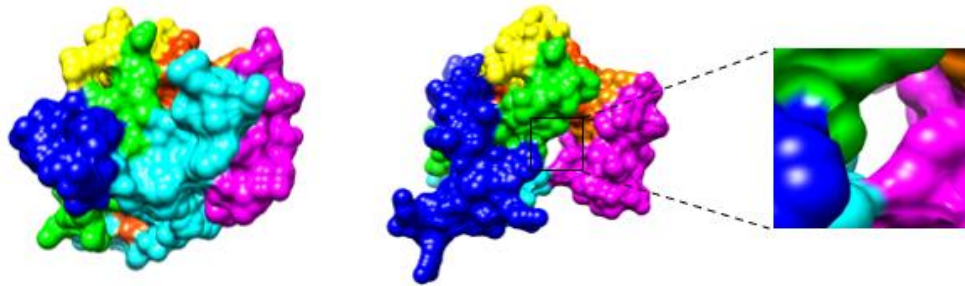
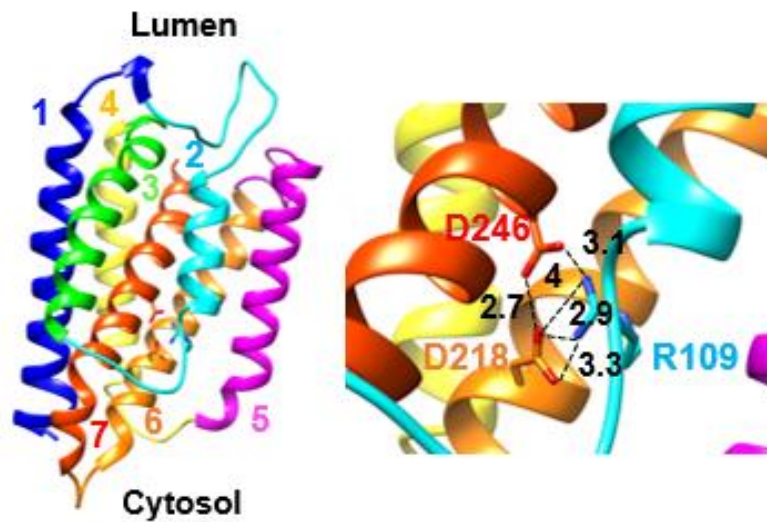


Figure 26: Structural models of US12 protein. Protein fold recognition models of US12 protein based on the crystal structures of *BsYetJ* were generated using Phyre2. A-C models of US12 protein in closed (A) and Open (B) states. In A and B, the side chains of residues are colored in cyan (Arg 109), dark yellow (Asp 218) and brown (Asp 246). Closed and open state of the model of the pUS12 – left column shows the model from the membrane view; middle column shows the closed model from luminal view, and the right column shows the enlarged regions of the models. (C) pUS12 in the closed (left column) and open (middle column) state with an enlarged view of the pore. The helices follow the following color code: TMD1 (Dark blue), TMD2 (Light blue), TMD3 (Green), TMD4 (Yellow), TMD5 (Purple), TMD6 (Dark yellow) and TMD7 (Brown). The TMDs are numbered for clarity.

A



B

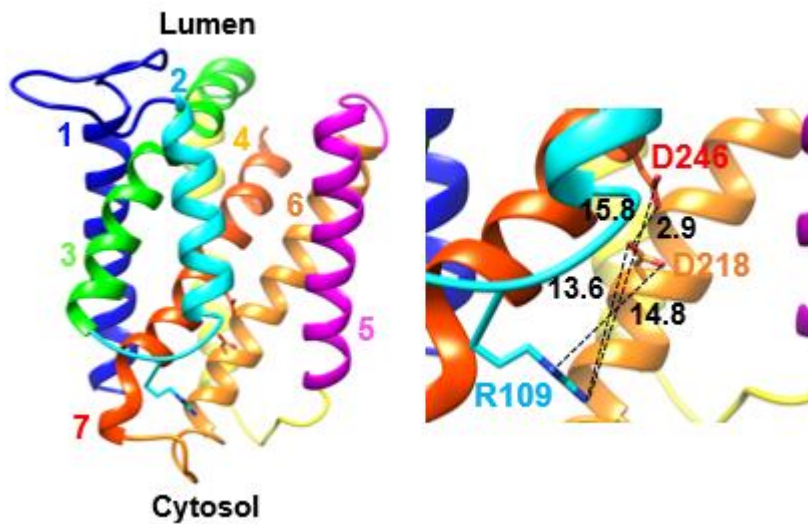


Figure 27: Distances between key residues of the predicted pUS12 pore measured in the closed (A) and open (B) model of pUS12: Enlarged images of the closed and open models of pUS12 along with the distances measured between the Arg (R109), and Aspartic acid residues (D218 and D246).

3.2.4 pUS12 functions as a calcium leak channel

3.2.4.1 Generation of T-REx system for inducible expression of pUS12HA

To experimentally verify the putative Ca²⁺ channel activity of pUS12, an appropriate cell system was generated by exploiting the Tetracycline – Regulated Expression (T-REx) system for TET-ON expression of proteins of interest. This system allows for rapid and efficient tetracycline-inducible

expression of proteins in mammalian cell lines, and it has been successfully used for the expression of Ca²⁺ channels (Kadeba et al., 2013).

To this end, the US12 ORF modified by the addition of a HA epitope at the 3' end was cloned into the pcDNA4/TO and the construct was then transfected into T-REx-293 cells. The T-REx-293 cells stably express the Tet repressor that in the absence of tetracycline forms a homodimer that binds with high affinity to the Tet operators (Tet O₂). Tet O₂ is located within the promoter region of the pcDNA4/TO (Hillen and Berens., 1994). When the Tet repressor is bound to the Tet O₂, the transcription of a downstream gene is repressed. However, with the addition of tetracycline, the Tet repressor binds tetracycline and undergoes to a conformational change that disrupt its interaction with Tet O₂. This results in the activation of transcription of the regulated gene. In summary, in the T-REx-293-pUS12HA cells, pUS12-HA is expressed only in the presence of externally added tetracycline.

The inducible expression of pUS12HA in T-REx-293-US12HA cells was thus validated through immunoblot analysis on whole cell protein extracts prepared cells uninduced (NI) or induced (I) with 1 µg/ ml of tetracycline for 48 h.

As depicted in **Figure 28**, a pUS12HA band of 28 kDa was observed in the extracts of the cells induced with tetracycline. Similarly, the expression of pUS21HA was detected only in extracts from T-REx-293-US21HA cells (Luganini et al. 2018). Moreover, a similar pattern of expression was observed for pUS18HA in T-REx-293-US18HA cells at 48 h post treatment (p.t).

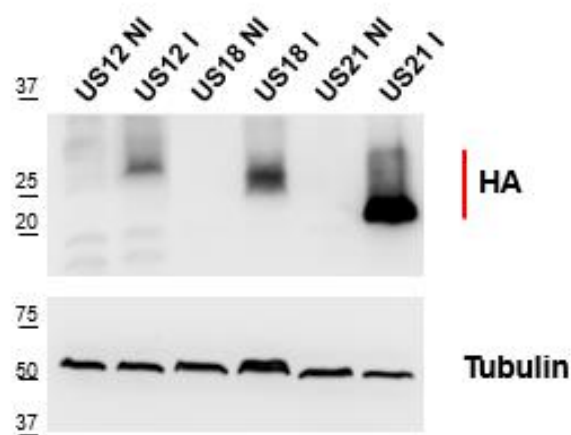
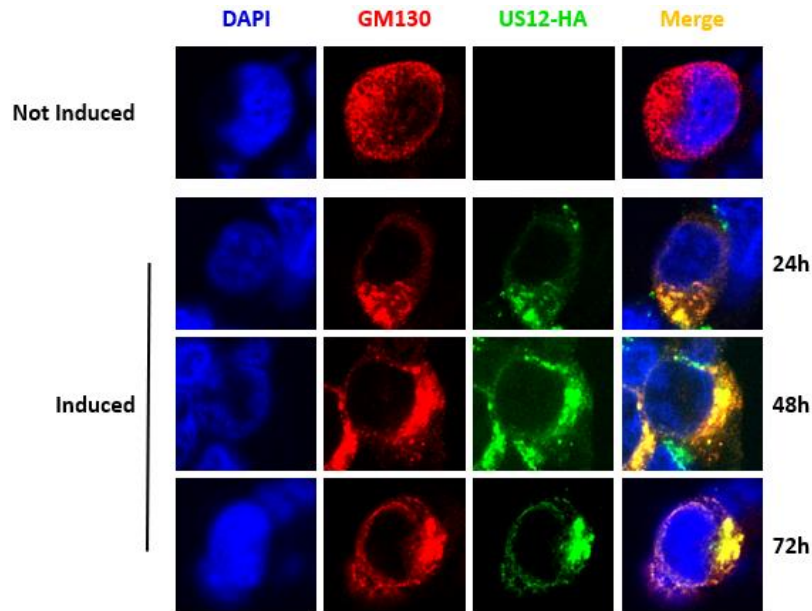


Figure 28: Inducible expression of pUS12HA, pUS18HA and pUS21HA in T-REx-293 cells. *T-REx-293-U12HA, T-REx-293-U18HA, or T-REx-293-21HA cells were either treated with 1 µg/ ml of tetracycline or not treated. Total protein cell extracts were prepared at 48 h post the tetracycline treatment. The extracts were loaded on a 15% SDS-PAGE (50 µg/ lane) and analysed with a α-HA or α-tubulin (TUB) mAbs. Tubulin was used as for protein load control.*

The inducible expression of pUS12HA in T-REx-293-US12HA cells was further confirmed by immunofluorescence analysis of the cells left untreated or treated with tetracycline 1 µg/ ml, for 24 h, 48 h, or 72 h. At these time points, induced cells were stained using α-HA mAb to detect pUS12 along with two Golgi markers, such as GM130 and TGN46. As shown in **Figure 29 (A and B)**,

the pUS12HA staining pattern almost completely overlapped that of GM130 and TGN46, thus indicating that pUS12HA, even in T-REX-293 cells and when expressed in isolation, localizes within Golgi-derived membranes.

A



B

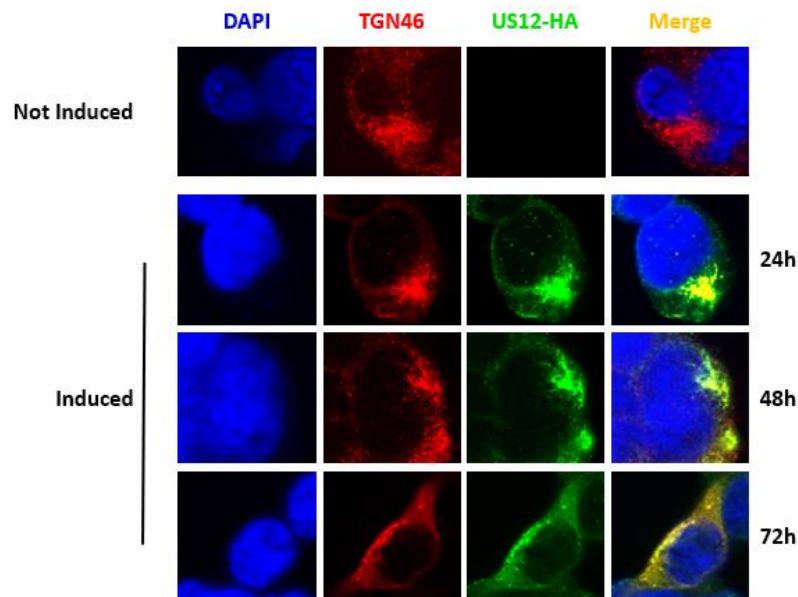


Figure 29: Co-localization of pUS12HA with GM130(A) and TGN46(B) in T-REX-293-US12HA cells. *T-REx-293-US12HA cells were either treated with 1 μ g/ml of tetracycline or left untreated and fixed at 24, 48 and 72 h p.t. Cells were then permeabilized and stained for pUS12HA, GM130, and TGN*

46.

3.2.4.2 Expression of pUS12 decreases the calcium content of intracellular stores

Once the expression of pUS12 in T-REx-293-US12HA cells was validated, we investigated whether pUS12 was indeed endowed of a Ca²⁺ channel function. To this end, cytosolic Ca²⁺ content was measured in T-REx-293-US12HA, T-REx-293-US18HA, and T-REx-293-US21HA cells. The T-REx-293-US21HA cells were used as positive control for a US12 protein family member with a Ca²⁺viroporin activity (Luganini et al., 2018). T-REx-293-US18HA was used as a negative control, since pUS18 does not contain neither the di-aspartyl pH sensor residues in TMD6 and 7, nor the Arg residue in TMD2 that constitute the latch amino acid required for closing the pore (Chang et al. 2014). The cells were grown on coverslips at a density of 40000 cells/ cm² and either treated (Induced, I) or not treated (Not-induced, NI) with 1 µg/ ml of tetracycline for 48 h.

Measurement of Ca²⁺ in the cytosol is carried out by a fluorescence-based assay. During the experiment, the cells are maintained in Ca²⁺ free extracellular solution. This is to avoid the calcium influx from the extracellular environment. The cells are then loaded with Fura-2 AM, a high affinity calcium fluorescent indicator that allows for ratiometric measurement for Ca²⁺ concentration. The probe can bind to calcium ions present only in the cytoplasm, but not to the calcium ions located into intracellular stores (ER and Golgi). When excited in the UV range at 340 nm and 380 nm, the ratio of the emissions of Fura-2 AM allows to quantify the amount of calcium ions present in the cytoplasm. To assess the intracellular store Ca²⁺ content in T-REx-293-derived cell lines uninduced (NI) or induced (I) with tetracycline for 48 h, the intracellular store Ca²⁺ pools were depleted with thapsigargin and ionomycin that cause an immediate Ca²⁺ efflux from ER and Golgi. In the presence of an extracellular Ca²⁺ buffer, Ca²⁺ influx from the extracellular environment is prevented and the ionomycin/ thapsigargin-releasable Ca²⁺ in the cytosol is solely produced from the intracellular stores, thus the measurement of cytosolic Ca²⁺ indicates the content of intracellular stores.

As shown in the **Figure 30**, in comparison to not-induced and induced T-REx-293-US18HA cells, here used as a negative control, the expression of pUS12HA significantly reduced the amount of releasable Ca²⁺ from intracellular stores upon stimulation with ionomycin/ thapsigargin. As expected, a similar result was observed also in induced T-REx-293-US21HA cells, used as a positive control.

This result suggested that like the pUS21, the pUS12 is endowed of a Ca²⁺ channel activity that may stimulate a passive leaking of Ca²⁺ from intracellular stores to the cytoplasm, thus decreasing their Ca²⁺ content.

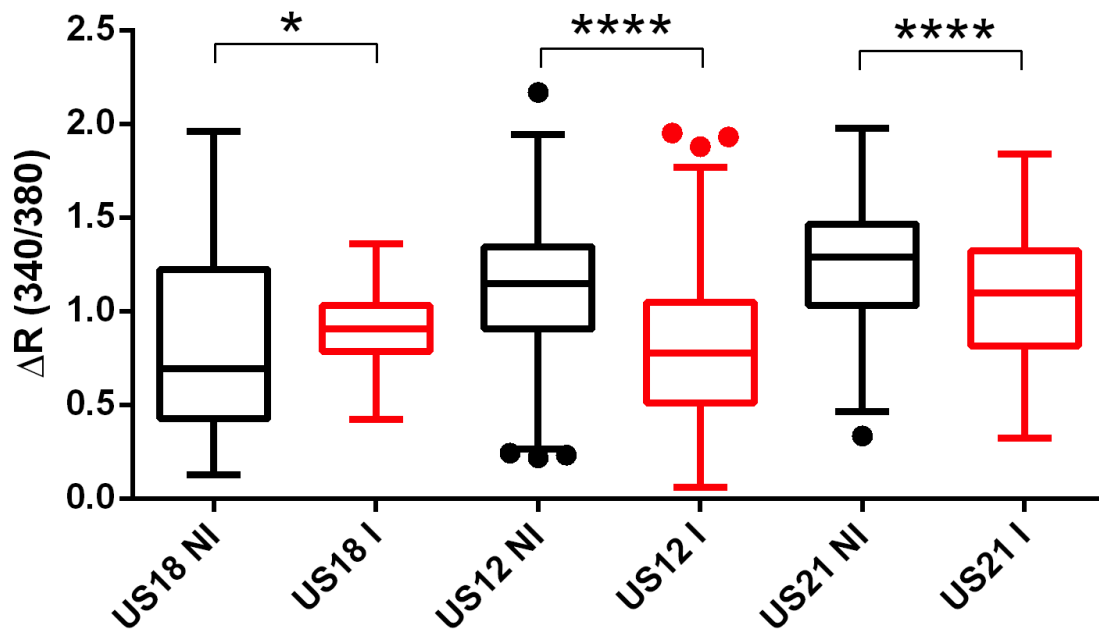


Figure 30: pUS12HA acts as a calcium channel. Boxplot summarizing the relative quantification of the peak amplitude of Ca^{2+} responses in not-induced (NI, black) and induced (I, red) T-REx-293-US12HA, T-REx-293-US18HA and T-REx-293-US21HA cells. * $P < 0.01$ and **** $P < 0.00001$ (student's *t*-test).

3.2.5 Mutation of aspartic acid residues of the putative US12 pore affects efficient HCMV replication in endothelial and epithelial cell lines

To investigate whether mutations of critical Asp residues within the pUS12 pore would impact the replication efficiency of HCMV in different cell types, we generated two further TR recombinant derivatives: TRUS12HA D218N and TRUS12HA D246N.

To determine their growth kinetics, HFFs, HMVECs, and ARPE-19 cells were infected at an MOI of 0.1 PFU/ cell with TRwt, TR Δ US12, TRUS12 stop, the revertant TRUS12HA, and the TRUS12HA D218N and TRUS12HA D246N. Then, the production of infectious viruses was measured at different days p.i.

In HFF fibroblasts, there was no difference between the growth rates of the mutant viruses in comparison to TRwt, TRUS12HA, and the TRUS12-deficient virus, thus indicating that mutated US12 proteins did not affect successful HCMV replication in this cell type (**Figure 31**).

In contrast, the growth kinetics of the US12-mutant viruses in the ARPE-19 cell line showed a 2-fold titer reduction at days 4, 6, 8, 10, and 12, as compared with the TRwt and TRUS12HA (**Figure 31**). Similarly, in HMVEC cells, the US12-mutant viruses showed a 2-fold reduction at days 6, 8, 10 and 12 in comparison with the TRwt and TRUS12HA (**Figure 31**).

Taken together, these results suggest that the D218 and D246 which are likely involved in viroporin activity of pUS12 are critical for the efficient HCMV replication in endothelial and epithelial cell lines.

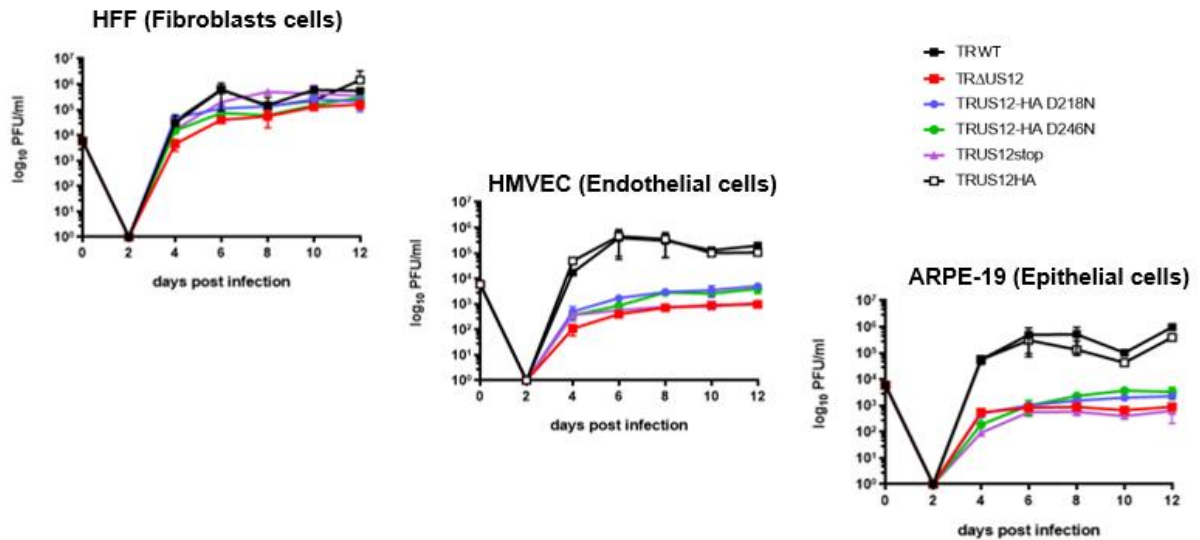


Figure 31. Asp 218 and Asp 246 mutations impact HCMV replication in epithelial and endothelial cells. *HFFs, ARPE-19, and HMVECs were infected with TRwt, TR Δ US12, TRUS12stop, TRUS12HA, TRUS12HA D218N or TRUS12HA D246N at an MOI of 0.1 PFU/cell. The extent of the virus replication at different times p.i was then determined by titrating the infectivity of the supernatants of the cell suspensions on HFFs and quantifying infectious viruses by IEA immunostaining. The data shown are the average of the results of two independent experiments \pm SD, performed in triplicate.*

3.3 Discussion

In this chapter, we investigated the requirement of pUS12 for productive replication of HCMV across in different cell types. We observed that the infectious viruses produced by HFFs cells infected with recombinant TR derivatives bearing inactivations of the US12 ORF failed to replicate productively in endothelial and epithelial cell lines, whereas they replicated normally in fibroblasts. The growth defect of genetically US12-deficient viruses was indeed due to mutations introduced into the US12 locus, as those in TR Δ US12 and TRUS12stop viruses, and not due to unwanted second-site mutations which otherwise could have affected the neighbouring or more distant genes, since the revertant TRUS12HA virus in which a functional US12 ORF was re-implanted in the TR Δ US12 background, replicated similarly to the TRwt in both endothelial and epithelial cells. Clearly further experiments are required to investigate the functional role of US12 in context of productive replication in these cell types relevant for the pathogenesis of HCMV. These further investigation might include: i) evaluation of the levels of IE, E and L gene/protein expression in epithelial and endothelial cells infected with US12-deficient viruses to understand which step is affected by the lack of US12; ii) evaluation of the nuclear accumulation of tegument viral pp65 protein and viral DNA in epithelial and endothelial cells infected with a US12-mutant virus to determine possible defects during virus attachment or entry or post-entry events, such as disassembly of virus particles, capsid translocation to the nuclear pores, and release of viral genomes into the nucleus.

The observation that the US12 gene is required for efficient HCMV replication in cell types relevant for HCMV infection and spread in the natural host, such as endothelial and epithelial cells, is somewhat different from what it has been observed for the US20 and US21 genes (Cavaletto et al., 2015; Luganini et al., 2018). In fact, US20-deficient viruses have been observed to grow normally in both fibroblasts and epithelial cell lines, while they showed an endothelial cell-specific growth defect (Cavaletto et al., 2015). In contrast, the lack of pUS21, has been observed to hamper severely the growth of the virus in both endothelial and epithelial cells (Luganini et al., 2018).

However, the growth phenotype of US12-null viruses seems to be more similar to that observed with US16-deficient viruses (Bronzini et al., 2012; Luganini et al., 2017). In fact, deletion or inactivation of the US16 ORF, impaired the HCMV ability to replicate in endothelial and epithelial cells (Bronzini et al., 2012). Investigations on the genetically US16-negative virions then showed that a failure in the entry phase in both endothelial and epithelial cells. The entry defect of genetically-negative US16 viruses was due to a severe reduction of the content of pentamer complex (gH-gL-UL128-UL130_UL131A) in extracellular viral particles (Luganini et al., 2017). It was therefore concluded that pUS16 is required for the production of virus progeny with a high pentamer content, thus allowing the efficient infection of both endothelial and epithelial cell lines (Luganini et al., 2017). The composition and content of the pentamer complex of genetically-negative US12 virions, however, remains to be determined to verify whether also the lack of pUS12 may impact on the content and/or composition of this HCMV envelope constituent. The

localisation of pUS12 within the cVAC of HCMV-infected cells can suggest a possible involvement of the protein in the maturation of HCMV infectious particles.

Then, to gain insights into the functional characterization of pUS12, its sequence was aligned against the whole protein database, finding interesting levels of amino acid identity with Bax-Inhibitor 1 (BI-1) (11.9%) and Golgi anti-apoptotic protein (GAAP) (14.9%), both belonging to the TMBIM family. These two TMBIM proteins have several regulatory activities and operate as 'stress integrator' pathway and have essential cellular adaptive responses to environmental changes, such as ER stress, autophagy, mitochondrial bioenergetics, and lysosomal functions (Rojas-Rivera and Hetz., 2015). In particular, BI-1 is an integral membrane protein that displays anti-apoptotic activity and it is located in membranes of endoplasmic reticulum (Bultynck et al., 2014) where it interacts with BCL-2 and BCL-XL. BI-1 also as shown to be a negative regulator of the ER stress sensor IRE1 α (Bultynck et al., 2011). During the ER stress, BI-1 was also observed to regulate the physiological amount of calcium ions (Bultynck et al., 2011). All these studies point out towards BI-1 being a Ca²⁺ channel-like protein that regulates the intra-ER Ca²⁺ concentrations by interacting with the IP3R (Rojas-Rivera et al., 2012; Kiviluoto et al., 2012; De Mattia et al., 2009).

GAAP, on the other hand, was first discovered in camelpox virus (CMLV). It was later found in other pox viruses like cowpox virus (CPXV) and strains of vaccinia virus (VACV), and also a human orthologue was determined (Gubser et al., 2007). Localizing in Golgi apparatus, both the human and viral GAAP (hGAAP and vGAAP) have protection activities against pro-apoptotic stimuli and form cation-selective channels (Carrara et al. 2012; Gubser et al. 2007). The hGAAP has shown to regulate the Ca²⁺ content of intracellular stores (Golgi apparatus and endoplasmic reticulum) (De Mattia et al. 2009; Carrara et al., 2015). In addition, hGAAP also promotes cell adhesion and migration via store-operated Ca²⁺ entry (SOCE) from the extracellular space (Saraiva et al., 2013). The multiple sequence alignment was performed between BsYetJ (the bacterial TMBIM homolog), hGAAP, CMLV_GAAP, hBI-1 and pUS12. This alignment revealed that the two aspartic acid residues that in BsYetJ play a crucial role in the pH-dependent channel gating (Chang et al., 2014) and are conserved in mammalian TMBIM family members, align perfectly with the pUS12 D218 and D246 residues (**Figure 25**). These findings suggested that, similar to the pUS21's Asp178 and Asp201 (Luganini et al., 2018), the D218 and D246 may constitute the di-aspartyl pH sensor of pUS12.

In BsYetJ the two aspartic acid residues Asp 171 and Asp195 form a di-aspartyl pH sensor that interact with the positively-charged Arg 60 in TMD2 in opening and closing of the pore. Protein modelling of pUS12, using as a template the BsYetJ structure, indeed predicted the existence of a putative pore within the US12 in which the interaction of D218 in TMD6 and D246 in TMD7 with their latch partner Arg109 located at the cytosolic end of TMD2, may regulate the opening and closing of the pore (**Figure 26**). In fact, Arg109 in TMD2 may form salt bridges with the negatively charged Asp218 and Asp246 at pH8, as observed in BsYetJ and pUS21 (Chang et al., 2014; Luganini et al., 2018). At pH 6, however, the protonation of the aspartic acid residue results in disrupting interactions with Arg109, thus leading to the opening of the pore in pUS12 (**figure 26 and 27**).

The experimental verification that like BsYetJ, BI-1, GAAP and pUS21, pUS12 was endowed of Ca²⁺ channel activity (**Figure 30**) allowed to conclude that pUS12 has a passive leak activity that lowers the Ca²⁺ present in the intracellular stores, likely the Golgi given that its localization in vesicles

derived from this organelle (**Figure 29**). Thus, pUS12 can be considered the second functional Ca^{2+} leak channel within the US12 gene family.

Regulation of Ca^{2+} homeostasis is crucial for cells' physiology because the Ca^{2+} ions act as secondary messengers which regulate many cellular processes, such as, metabolism, protein phosphorylation, cell proliferation, programmed cell death (PCD), and many physiological cell responses to environmental changes and stresses (Berridge et al., 2003). The cytoplasmic Ca^{2+} levels should be maintained within the nanomolar range (around 100 nM) in eukaryotes, as high cytosolic Ca^{2+} concentrations may result in PCD (Pinton et al., 2008). To maintain such low levels of cytosolic levels, a network of transport and buffering have been evolved to control temporal and spatial Ca^{2+} gradients by pumping it either out of the cell or into intracellular organelles, such as ER and Golgi, thus allowing rapid cellular responses to the variations of these gradients. The intracellular Ca^{2+} compartments have in fact Ca^{2+} concentration ranging between 300-500 μM (Camello et al., 2002; Rizzuto et al., 1998). Under the resting conditions, Ca^{2+} content in intracellular stores regulate to equilibrate between the active Ca^{2+} uptake and passive Ca^{2+} leak. Ca^{2+} signaling can thus be derived by rising the cytoplasmic Ca^{2+} concentration either by uptake of extracellular Ca^{2+} or release the Ca^{2+} from intracellular stores, which results in changes of the free Ca^{2+} concentration. Due to the essential role of Ca^{2+} homeostasis for cells, it is not unexpected that viruses have evolved tools to manipulate cellular Ca^{2+} signaling to favor their replication (Zhou et al., 2009; Saurav et al., 2021). To date, several ion channels of viral origin have been identified and designated as viroporins. Out of these, only a few have shown to act as Ca^{2+} channels (Hyser and Estes., 2015). Overall, most viroporins so far identified have been identified in RNA viruses as are proton channels or non-specific monovalent cation channels (Hyser and Estes., 2015). Rotavirus NSP4 and Picornavirus 2B among RNA viruses, and SV40 virus VP4 and CMLV GAAP, among DNA viruses, have been identified as Ca^{2+} channels (Scott and Griffin., 2015). Among Herpesviruses, the HCMV UL37x1 protein (vMIA, viral Mitochondria-localized inhibitor of apoptosis) has been suggested as a candidate viroporin able to dysregulate Ca^{2+} homeostasis, although no functional evidence of it as Ca^{2+} channel have been reported. However, UL37x1 is known to traffic from mitochondria to ER and to block Bax-mediated apoptosis by directly interacting with Bax and sequestering it at mitochondria membranes, thus it has been defined as viral Mitochondria-localized inhibitor of apoptosis (vMIA) (Arnoult et al., 2004). Immunofluorescence studies, suggested that UL37x1 may induce cell rounding and swelling, and the release of Ca^{2+} from ER (Sharon-Friling et al., 2014). Lowering of ER Ca^{2+} store levels by UL37x1 has been suggested to exert protective effects on intrinsic apoptosis, which contributes to the overall activity of UL37x1 as vMIA (Sharon-Friling et al., 2014).

Viroporins can be classified based on their topology. The Class I viroporins contain proteins with single TMD, Class II contain proteins with two TMDs. These classes are further classified based on the orientation of their termini: subclass A with luminal N-terminus and cytosolic C-terminus, and subclass B with luminal C-terminus and cytosolic N-terminus (Hyser and Estes., 2015). Moreover, a third class of viroporins has been proposed to include viral-encode ion channels containing 6-7 TMDs, such as the vGAAP (Carrara et al., 2017). This third class of viroporins thus include the CMLVGAAP and the pUS21 of HCMV (Luganini et al., 2018). Since the pUS12 also show viroporin activity and it has structural similarity to pUS21 with GAAP, it can also be considered to be a class

III viroporin.

The findings of pUS12 as a Ca^{2+} -conducting viroporins, could allow to hypothesize some of its functions. From the phylogenetic point of view, pUS12 and hGAAP have an identity and similarity of amino acid of 14.9% and 30.7% respectively, suggesting an evolutionary conservation of the structural protein scaffold of cellular TMBIM origin. These conservations are only observed in two US12 family proteins: pUS12 and pUS21. pUS21 has a higher percentage of similarity with hGAAP (17.4% identity and 32.9% similarity) compared to pUS12.

In response to a viral infection, many cells undergo apoptosis. Thus, many viruses have evolved mechanisms to modulate the host cell apoptosis. We can believe that the presence of two viroporins in the US12 gene family can contribute to the HCMV toolbox to counteract premature death of infected cells. pUS12 is an early protein which is localized in the Golgi-derived membrane in cVAC. In contrast, pUS21 is a late protein and is localized in the Endoplasmic reticulum (ER) (Luganini et al., 2018). By deploying two different viroporins located within the two main intracellular Ca^{2+} stores, and expressed within time frames that cover almost all the length of the replicative cycle, HCMV could reduce the Ca^{+} content of intracellular stores so reducing the cell susceptibility to intrinsic pro-apoptotic stimuli that unavoidably arise during host cell infection. In addition, it is also intriguing the localization of pUS12 within the cVAC, where HCMV acquires its final tegument and envelope and starts the final egression phase. Related to this, when the putative di-aspartyl pH sensor residues of pUS12 (D218 and D246) was mutated in the context of an infectious TR recombinant virus, a 2-fold reduction of viral growth was observed in endothelial and epithelial cells. Thus, it could be hypothesized that the integrity of the di-aspartyl pH sensor of pUS12, and likely its viroporin activity, is required within the cVAC of producer cells to contribute to generate HCMV virions fully competent for efficient infection and replication in endothelial and epithelial cells. However, further investigations are required to experimentally prove this hypothesis.

In conclusion, the main findings of this chapter include the first evidence of pUS12 as tropism factor required for efficient HCMV productive replication in endothelial and epithelial cells, as well as the identification of pUS12 as type III viroporin that may impact cellular Ca^{2+} homeostasis. The determination of this biochemical function of pUS12 paves the way for further studies to investigate the importance of pUS12's functions in the context of the last phases of HCMV replication.

Chapter 4 - Exploitation of the structures of US12 and US21 proteins for the identification of compounds with antiviral activity

4.1 Materials and Methods

4.1.1 Structure-based virtual screening

The Drug Bank (<https://go.drugbank.com/>) was interrogated to search for Calcium Channel Blockers (CCBs) compounds through the code “Voltage dependent calcium channels”. Then, among the 1212 molecules that were available for the search term, 249 CCBs were selected for further analysis. Using this CCB library, an *in silico* structure-based virtual screening was performed on targets represented by the predicted three-dimensional structure of pUS12 and pUS21. To this end, the CCB library was loaded on the AutoDock software v4 (Morris et al., 1998) obtained from the Yasara platform, along with the structures of either pUS12 or pUS21. The binding energy and the dissociation constant between each CCB molecules and the pUS12 and pUS21 structures were calculated by the software. The binding energy is the sum of the intermolecular forces that acts upon the receptor and ligand process (Matossian et al., 2014). In our *in silico* analysis, the binding energy is between a CCB molecule and the structure of either pUS1 or pUS21. More the binding energy, less chances of the ligand-protein interactions to be broken. The various bond interactions between the molecules and the protein structures were further analysed by the Discovery Studio Client software (BIOVIA, Dassault Systèmes, Discovery studio client, 21.1, San Diego: Dassault Systèmes, 2021).

4.1.2 Cells and culture conditions

Low passage number of human foreskin fibroblasts (HFFs) were grown as a monolayer in Dulbecco Modified Eagle’s Medium (DMEM) (Euroclone) supplemented with 10% Fetal Bovine Serum (FBS) (Euroclone), 2 mM glutamine, 1 mM sodium pyruvate, 100 U/ ml penicillin and 100 µg/ ml streptomycin sulphate.

4.1.3 BAC recombineering and virus preparations

The HCMV TR BAC was used to generate the mutant viruses. BAC recombineering was performed to generate the recombinant HCMV viruses. The TR Δ US12 BAC was generated as described in Chapter 2, while the generation of the TRUS21stop BAC was described previously by Lukanini et al., 2018.

The TR Δ US12-US21stop BAC clone (**Figure 32**), is a double mutant BAC derivative in which the US12 ORF is replaced by GalK-kan cassette and the US21 ORF has a stop codon inserted at the 5’ end of its ORF (**Figure 32**). Thus, both US12 ORF and US21 ORF are inactivated. To generate the TR Δ US12-US21stop BAC, first the new set of primers US12F and US12R (**Table 5**) was used to generate the Δ US12 cassette. The 3’ end of the forward and reverse primers are specific to sequence that amplify a galK-kan cassette from the pgalk-kan, while 50 bp at their 5’ end tail are homologous to the sequences flanking the US12 ORF (**Table 1**). Then, 100 ng of the Δ US12 galK-kan cassette was electroporated in *E. coli* SW102 cells containing the TR US21 stop BAC. Since *E. coli* SW102 express γ -red encoded recombination proteins (exo, bet, gamma) upon temperature shifting, bacteria were

grown at 32° C and then at 42° C for 15 minutes before electroporation to induce the expression of recombination machinery. After electroporation, cells are recovered for 1 h at 32° C, and then plated on LB agar plates containing 15 µg/ml Chloramphenicol (Caf) and 25 µg/ ml kanamycin (Kan) for 24-48 h.

The colonies that appeared on the plates were re-streaked on MacConkey agar plates containing 0.2% galactose and 15 µg/ ml Caf. Several single Gal-positive TRΔUS12-US21stop clones that produced bright red colour colonies were further characterized for US12 replacement by PCR. Recombinant TRΔUS12-US21stop BAC was then purified from SW102 cells with NucleoBond Xtra BAC (Macherey-Nagel) according to the manufacturer instructions. In this BAC clone, the US12 cassette is replaced by Galk-kan cassette and the US21 ORF has a stop codon inserted at the 5' end of its ORF (**Figure 32**).

Infectious recombinant HCMV viruses TRΔUS12, TRUS21stop and TRΔUS12-US21stop were reconstituted in HELFs by co-transfection of the correspondent recombinant BAC and a plasmid expressing HCMV pp71 using SuperFect transfection reagent (Qiagen), according to the manufacturer instructions. Transfected HELFs were then cultured until a marked cytopathic effect were observed.

Viral stocks were prepared by infecting HFF cells at a virus-to-cell ratio of 0.01. Cells were supplemented with 5% heat inactivated FBS and cultured until a marked cytopathic effect was observed. Viral stocks were titrated using a plaque assay based on the IEA (IE1+IE2) indirect immunoperoxidase staining procedure on HFF cells as described (Cavaletto et al., 2015; Luganini et al., 2017).

Table 5: *Oligonucleotides used for PCR and sequencing*

Primer Name	Sequence 5' → 3'
US12F	AAACTTGCCGGGTACCTAAAGCCCCGACGACTGTTTCGTCGAGCACCCGTCCTGTTGACAA TTAATCATCG
US12R	GCGGGGGCACCCGGACAGTACGACAGATTAGGTGATAGAAACGTTTTTTTCTCAGCAAAA GTTCGATTTA

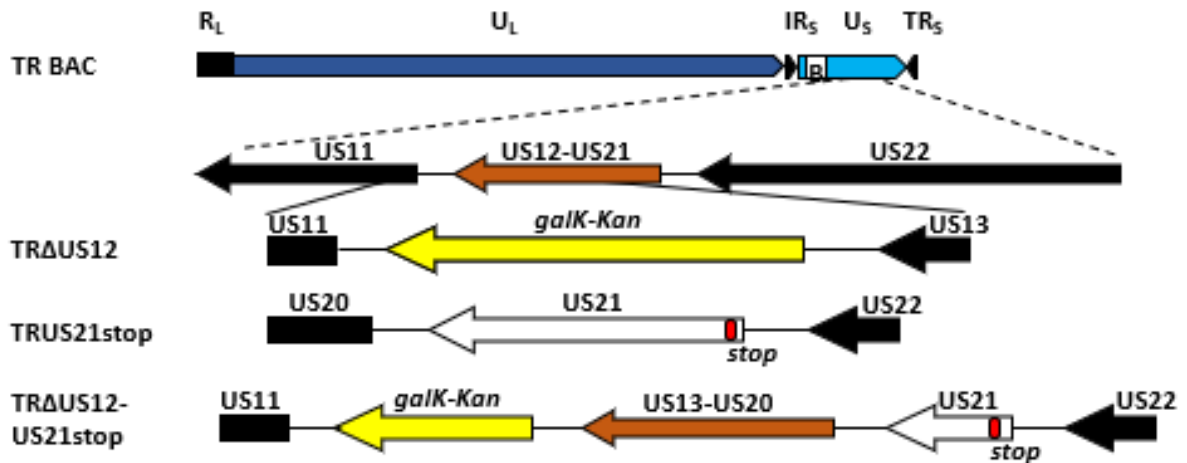


Figure 32: Schematic representation of the TR Δ US12, TRUS21stop, and TR Δ US12-US21stop BACs. The *Galk-Kan* cassette replaced the US12 ORF in the TR Δ US12. In TRUS21 stop, a stop codon was added at the 5' end of US21 ORF, such that, the translation of the US21 ORF is interrupted by the stop codon resulting in the inactivation of the expression of US21. In TR Δ US12-US21 stop, the US12 ORF is replaced by the *Galk-Kan* cassette and along with this a stop codon is at the 5' end of US21 ORF.

4.1.4 Preparation of stock solutions of the CCBs

Some of the CCBs selected by the structure-based virtual screening were purchased from Merck Sigma. Efonidipine, niguldipine, azelnidipine, and lercanidipine were then resuspended in DMSO to obtain a stock concentration of 50 mM that was stored at -20° C protected from light.

4.1.5 Cell Cytotoxicity assay

To evaluate the cytotoxicity of the CCBs, HFF cells were seeded in clear bottom 96-well plates (12,000 cells/well). After 24 h, cells were treated with increasing concentrations of the vehicle (DMSO or of the different CCB starting from 1.25 μ M to 400 μ M. For the background correction, wells with only DMEM and no cells were also included. After five days of incubation, cells were processed for the measurement of cell viability using the 3-(4,5-dimethylthiazol-2-yl)-2,5-diphenyltetrazolium bromide (MTT) method (Pauwels et al., 1988). After the background subtraction, the values were analysed with GraphPad Prism to calculate the cell cytotoxicity 50 (CC₅₀) values.

4.1.6 Antiviral assay

A focus forming reduction assay (FFRA) was performed to measure the effect of CCB molecules on the replication of TRwt, TR Δ US12, TRUS21 stop, and TR Δ US12-US21 stop viruses. FFRA exploits an Immediate-Early proteins (IEA) immunostaining to detect foci of HCMV-infected host cell. To this end, 20,000 HFF cells were plated in 96-well flat bottom plates. The plates were incubated overnight

at 37° C, 5% CO₂. The next day, cells were treated with non-cytotoxic ranges of the CCB molecules in triplicates starting from 1 h before infection with MOI 100 PFU/ well of TRwt, TRΔUS12, TRUS21 stop or TRΔUS12–US21 stop viruses. The virus attachment was facilitated by performing a centrifugation at 2000 rpm for 30 mins at RT. The cells were then incubated for 2 h at 37° C. After 2 h, viral inoculum were removed and cells were incubated in DMEM medium containing 5% FBS, 1.2% methylcellulose, and non-cytotoxic concentrations of the CCB molecules. Plates were then incubated at 37° C for seven days.

Then, cells were fixed with 50% acetone+50% methanol and foci of infected HFFs were detected by a mouse mAb IEA (IE1+IE2) (Virusys) followed by immunoperoxidase staining using Vectastain ABC-HRP kit. Foci of IEA-positive cells were then microscopically counted and results analyzed using the GraphPad Prism software.

4.1.7 Statistical analysis

The EC₅₀±SD values were analyzed for significance using the student's t-test and P values <0.05 were considered significant. The statistical tests were performed using GraphPad Prism.

4.2 Results

4.2.1 Structure-based virtual screening identifies CCB molecules that target the pUS12 and pUS21 predicted structures

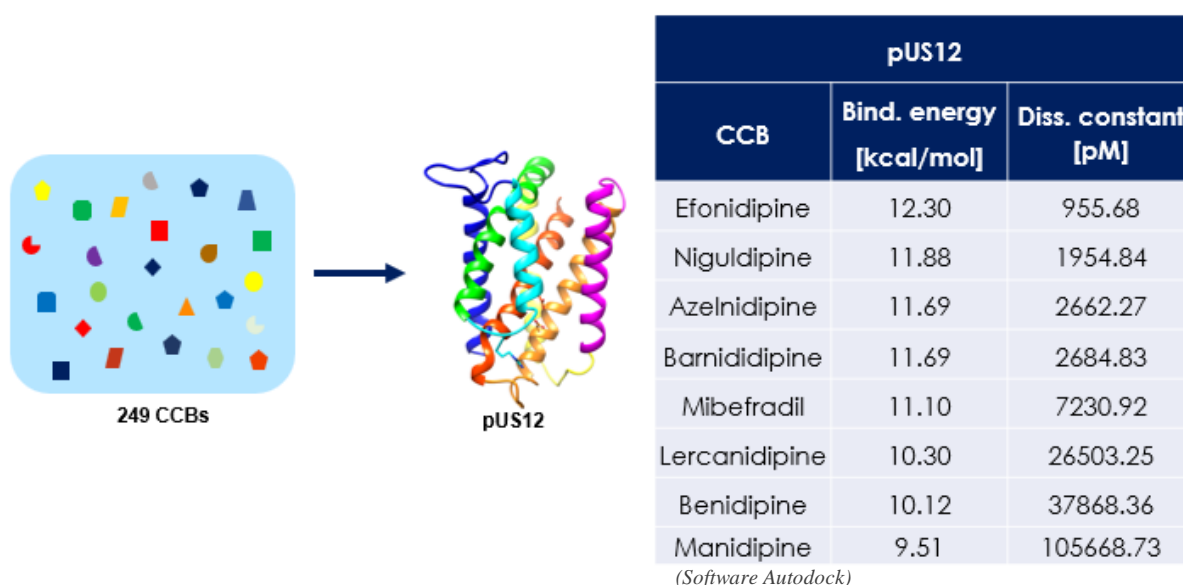
Based upon the knowledge acquired by studying the pUS12 and pUS21 viroporins, we thought that it could be of interest to exploit their predicted protein structures to identify molecules that may interfere with their viroporin activity and perhaps affect HCMV replication.

With this in mind, we launched a computational drug repurposing attempt based on the pUS12 and pUS21 putative structure models as targets for molecular docking, binding free energy calculations, and thus to predict protein-ligand interactions. Therefore, using the AutoDock suite, we performed an *in silico* structure-based virtual screening of a library of 249 Calcium Channel Blockers (CCBs) compounds that were selected from an online drug database. The predicted pore cavities structures of the US12 and US21 viroporin were thus used as drug targets. CCBs are a group of antihypertensive drugs that disrupt the movement of Ca^{2+} through calcium channels.

The *in silico* screening allowed to select different dihydropyridines (DHPs) CCBs molecules as suitable binding partners of pUS12 and pUS21 (**Figure 33**)

Especially, among the 8 DHPs identified as those with the best binding energy values, efonidipine, niguldipine and azelnidipine were predicted to interact with both pUS12 and pUS21 with the highest binding energy and the low disassociation constants (**Figure 33**).

A



B

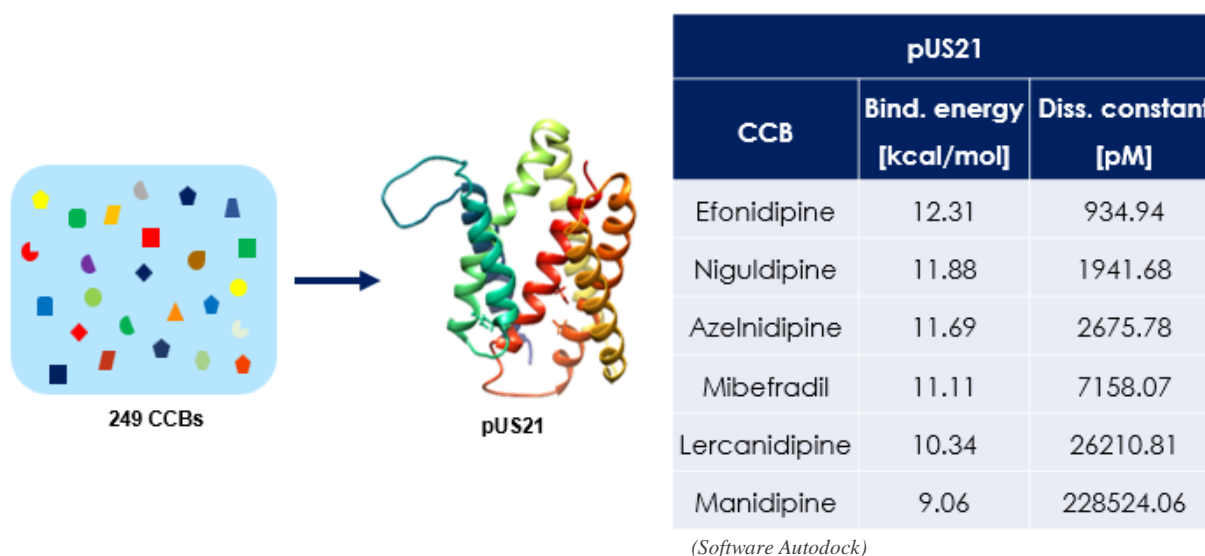


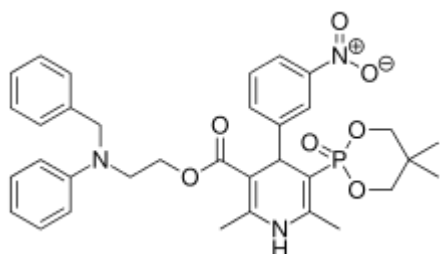
Figure 33: Results of the *in silico* structure-based virtual screening of a CCB library using the predicted structures of pUS12 (A) and pUS21 (B) as molecular targets. *In silico* molecular docking was performed using the AutoDock software and resulted in identifying potential interacting CCBs molecules.

Dihydropyridines are a type of CCB that block the activity of calcium channels located in the heart, muscle cells, and arterial blood vessels, thereby reducing the entry of calcium ions into cells. DHPs represent one of the most important heterocyclic scaffolds found in many drugs, and not limited to L-type CCBs (antihypertensive) (Bandyopadhyay et al., 2017).

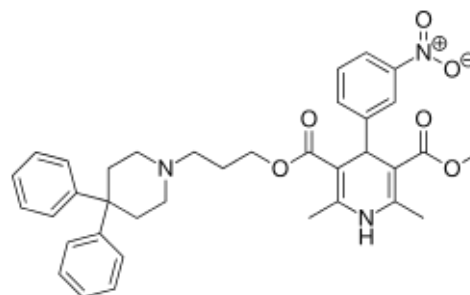
Efonidipine was launched in 1995 as a CCB able to block both L and T-type Ca^{2+} ion channels (Tanaka and Shigenobu., 2002) (**Figure 34 A**). Niguldipine is a diarylmethane and along with being a CCB, it

is also a α 1-adrenergic antagonist (**Figure 34 B**). Azelnidipine is relatively a new CCB drug that has been approved in Japan for hypertension and it has its selectivity for L-type calcium channel (**Figure 34 C**). Among remaining selected CCBs, lercanidipine (**Figure 34 D**), also known with the trade name Zanidip and approved as an anti-hypertensive drug in 1997, was considered for further analysis.

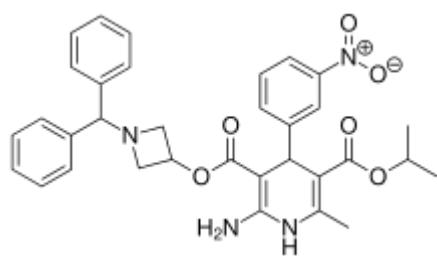
A



B



C



D

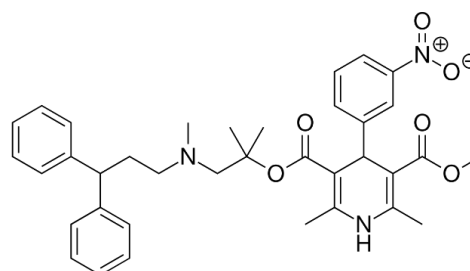
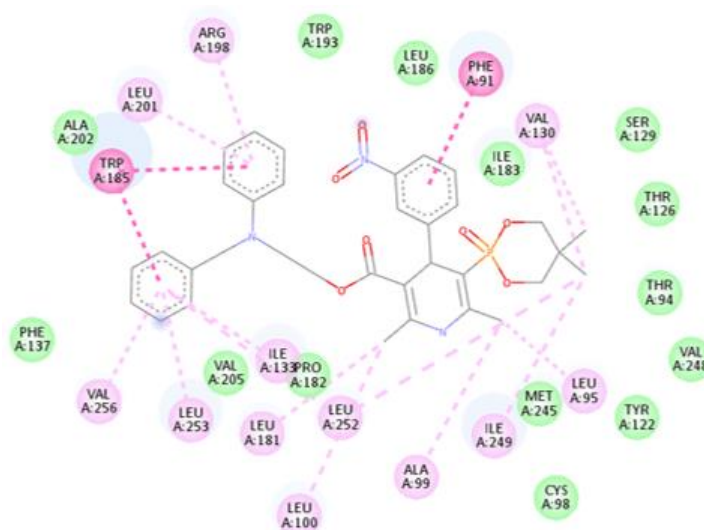
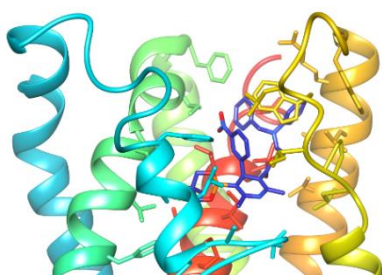


Fig 34: Chemical structures of the selected DHPs calcium channel blockers. A) efonidipine, B) niguldipine, C) azelnidipine and D) lercanidipine.

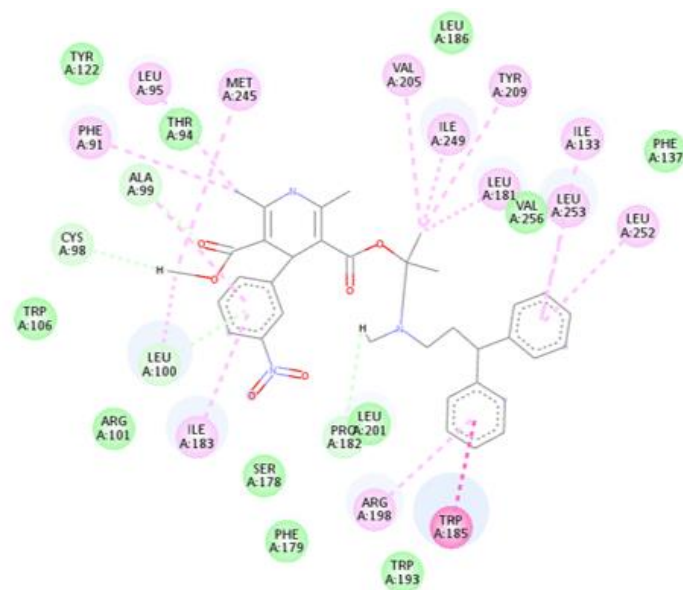
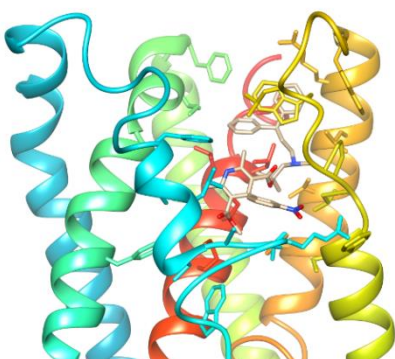
Then, the binding mode of two representative DHPs, namely efonidipine and lercanidipine, was further analyzed within the putative pore of pUS12 and of pUS21 by using the Discovery Studio platform (BIOVIA, Dassault Systèmes, Discovery studio client, 21.1, San Diego: Dassault Systèmes, 2021).

Especially, the efonidipine was predicted to bind within the putative pore structures of both pUS12 (**Figure 35 A**) and pUS21 (**Figure 36 A**) and to engage the surrounding amino acid residues by various types of interactions, such as Van der Waals bonds, carbon-hydrogen bonds, Pi-donor hydrogen bonds, Pi-Pi stacked interactions, Alkyl interactions, and Pi-alkyl interactions.

A) Efonidipine



B) Lercanidipine



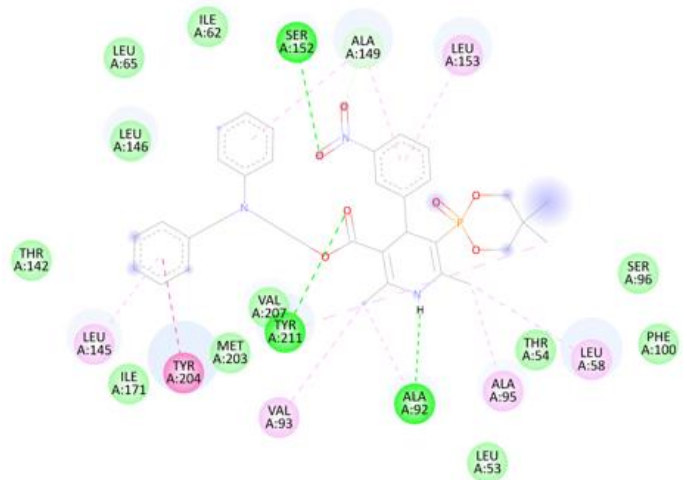
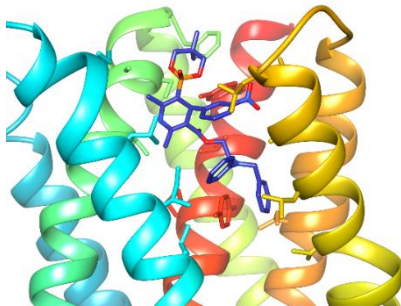
Interactions

- van der Waals
- Carbon Hydrogen Bond
- Pi-Donor Hydrogen Bond
- Pi-Pi Stacked
- Alkyl
- Pi-Alkyl

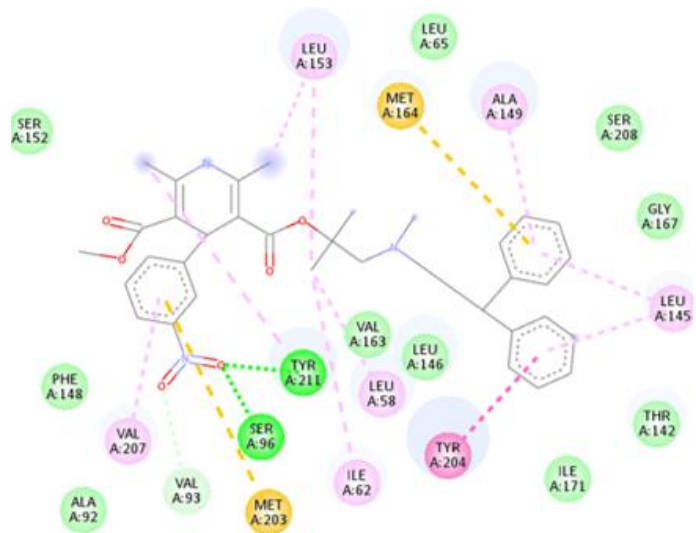
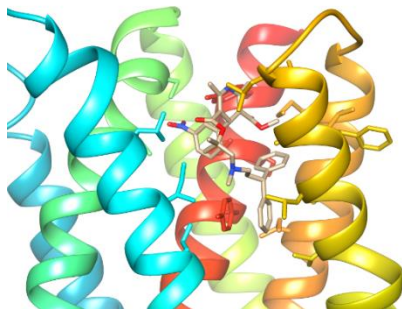
Figure 35: Molecular docking between efonidipine (A) and lercanidipine (B) and the pUS12 structure. The CCB molecules bind within the pUS12 structure by interacting with different amino acids of the protein that is surrounding the molecule via various types of interactions. Molecular docking prediction made by the Discovery Studio software.

Also, the lercanidipine was predicted to establish different types of interactions with both pUS12 (Figure 35 A) and pUS21 structures (Figure 36 B).

A) Efonidipine



B) Lercanidipine



Interactions

■	van der Waals
■	Carbon Hydrogen Bond
■	Pi-Donor Hydrogen Bond
■	Pi-Pi Stacked
■	Alkyl
■	Pi-Alkyl

Figure 36: Molecular docking between efonidipine (A) and lercanidipine (B) and the US21 protein structure. The CCB molecules bind with the pUS21 within the inner TMD structure s by various types of interactions. This image illustrates the molecular docking prediction made by the Discovery Studio

software.

4.2.2 Effect of selected CCB molecules on HCMV replication

Prompted by these appealing predictions, we tested the four selected CCBs for a possible inhibitory activity against the HCMV TRwt strain and three TR derivatives in which the genes encoding US12 and US21 were inactivated one at a time or both. To this end, Focus Forming Reduction Assay (FFRA) were performed in HFFs infected with TRwt, TRUS21 stop, TR Δ US12 or TR Δ US12-US21stop.

The antiviral effect of the tested CCBs was measured as 50% Effective Concentration (EC₅₀). To assess the cytotoxicity of CCBs, viability cell assay were performed for the different molecules on uninfected HFF cells to measure the value of 50% Cytotoxic Concentration (CC₅₀). Since the Selectivity Index (SI) is equivalent to the ratio of CC₅₀ to EC₅₀, high SI values indicate safe and effective compound (**Table 6**).

Efonidipine produced a CC₅₀ concentration of 339.7 μ M in HFF cells. When the antiviral effect of efonidipine was measured against the different HCMV, the double mutant (TR Δ US12 US21 stop) showed a 2-fold increase in the EC₅₀ value (EC₅₀ 7.04 μ M) compared to the TRwt virus (EC₅₀ 3.27 μ M). The two single mutant viruses (TR Δ US12 and TRUS21 stop) also showed higher EC₅₀ values compared to that of TRwt, of 4.60 and 5.15 μ M, respectively. (**Figure 37 A**).

Lercanidipine showed an CC₅₀ concentration 126.5 μ M in HFF cells. Likely to efonidipine, the lercanidipine showed a EC₅₀ value of 2.91 μ M for TRwt that was measured increased for TR Δ US12 at 5.04 μ M, and at 4.96 μ M for TRUS21 stop. Again, the EC₅₀ value measured for the double mutant virus in which US12 and US21 were both inactivated, showed an increase by 3-fold (EC₅₀ 7.50 μ M) compared to that measured for TRwt. (**Figure 37 B**).

The effect of niguldipine on HFF cells viability allowed to asses a CC₅₀ value of 187.4 μ M. Niguldipine potently inhibited TRwt replication with a EC₅₀ 1.060 μ M. When tested against TR Δ US12, it showed a EC₅₀ of 1.393 μ M, while against the TRUS21 stop virus the measured EC₅₀ was 2.111 μ M. However, in the absence of functional US12 and US21 genes, there was a 2-fold increase of the EC₅₀ values (3.183 μ M) for the TR Δ US12-US21stop virus as compared to the TRwt (**Figure 37 C**).

Finally, a CC₅₀ of 194.89 μ M was measured in HFF cells for azelnidipine. Its antiviral activity against TRwt produced an EC₅₀ of 1.628 μ M. Azelnidipine was active against both TR Δ US12 and TRUS21 stop viruses with EC₅₀ 2.414 and 2.155 μ M, respectively. Again, the absence of both US12 and US21 genes caused a 5-fold increase of the EC₅₀ values (5.231 μ M) measured for the TR Δ US12-US21stop virus compared to that observed for TRwt (**Figure 37 D**).

Taken together, these results indicate that all the selected CCBs exerted a potent antiviral activity against HCMV TRwt replication in the low-micromolar range. Intriguingly, an increase of more than 2-fold in the EC₅₀ values of mutant viruses compared to TRwt was observed, particularly when both US12 and US21 were both inactivated, thus suggesting a likely involvement of pUS12 and pUS21 viroporin activity in the overall antiviral activity of these CCBs against HCMV. A significant difference in the EC₅₀ values was in fact measured between the TRwt and TR Δ US12-US21 stop viruses (**Figure 38**).

Although further investigations are required to confirm that indeed is the binding of the selected CCBs within the putative pUS12 and pUS21 pores that contributes to the observed antiviral activity,

this result is evocative of CCBs as possible candidates for repurposing drugs against HCMV.

Table 6: Antiviral activity of the different CCBs against TR viruses.

	Efonidipine μM (CC_{50} 339.7 μM)		Lercanidipine μM (CC_{50} 126.5 μM)		Niguldipine μM (CC_{50} 187.4 μM)		Azelnidipine μM (CC_{50} 194.89 μM)	
	EC_{50}	SI	EC_{50}	SI	EC_{50}	SI	EC_{50}	SI
TRWT	3.27	103.88	2.91	43.47	1.060	176.79	1.628	119.71
TR Δ US12	4.60	73.84	5.04	25.09	1.393	134.24	2.414	80.73
TRUS21 stop	5.15	65.96	4.96	25.50	2.111	88.77	2.155	90.43
TR Δ US12-US21 stop	7.04	48.25	7.50	16.86	3.183	58.87	5.231	37.25

The 50% Effective concentration (EC_{50}) and 50% Cytotoxic concentration (CC_{50}) values were calculated by the GraphPad Prism software. Selectivity Index (SI) values were determined as the ratio between CC_{50} and EC_{50} .

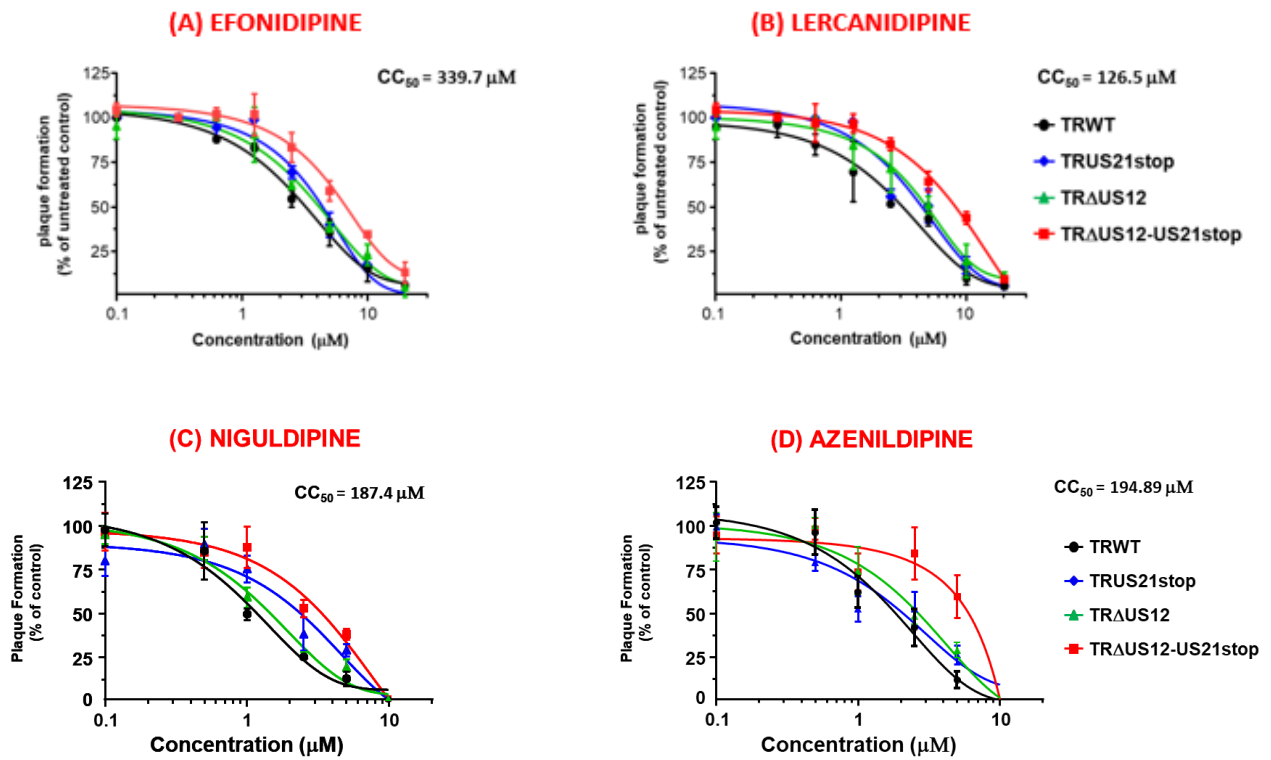


Figure 37: Effect of selected CCB molecules on different TR viruses. HFF cells were infected with 100 PFU/ well of TRwt, TRΔUS12, TRUS21 stop and TRΔUS12 US21 stop viruses. The cells were treated with increasing concentration of (A) Efonidipine, (B) Lercanidipine, (C) Niguldipine and (D) Azelnidipine 1 h before, during the virus adsorption and post infection (maintained throughout the experiment). The virus replication was quantified after 7 days p.i by FFRA. To determine the cell viability, after 5 days of incubation of HFF cells with the CCB molecules, an MTT assay was performed. EC_{50} and CC_{50} values were calculated using the software GraphPad Prism.

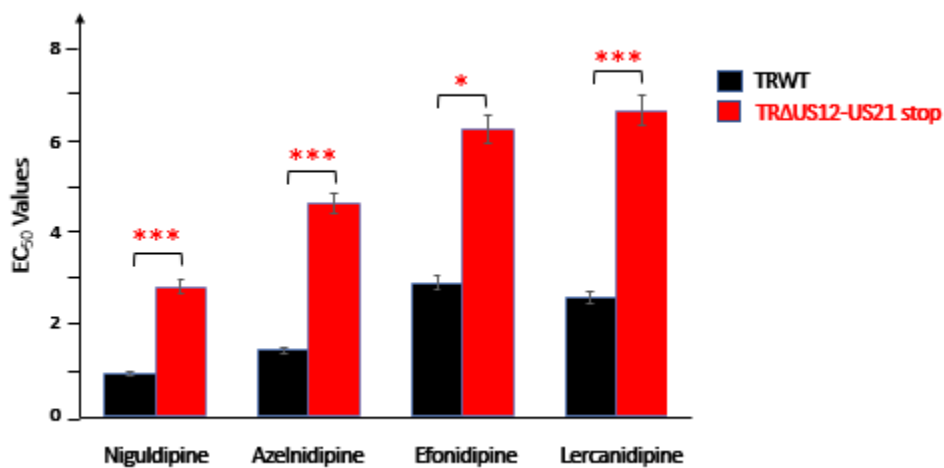


Figure 38: Comparison of the EC_{50} values between the TRwt and TRΔUS12-US21 stop. Comparison of the EC_{50} values between the TRwt and TRΔUS12-US21stop for each of the CCB molecule. Data are analysed by unpaired t-test. * $P < 0.01$, ** $P < 0.001$, *** $P < 0.0001$.

4.3 Discussion

Viroporins are ion channels encoded by many viruses that may contribute to efficient virus replication and thereby viral pathogenesis (Nieva et al., 2012). Due to their importance for the viral life cycle, viroporins are potential targets for antiviral drug development and antiviral therapy. The pharmacological targeting of viroporins is a recognized, yet largely unexplored, therapeutic strategy, so far only used for Influenza A with the drugs amantadine and rimantadine (Scott and Griffin., 2015). Amantadine in fact targets the M2, a virus-encoded proton channel required for the uncoating of Influenza A virus (Pinto et al., 1992). Relevant to this advancement, the identification and characterization of new viroporins able to dysregulate cellular ion homeostasis may represent an important avenue for the identification of new effective antiviral agents and the development of new therapeutical strategies.

Ion channel therapeutics have been used in areas like cardiac medicines. Among these drugs, calcium channel antagonists, also known as the Calcium Channel blockers (CCB) are widely used for many disease indications. The use of CCBs started as early as 1970s and they were prescribed for alterations of heart and blood vessels, such as hypertension, angina, some abnormal heart rhythms, and the Raynaud's phenomenon ("Calcium Channel Blockers - StatPearls - NCBI Bookshelf"). The CCBs are classified into two major categories, either non-dihydropyridines or dihydropyridines. The dihydropyridines include many drugs which the name ending in "pine." By hampering the Ca^{2+} flux through cellular calcium channels, the two CCB classes both help to relax and widen arteries. However, the non-dihydropyridines also has an additional effect on heart's conduction system and can help to control heart rhythms (Cooper and Dimri., 2022).

The calcium channel antagonists bind to the L-type voltage-gated calcium channels in the heart, vascular smooth muscles and pancreas, thus blocking the inward flow of calcium ions. As a result, the blood vessels relax, and the heart muscles receives more oxygenated blood.

Interestingly, verapamil, a drug used to treat hypertension, atrial fibrillation and angina was successful in containing the Influenza A virus (Alam et al., 2016). Compounds blocking the L-type calcium channels like nimodipine, diltiazem was found to inhibit the Ebola virus in vivo (Sakurai et al., 2015). Verapamil was also observed to modulate endosomal trafficking by inhibiting both Ca^{2+} and K^{+} channels in SV40 (Dobson et al., 2020). Taken together these observations, the exploitation by some viruses of Ca^{2+} signaling may lead to hypothesize the re-purposing of Calcium Channel Blockers as antiviral agents.

The US12 and US21 proteins of HCMV function as calcium ion channels and therefore we thought that it could be of interest to exploit their predicted protein structures as drug targets to identify CCBs molecules that may interfere with their viroporin activity, thus affecting HCMV replication. An *in silico* virtual screening approach was thus adopted to filter out specific CCB molecules from a virtual collection of CCBs and to obtain molecules with the best docking properties. To this end, a structure-based virtual screening was performed by means of to identify molecules of a CCB library with best the binding energy and disassociation constant.

Four CCB molecules were selected on the basis of the predicted best binding energy, favorable dissociation constants against both pUS12 and pUS21, and commercial availability. They were Niguldipine, Azelnidipine, Lercanidipine and Efonidipine.

Niguldipine is a compound belonging to the class of diphenylmethanes. Niguldipine has a high affinity towards the calcium ion channels and also towards a subtype of α -1 adrenoceptors (Boer et al., 1989). It binds to the α -1 adrenergic receptor and inhibits the binding of other substance, thereby the influx of Ca^{2+} into the smooth muscle cells is reduced and prevents the smooth muscle contraction (Schwinn and Price., 1999). Niguldipine was approved by the US Food and Drug Administration (FDA) and European Agency for the Evaluation of Medicinal Products (EMA) as an antihypertensive drug (Amaral and Kunzelmann., 2007).

Azelnidipine is also a diphenylmethane derivative jointly developed by Ube industries, Ltd. (Yamguchi, Japan) and Daiichi Sankyo Co, Ltd. (Tokyo, Japan) and launched in 2003. Azelnidipine has been approved by the FDA, European Chemical Agency (ECHA), Japan and China for its use as an antihypertensive drug (Wellington and Scott., 2003). The antihypertensive effect of azelnidipine is based on the inhibition of transmembrane Ca^{2+} influx throughout the voltage-dependent channels of vascular smooth muscle cells (Chen et al., 2015). Azelnidipine has a selectivity to L-type Ca^{2+} channels and has a strong lipophilicity and affinity to membranes of vascular smooth muscle cells. It has a gradual onset of action and produces a long-lasting decrease in blood pressure, with only a small increase in heart rate (Wellington and Scott., 2003).

Lercanidipine, commercially known as Zandip, is a diphenylmethane compound that was approved by FDA, Europe and UK in a total of 61 countries as an anti-hypertensive calcium channel blocker (<https://www.recordati.com/public/pub.aspx?id=357>) in 2002. Lercanidipine acts as a competitive antagonism of L-type calcium channels, thus leading to smooth muscle relaxation and vasodilation (Herbette et al., 2010). Lercanidipine inhibits the influx of extra cellular calcium by possibly deforming the channel, inhibiting ion-control gating mechanisms, and/ or interfering with the release of calcium from the sarcoplasmic reticulum. The decrease in intracellular calcium inhibits the contractile processes of the myocardial smooth muscle cells, causing dilation of the coronary and systemic arteries, increased oxygen delivery to the myocardial tissue, decreased total peripheral resistance, decreased systemic blood pressure and decreased afterload (McClellan and Jarvis., 2000).

Efonidipine was launched in 1995 by Shionogi and Co. under the name Landel. It was later approved by FDA and also Drug Controller General of India (DCGI) and marketed with the brand name Efonta (Ajanta Pharma Ltd. India) and Efnocar (Zuventus health care Ltd. India) (Patel et al., 2019). Efondipine is an antihypertensive and antianginal drug that blocks both the L- and T- type Ca^{2+} channels. Because of its inhibition to T-type Ca^{2+} channels, efonidipine acting on SA node (sinoatrial node) prolong phase-4 depolarization decreasing the heart rate. Along with this, the demand for myocardial oxygen also reduces and there is an increase of the blood flow to the coronary arteries and thereby reduces the chances of myocardial ischemia (Tanaka and Shigenobu., 2002). Efonidipine in addition to this, also increases the glomerular filtration rate (GFR) without increasing intra-glomerular pressure and filtration (Hayashi et al., 2010). This increase leads to the prevention of renal damage that is associated with hypertension.

The effects of these CCBs on the replication of HCMV. The TRwt was indeed observed to be very sensitive to the four CCBs, with EC₅₀ values ranging from 1 μM for nifedipine to 3.27 μM for efonidipine (**Table 6**). As for comparison, for the TR strain, an EC₅₀ value of 3 μM was measured for ganciclovir (GCV), the reference antiviral agent for HCMV. Interestingly, the EC₅₀ values measured for all the tested CCBs when the double mutant virus TRΔUS12-US21stop was examined, were increased by two-fold as compared to those of TRwt. This observation may thus suggest an involvement of pUS12 and pUS21 viroporin activity in the overall antiviral activity of these CCBs against HCMV.

Although further investigations are required to confirm that indeed is the binding of the selected CCBs within the putative pUS12 and pUS21 pores that contributes to the observed antiviral activity, the results presented in this chapter suggest that the anti-HCMV activity of the four CCB molecules may be due, at least in part, to their predicted ability to bind to pUS12 and pUS21 structures, thus interfering with their function, and in doing so, affecting the efficient HCMV replication. However, we can assume that the specific targeting of pUS12 and pUS21 by the selected CCBs may contribute to the overall anti-HCMV that we have observed by adding up or synergizing with the inhibition of the activity of cellular channels that can be blocked by these CCBs.

Moreover, these results further sustain that viroporins may represent a source of yet unexplored antiviral targets that spans through various virus families, and that may be considered for new paths for antiviral drug discovery. Moreover, given the low mutation rates in DNA viruses, identifying viroporins, such as U12 and US21, as drug targets is an attractive scenario for the identification and development of new antiviral agents. Finally, these results are evocative of CCBs as possible candidates for repurposing approved drugs against HCMV to design and develop new intervention strategies.

References

References

- Ahn J, Jang W, Hayward G. "The Human Cytomegalovirus IE2 and UL112-113 Proteins Accumulate in Viral DNA Replication Compartments That Initiate from the Periphery of Promyelocytic Leukemia Protein-Associated Nuclear Bodies (PODs or ND10)." *Journal of Virology*. **1999**.73 (12): 10458–71. <https://doi.org/10.1128/JVI.73.12.10458-10471.1999>.
- Alam M, Mostafa A, Kanrai P, Müller C, Dzieciolowski J, Lenz E, Kuznetsova I, Schult-Dietrich P, Ziebuhr J, Dietrich U, Pleschka S. "Verapamil Has Antiviral Activities That Target Different Steps of the Influenza Virus Replication Cycle." *Journal of antivirals and Antiretrovirals*. **2016**.8(4). 121-130.<https://www.longdom.org/open-access/verapamil-has-antiviral-activities-that-target-different-steps-of-theinfluenza-virus-replication-cycle-jaa-1000147.pdf>.
- Amaral M, Kunzelmann K. "Molecular Targeting of CFTR as a Therapeutic Approach to Cystic Fibrosis." *Trends in Pharmacological Sciences*.**2007**.28 (7): 334–41. <https://doi.org/10.1016/J.TIPS.2007.05.004>.
- Arnoult D, Bartle L, Skaletskaya A, Poncet D, Zamzami N, Park P, Sharpe J, Youle R, Goldmacher V. "Cytomegalovirus Cell Death Suppressor VMIA Blocks Bax- but Not Bak-Mediated Apoptosis by Binding and Sequestering Bax at Mitochondria." *Proceedings of the National Academy of Sciences of the United States of America*.**2004**.101 (21): 7988–93. https://doi.org/10.1073/PNAS.0401897101/SUPPL_FILE/01897SUPPTEXT.HTML.
- Bandyopadhyay D, Salazar T, Gonzalez A. "Dihydropyridines as Calcium Channel Blockers: An Overview." *Journal of Analytical & Pharmaceutical Research*.**2017**.5 (4): 5–7. <https://doi.org/10.15406/japlr.2017.05.00148>.
- Behnke J, Eskelinen E, Saftig P, and Schröder B. "Two Dileucine Motifs Mediate Late Endosomal/Lysosomal Targeting of Transmembrane Protein 192 (TMEM192) and a C-Terminal Cysteine Residue Is Responsible for Disulfide Bond Formation in TMEM192 Homodimers." *Biochemical Journal*. **2011**. 434. (2): 219–31. <https://doi.org/10.1042/BJ20101396>.
- Berridge M, Bootman M, Roderick H. "Calcium Signalling: Dynamics, Homeostasis and Remodelling." *Nature Reviews. Molecular Cell Biology*. **2003**. 4 (7): 517–29. <https://doi.org/10.1038/NRM1155>.
- Bodaghi B, Jones T, Zipeto D, Vita C, Sun L, Laurent L, Seisdedos F, Virelizier J, Michelson S. "Chemokine Sequestration by Viral Chemoreceptors as a Novel Viral Escape Strategy: Withdrawal of Chemokines from the Environment of Cytomegalovirus- Infected Cells." *Journal of Experimental Medicine*. **1998**.188 (5): 855–66. <https://doi.org/10.1084/JEM.188.5.855>.
- Boeckh M, Geballe A. "Cytomegalovirus: Pathogen, Paradigm, and Puzzle." *The Journal of Clinical Investigation*. **2011**. 121 (5): 1673–80. <https://doi.org/10.1172/JCI45449>.
- Boer R, Grassegger A, Schudt C, Glossmann H. "(+)-Niguldipine Binds with Very High Affinity to Ca²⁺ Channels and to a Subtype of A1-Adrenoceptors." *European Journal of Pharmacology: Molecular Pharmacology*. **1989**.172 (2): 131–45. [https://doi.org/10.1016/0922-4106\(89\)90004-7](https://doi.org/10.1016/0922-4106(89)90004-7).

Braulke T, Bonifacino J. "Sorting of Lysosomal Proteins." *Biochimica et Biophysica Acta - Molecular Cell Research*. **2009**. 1793 (4): 605–14. <https://doi.org/10.1016/J.BBAMCR.2008.10.016>.

Britt W, Prichard M. "New Therapies for Human Cytomegalovirus Infections." *Antiviral Research*. **2018**.159 (11): 153–74. <https://doi.org/10.1016/J.ANTIVIRAL.2018.09.003>.

Bronzini M, Luganini A, Dell'Oste V, De Andrea M, Landolfo S, Gribaudo G. "The US16 Gene of Human Cytomegalovirus Is Required for Efficient Viral Infection of Endothelial and Epithelial Cells." *Journal of Virology*. **2012**.86 (12): 6875–88. <https://doi.org/10.1128/jvi.06310-11>.

Bultynck G, Kiviluoto S, Henke N, Ivanova H, Schneider L, Rybalchenko V, Luyten T. "The C Terminus of Bax Inhibitor-1 Forms a Ca²⁺ Permeable Channel Pore." *Journal of Biological Chemistry*. **2011**.287(4).2544-57.<https://doi.org/10.1074/jbc.M111.275354>.

Bultynck G, Kiviluoto S, Methner A. "Bax Inhibitor-1 Is Likely a PH-Sensitive Calcium Leak Channel, Not a H⁺/Ca²⁺ Exchanger." *Science Signaling*.**2014**.7 (343).pe22. <https://doi.org/10.1126/SCISIGNAL.2005764>.

Butcher J, Aitken J, Mitchell J, Gowen B, Dargan D. "Structure of the Human Cytomegalovirus B Capsid by Electron Cryomicroscopy and Image Reconstruction." *Journal of Structural Biology*. **1998**.124 (1): 70–76. <https://doi.org/10.1006/jsbi.1998.4055>.

"Calcium Channel Blockers - StatPearls - NCBI Bookshelf." Accessed January 9, 2023. <https://www.ncbi.nlm.nih.gov/books/NBK482473/>.

Camello C, Lomax R, Petersen O, Tepikin A. "Calcium Leak from Intracellular Stores—the Enigma of Calcium Signalling." *Cell Calcium*.**2002**.32 (5–6): 355–61. <https://doi.org/10.1016/S0143416002001926>.

Carrara G, Parsons M, Saraiva N, Smith G. "Golgi Anti-Apoptotic Protein: A Tale of Camels, Calcium, Channels and Cancer." *Open Biology*. **2017**.7 (5).170045. <https://doi.org/10.1098/rsob.170045>.

Carrara G, Saraiva N, Parsons M, Byrne B, Prole D, Taylor C, Smith G. "Golgi Anti-Apoptotic Proteins Are Highly Conserved Ion Channels That Affect Apoptosis and Cell Migration." *Journal of Biological Chemistry*. **2015**.290 (18): 11785–801. <https://doi.org/10.1074/JBC.M115.637306>.

Carrara G, Saraivas N, Gubers C, Johnson B, Smith G. "Six-Transmembrane Topology for Golgi Anti-Apoptotic Protein (GAAP) and Bax Inhibitor 1 (BI-1) Provides Model for the Transmembrane Bax Inhibitor-Containing Motif (TMBIM) Family." *The Journal of Biological Chemistry*. **2012**.287 (19): 15896–905. <https://doi.org/10.1074/JBC.M111.336149>.

Cavaletto N, Luganini A, Gribaudo G. " Inactivation of the Human Cytomegalovirus US20 Gene Hampers Productive Viral Replication in Endothelial Cells ." *Journal of Virology*. **2015**. 89 (21): 11092–106. <https://doi.org/10.1128/jvi.01141-15>.

Chambers J, Angulo A, Amaratunga D, Guo H, Jiang Y, Wan J, Bittner A. "DNA Microarrays of the Complex Human Cytomegalovirus Genome: Profiling Kinetic Class with Drug Sensitivity of Viral Gene

Expression." *Journal of Virology*.**1999**.73 (7): 5757–66. <https://doi.org/10.1128/jvi.73.7.5757-5766.1999>.

Chang Y, Bruni R, Kloss B, Assur Z, Kloppmann E, Rost B, Hendrickson W, Liu Q. "Structural Basis for a PH-Sensitive Calcium Leak across Membranes." *Science*.**2014**.344 (6188): 1131–35. <https://doi.org/10.1126/science.1252043>.

Chee S, Bankier A, Beck S, Bohni R, Brown C, Cerny R, Horsnell T. "Analysis of the Protein-Coding Content of the Sequence of Human Cytomegalovirus Strain AD169." *Current Topics in Microbiology and Immunology*. **1990**.154: 125–69. https://doi.org/10.1007/978-3-642-74980-3_6/COVER.

Chen L, Zhang Y, Luo J, Zhang W. "Clinical Use of Azelnidipine in the Treatment of Hypertension in Chinese Patients." *Therapeutics and Clinical Risk Management*.**2015**. 11 (2): 309–18. <https://doi.org/10.2147/TCRM.S64288>.

Claros M, Heijne G. "TopPred II: An Improved Software for Membrane Protein Structure Predictions." *Computer Applications in the Biosciences: CABIOS*.**1994**.10 (6): 685–86. <https://doi.org/10.1093/BIOINFORMATICS/10.6.685>.

Compton T. "Receptors and Immune Sensors: The Complex Entry Path of Human Cytomegalovirus." *Trends in Cell Biology*. **2004**. 14 (1): 5–8. <https://doi.org/10.1016/j.tcb.2003.10.009>.

Cooper D, Dimri M. "Calcium Channels". *Biochemistry StatPearls*.**2022**. July. <https://www.ncbi.nlm.nih.gov/books/NBK562198/>.

Damme V, Loock M. "Functional Annotation of Human Cytomegalovirus Gene Products: An Update." *Frontiers in Microbiology*.**2014**.19(5).218. <https://doi.org/10.3389/FMICB.2014.00218/ABSTRACT>.

Das S, Pellett P. "Members of the HCMV US12 Family of Predicted Heptaspanning Membrane Proteins Have Unique Intracellular Distributions, Including Association with the Cytoplasmic Virion Assembly Complex." *Virology*. **2007**. 361 (2): 263–73. <https://doi.org/10.1016/j.virol.2006.11.019>.

Das S, Pellett P. "Spatial Relationships between Markers for Secretory and Endosomal Machinery in Human Cytomegalovirus-Infected Cells versus Those in Uninfected Cells." *Journal of Virology*. **2011**. 85 (12): 5864–79. <https://doi.org/10.1128/JVI.00155-11>.

Davison A, Dolan A, Akter P, Addison C, Dargan D, Alcendor D, McGeoch D, Hayward G. "The Human Cytomegalovirus Genome Revisited: Comparison with the Chimpanzee Cytomegalovirus Genome." *Journal of General Virology*.**2003**. 84 (1): 17–28. <https://doi.org/10.1099/VIR.0.18606-0/CITE/REFWORKS>.

Dobson S, Mankouri J, Whitehouse A. "Identification of Potassium and Calcium Channel Inhibitors as Modulators of Polyomavirus Endosomal Trafficking." *Antiviral Research*.**2020**.179 (7).104819. <https://doi.org/10.1016/J.ANTIVIRAL.2020.104819>.

Dolan A, Cunningham C, Hector R, Hassan-Walker A, Lee L, Addison C, Dargan D. "Genetic Content

of Wild-Type Human Cytomegalovirus.” *Journal of General Virology*.**2004**.85 (5): 1301–12. <https://doi.org/10.1099/VIR.0.79888-0/CITE/REFWORKS>.

Dunn W, Chou C, Li H, Hai R, Patterson D, Stolc V, Zhu H, Liu F. “Functional Profiling of a Human Cytomegalovirus Genome.” *Proceedings of the National Academy of Sciences of the United States of America*.**2003**.100(24).14223–28.

https://doi.org/10.1073/PNAS.2334032100/SUPPL_FILE/4032FIG5.PDF.

Mocarski E, Shenk T, Griffiths P, Pass R. “Cytomegaloviruses — Princeton University.” *Fields Virology*.**2013**. <https://collaborate.princeton.edu/en/publications/cytomegaloviruses>.

Fernández M, Segura M, Solé C, Colino A, Comella J, Ceña V. “Lifeguard/Neuronal Membrane Protein 35 Regulates Fas Ligand-Mediated Apoptosis in Neurons via Microdomain Recruitment.” *Journal of Neurochemistry*.**2007**.103 (1): 190–203. <https://doi.org/10.1111/J.1471-4159.2007.04767.X>.

Fielding C, Aicheler R, Stanton R, Wang E, Han S, Seirafian S, Davies J. “Two Novel Human Cytomegalovirus NK Cell Evasion Functions Target MICA for Lysosomal Degradation.” *PLoS Pathogens*.**2014**.10 (5). <https://doi.org/10.1371/journal.ppat.1004058>.

Fiorio Pla A, Genova T, Pupo E, Tomatis C, Genazzani A, Zaninetti R, Munaron L. “Multiple Roles of Protein Kinase A in Arachidonic Acid-Mediated Ca²⁺ Entry and Tumor-Derived Human Endothelial Cell Migration.” *Molecular Cancer Research*.**2010**.8 (11): 1466–76. <https://doi.org/10.1158/1541-7786.mcr-10-0002/79374/am/multiple-roles-of-protein-kinase-a-on-arachidonic>.

Fiorio Pla A, Avanzato D, Munaron L, Ambudkar I. “Ion Channels and Transporters in Cancer. 6. Vascularizing the Tumor: TRP Channels as Molecular Targets.” *American Journal of Physiology - Cell Physiology*.**2012**.302(1):9–15.

<https://doi.org/10.1152/AJPCELL.00280.2011/ASSET/IMAGES/LARGE/ZH00121167600002.JPEG>.

Fortunato E, Spector D. “Regulation of Human Cytomegalovirus Gene Expression.” *Advances in Virus Research*.**1999**.54 (C): 61–128. [https://doi.org/10.1016/S0065-3527\(08\)60366-8](https://doi.org/10.1016/S0065-3527(08)60366-8).

Gao J, Murphy P. “Human Cytomegalovirus Open Reading Frame US28 Encodes a Functional Beta Chemokine Receptor.” *Journal of Biological Chemistry*.**1994**.269 (46): 28539–42. [https://doi.org/10.1016/S0021-9258\(19\)61936-8](https://doi.org/10.1016/S0021-9258(19)61936-8).

Gatherer D, Seirafian S, Cunningham C, Holton M, Dargan D, Baluchova K, Hector R. “High-Resolution Human Cytomegalovirus Transcriptome.” *Proceedings of the National Academy of Sciences of the United States of America*.**2011**.108 (49): 19755–60. <https://doi.org/10.1073/pnas.1115861108>.

Gerna G, Kabanova A, Lilleri D. “Human Cytomegalovirus Cell Tropism and Host Cell Receptors.” *Vaccines*.**2019**.7 (3): 1–18. <https://doi.org/10.3390/vaccines7030070>.

Gerna G, Zipeto D, Percivalle E, Parea M, Revello M, Maccario R, Peri G, Milanese G. “Human Cytomegalovirus Infection of the Major Leukocyte Subpopulations and Evidence for Initial Viral Replication in Polymorphonuclear Leukocytes from Viremic Patients.” *The Journal of Infectious*

Diseases. **1992**.166 (6): 1236–44. <https://doi.org/10.1093/INFDIS/166.6.1236>.

Gretch D, Gehrz R, Stinski M. “Characterization of a Human Cytomegalovirus Glycoprotein Complex (GcI).” *Journal of General Virology*. **1988**.69 (6): 1205–15. <https://doi.org/10.1099/0022-1317-69-6-1205/CITE/REFWORKS>.

Griffiths P. “Herpesviruses as Unrecognised Components of the Pathogenesis of Chronic Diseases.” *Reviews of Medical Virology*. **2000**. 10(5). 281-3. <https://doi.org/10.1002/1099-1654>.

Gubser C, Bergamaschi D, Hollinshead M, Lu X, Kuppeveld F, Smith G. “A New Inhibitor of Apoptosis from Vaccinia Virus and Eukaryotes.” *PLOS Pathogens*.**2007**.3 (2): e17. <https://doi.org/10.1371/JOURNAL.PPAT.0030017>.

Guo G, Xu M, Chang Y, Luyten T, Seitaj B, Liu W, Zhu P. “Ion and PH Sensitivity of a TMBIM Ca²⁺ Channel.” *Structure*. **2019**. 27 (6): 1013-1021. <https://doi.org/10.1016/j.str.2019.03.003>.

Guo Y, Huang E. “Characterization of a Structurally Tricistronic Gene of Human Cytomegalovirus Composed of U(s)18, U(s)19, and U(s)20.” *Journal of Virology*.**1993**. 67 (4): 2043–54. <https://doi.org/10.1128/JVI.67.4.2043-2054.1993>.

Gurczynski S, Das S, Pellett P. “Deletion of the Human Cytomegalovirus US17 Gene Increases the Ratio of Genomes per Infectious Unit and Alters Regulation of Immune and Endoplasmic Reticulum Stress Response Genes at Early and Late Times after Infection.” *Journal of Virology*.**2014**.88 (4): 2168–82. <https://doi.org/10.1128/JVI.02704-13>.

Hai R, Chu A, Li H, Umamoto S, Rider P, Liu F. “Infection of Human Cytomegalovirus in Cultured Human Gingival Tissue.” *Virology Journal*. **2006**.3(84).<https://doi.org/10.1186/1743-422X-3-84>.

Hayashi K, Homma K, Wakino S, Tokuyama H, Sugano N, Saruta T, Itoh H. “T-Type Ca Channel Blockade as a Determinant of Kidney Protection.” *The Keio Journal of Medicine*. **2010**.59 (3): 84–95. <https://doi.org/10.2302/KJM.59.84>.

Herbette L, Vecchiarelli M, Leonardi A, Sartani A. “Lercanidipine: Short Plasma Half-Life, Long Duration of Action and High Cholesterol Tolerance. Updated Molecular Model to Rationalize Its Pharmacokinetic Properties.” *Blood Pressure*.**2010**.7 (sup2): 10–17. <http://Dx.Doi.Org/10.1080/080370598438998>.

Hillen W, Berens C. “MECHANISMS UNDERLYING EXPRESSION OF TN10 ENCODED TETRACYCLINE RESISTANCE.” *Annual Reviews*.**2003**.48 (11): 345–69. <https://doi.org/10.1146/ANNUREV.MI.48.100194.002021>.

Holzerlandt R, Orengo S, Kellam P, Mar Albà M. “Identification of New Herpesvirus Gene Homologs in the Human Genome.” *Genome Research*.**2002**.12 (11): 1739–48. <https://doi.org/10.1101/GR.334302>.

Hu L, Smith T, Goldberger G. “LFG: A Candidate Apoptosis Regulatory Gene Family.” *Apoptosis : An International Journal on Programmed Cell Death*.**2009**.14 (11): 1255–65.

<https://doi.org/10.1007/S10495-009-0402-2>.

Hyser J, Estes M. "Pathophysiological Consequences of Calcium-Conducting Viroporins." *Annual Review of Virology*. **2015**. 2 (1): 473. <https://doi.org/10.1146/ANNUREV-VIROLOGY-100114-054846>.

Isaacson M, Compton T. "Human Cytomegalovirus Glycoprotein B Is Required for Virus Entry and Cell-to-Cell Spread but Not for Virion Attachment, Assembly, or Egress." *Journal of Virology*. **2009**. 83 (8): 3891–3903. <https://doi.org/10.1128/JVI.01251-08/ASSET/3CD0F013-C466-466E-84B2-FA6BABF37C2D/ASSETS/GRAPHIC/ZJV0080917580006.JPEG>.

Jones T, Wiertz Et, Sun L, Kenneth N, Nelson J, Ploeght H. "Genetic Engineering of Viruses and of Virus Vectors". *Proceedings of the National Academy of Sciences of the United States of America*. **1996**. 93: 11327–33. [10.1073/pnas.93.21.11287](https://doi.org/10.1073/pnas.93.21.11287).

Kadeba P, Vasauskas A, Chen H, Wu S, Scammell J, Cioffi D. "Regulation of Store-Operated Calcium Entry by FK506-Binding Immunophilins." *Cell Calcium*. **2013**. 53 (4): 275. <https://doi.org/10.1016/J.CECA.2012.12.008>.

Kalejta R. "Functions of Human Cytomegalovirus Tegument Proteins Prior to Immediate Early Gene Expression." *Current Topics in Microbiology and Immunology*. **2008**. 325: 101–15. https://doi.org/10.1007/978-3-540-77349-8_6/COVER.

Kalejta R. "Tegument Proteins of Human Cytomegalovirus." *Microbiology and Molecular Biology Reviews*. **2008**. 72 (2): 249–65. <https://doi.org/10.1128/MMBR.00040-07>.

Kari B, Cooper W, Goertz R, Radeke B. "The Human Cytomegalovirus UL100 Gene Encodes the GC-II Glycoproteins Recognized by Group 2 Monoclonal Antibodies." *Journal of General Virology*. **1994**. 75 (11): 3081–86. <https://doi.org/10.1099/0022-1317-75-11-3081/CITE/REFWORKS>.

Karlin S, Mocarski E, Schachtel G. "Molecular Evolution of Herpesviruses: Genomic and Protein Sequence Comparisons." *Journal of Virology*. **1994**. 68(3):1886–1902. <https://doi.org/10.1128/JVI.68.3.1886-1902.1994>.

Kelley L, Mezulis S, Yates C, Wass M, Sternberg M. "The Phyre2 Web Portal for Protein Modeling, Prediction and Analysis." *Nature Protocols*. **2015**. 10(6):845–58. <https://doi.org/10.1038/NPROT.2015.053>.

Kiviluoto S, Schneider L, Luyten T, Vervliet T, Missiaen L, Smedt H, Parys J, Methner A, Bultynck G. "Bax Inhibitor-1 Is a Novel IP₃ Receptor-Interacting and -Sensitizing Protein." *Cell Death & Disease*. **2012**. 3 (8). <https://doi.org/10.1038/CDDIS.2012.103>.

Krogh A, Larsson B, Heijne G, Sonnhammer E. "Predicting Transmembrane Protein Topology with a Hidden Markov Model: Application to Complete Genomes." *Journal of Molecular Biology*. **2001**. 305 (3): 567–80. <https://doi.org/10.1006/JMBI.2000.4315>.

Landolfo S, Gariglio M, Gribaudo G, Lembo D. "The Human Cytomegalovirus." *Pharmacology and Therapeutics Elsevier Inc*. **2003**. 98. 269-297. [https://doi.org/10.1016/S0163-7258\(03\)00034-2](https://doi.org/10.1016/S0163-7258(03)00034-2).

Lesniewski M, Das S, Skomorovska-Prokvolit Y, Wang F, Pellett P. "Primate Cytomegalovirus US12 Gene Family: A Distinct and Diverse Clade of Seven-Transmembrane Proteins." *Virology*. **2006**.354 (2): 286–98. <https://doi.org/10.1016/J.VIROL.2006.06.035>.

Lisak D, Schacht T, Enders V, Habicht J, Kiviluoto S, Schneider J, Henke N, Bultynck G, Methner A. "The Transmembrane Bax Inhibitor Motif (TMBIM) Containing Protein Family: Tissue Expression, Intracellular Localization and Effects on the ER CA²⁺-Filling State." *Biochimica et Biophysica Acta (BBA) - Molecular Cell Research*.**2015**.1853(9):2104–14. <https://doi.org/10.1016/J.BBAMCR.2015.03.002>.

Liu Q. "TMBIM-Mediated Ca²⁺ Homeostasis and Cell Death." *Biochem Biophys Acta*. **2017**.1864(6).850-857.<https://doi.org/10.1016/j.bbamcr.2016.12.023>.

Lu Y, Ma Y, Liu Z, Han L, Gao S, Zheng B, Liu C. "A Cluster of 3' Coterminal Transcripts from US12–US17 Locus of Human Cytomegalovirus." *Virus Genes*.**2016**.52 (3): 334–45. <https://doi.org/10.1007/S11262-016-1308-Z/FIGURES/7>.

Luganini A, Cavaletto N, Raimondo S, Geuna S, Gribaudo G. "Loss of the Human Cytomegalovirus US16 Protein Abrogates Virus Entry into Endothelial and Epithelial Cells by Reducing the Virion Content of the Pentamer." *Journal of Virology*.**2017**.91 (11): 1–18. <https://doi.org/10.1128/jvi.00205-17>.

Luganini A, Di Nardo G, Munaron L, Gilardi G, Fiorio Pla A, Gribaudo G. "Human Cytomegalovirus US21 Protein Is a Viroporin That Modulates Calcium Homeostasis and Protects Cells against Apoptosis." *Proceedings of the National Academy of Sciences of the United States of America*. **2018**.115 (52): E12370–77. <https://doi.org/10.1073/pnas.1813183115>.

Matossian M, Vangelder C, Papagerakis P, Zheng L, Wolf L, Papagerakis S. "In Silico Modeling of the Molecular Interactions of Antacid Medication with the Endothelium: Novel Therapeutic Implications in Head and Neck Carcinomas." *International Journal of Immunopathology and Pharmacology*. **2014**.27 (4): 573–83. <https://doi.org/10.1177/039463201402700413>.

Mattia F, Gubser C, Dommelen M, Jan Visch H, Distelmaier F, Postigo A, Luyten T. "Human Golgi Antiapoptotic Protein Modulates Intracellular Calcium Fluxes." *Molecular Biology of the Cell*. **2009**. 20 (16): 3638–45. <https://doi.org/10.1091/MBE.E09-05-0385/ASSET/IMAGES/LARGE/ZMK0160991530004.JPEG>.

McClellan K, Jarvis B. "Lercanidipine: A Review of Its Use in Hypertension." *Drugs*. **2000**. 60 (5): 1123–40. <https://doi.org/10.2165/00003495-200060050-00009/FIGURES/4>.

Meesing A, Razonable R. "New Developments in the Management of Cytomegalovirus Infection After Transplantation". *Drugs*. **2018**. 78: 1085–1103. <https://doi.org/10.1007/s40265-018-0943-1>.

Meier J, Stinski M. "Regulation of Human Cytomegalovirus Immediate-Early Gene Expression." *Intervirology*. **1996**.39 (5–6): 331–42. <https://doi.org/10.1159/000150504>.

Mocarski E. "Immune Escape and Exploitation Strategies of Cytomegaloviruses: Impact on and Imitation of the Major Histocompatibility System." *Cellular Microbiology*.**2004**. 6 (8): 707–17. <https://doi.org/10.1111/J.1462-5822.2004.00425.X>.

Morris G, Goodsell D, Halliday R, Huey R, Hart W, Belew R, Olson A. "Automated Docking Using a Lamarckian Genetic Algorithm and an Empirical Binding Free Energy Function." *Journal of Computational Chemistry*.**1998**.19 (14): 1639–62. [https://doi.org/10.1002/\(SICI\)1096-987X\(19981115\)19:14<1639::AID-JCC10>3.0.CO;2-B](https://doi.org/10.1002/(SICI)1096-987X(19981115)19:14<1639::AID-JCC10>3.0.CO;2-B).

Murphy E, Shenk T. "Human Cytomegalovirus Genome." *Current Topics in Microbiology and Immunology*. **2008**. 325. 1–19. https://doi.org/10.1007/978-3-540-77349-8_1.

Murphy E, Yu D, Grimwood J, Schmutz J, Dickson M, Jarvis M, Hahn G, Nelson J, Myers R, Shenk T. "Coding Potential of Laboratory and Clinical Strains of Human Cytomegalovirus." *Proceedings of the National Academy of Sciences of the United States of America*.**2003**.100 (25). 14976. <https://doi.org/10.1073/PNAS.2136652100>.

Nelson J, Gnann J, Ghazal P. "Regulation and Tissue-Specific Expression of Human Cytomegalovirus." *Current Topics in Microbiology and Immunology*. **1990**.154. 75–100. https://doi.org/10.1007/978-3-642-74980-3_4/COVER.

Nieva L, Madan V, Carrasco L. "Viroporins: Structure and Biological Functions." *Nature Reviews Microbiology*. **2012**. 10 (8). 563–74. <https://doi.org/10.1038/nrmicro2820>.

Nugent T, Jones D. "Transmembrane Protein Topology Prediction Using Support Vector Machines." *BMC Bioinformatics* **2009**.10 (5). 159. <https://doi.org/10.1186/1471-2105-10-159>.

Oka T, Sayano T, Tamai S, Yokota S, Kato H, Fujii G, Mihara K. "Identification of a Novel Protein MICS1 That Is Involved in Maintenance of Mitochondrial Morphology and Apoptotic Release of Cytochrome C." *Molecular Biology of the Cell*. **2008**.19 (6): 2597. <https://doi.org/10.1091/MBC.E07-12-1205>.

Patel G, Adeshra S, Meshram D. "A Review on Properties, Application, and Analytical Methods of an Antihypertensive Drug Efonidipine." *Journal of Health Sciences & Research*. **2019**. 10 (2): 52–56. <https://doi.org/10.5005/JP-JOURNALS-10042-1084>.

Pauwels R, Balzarini J, Baba M, Snoeck R, Schols D, Herdewijn P, Desmyter J, De Clercq E. "Rapid and Automated Tetrazolium-Based Colorimetric Assay for the Detection of Anti-HIV Compounds." *Journal of Virological Methods*. **1988**.20 (4): 309–21. [https://doi.org/10.1016/0166-0934\(88\)90134-6](https://doi.org/10.1016/0166-0934(88)90134-6).

Penfold M, Mocarski E. "Formation of Cytomegalovirus DNA Replication Compartments Defined by Localization of Viral Proteins and DNA Synthesis." *Virology*.**1997**.239 (1): 46–61. <https://doi.org/10.1006/VIRO.1997.8848>.

Pinto L, Holsinger L, Lamb R. "Influenza Virus M2 Protein Has Ion Channel Activity." *Cell*. **1992**. 69 (3): 517–28. [https://doi.org/10.1016/0092-8674\(92\)90452-I](https://doi.org/10.1016/0092-8674(92)90452-I).

Pinton P, Giorgi C, Siviero R, Zecchini E, Rizzuto R. "Calcium and Apoptosis: ER-Mitochondria Ca²⁺ Transfer in the Control of Apoptosis." *Oncogene*.**2008**.27 (50): 6407–18. <https://doi.org/10.1038/ONC.2008.308>.

Reimers K, Choi C, Bucan V, Vogt P. "The Bax Inhibitor-1 (BI-1) Family in Apoptosis and Tumorigenesis." *Current Molecular Medicine*.**2008**.8 (2): 148–56. <https://doi.org/10.2174/156652408783769562>.

Rigoutsos I, Novotny J, Huynh T, Chin-Bow S, Parida L, Platt C, Shenk T. "In Silico Pattern-Based Analysis of the Human Cytomegalovirus Genome." *Journal of Virology*.**2003**.77 (7): 4326–44. <https://doi.org/10.1128/JVI.77.7.4326-4344.2003/ASSET/B500D22A-6642-4977-9AC3-8658B347BB68/ASSETS/GRAPHIC/JV0731373004.JPEG>.

Rizzuto R, Pinton P, Carrington W, Fay F, Fogarty K, Lifshitz L, Tuft P. "Close Contacts with the Endoplasmic Reticulum as Determinants of Mitochondrial Ca²⁺ Responses." *Science*.**1998**. 280 (5370): 1763–66. <https://doi.org/10.1126/SCIENCE.280.5370.1763>.

Rojas-Rivera, D, Armisen R, Colombo A, Martínez G, Eguiguren A, Díaz A, Kiviluoto S. "TMBIM3/GRINA Is a Novel Unfolded Protein Response (UPR) Target Gene That Controls Apoptosis through the Modulation of ER Calcium Homeostasis." *Cell Death and Differentiation*. **2012**.19 (6): 1013. <https://doi.org/10.1038/CDD.2011.189>.

Rojas-Rivera, D, Hetz C. "TMBIM Protein Family: Ancestral Regulators of Cell Death." *Oncogene* **2015**.34 (3): 269–80. <https://doi.org/10.1038/onc.2014.6>.

Sakurai Y, Kolokoltsov A, Chen C, Tidwell M, Bauta W, Klugbauer N, Grimm C, Wahl-Schott C, Biel M, Davey R. "Two-Pore Channels Control Ebola Virus Host Cell Entry and Are Drug Targets for Disease Treatment." *Science*.**2015**.347 (6225): 995–98. https://doi.org/10.1126/SCIENCE.1258758/SUPPL_FILE/SAKURAI.SM.PDF.

Sanchez V, Sztul E, Britt W. "Human Cytomegalovirus Pp28 (UL99) Localizes to a Cytoplasmic Compartment Which Overlaps the Endoplasmic Reticulum-Golgi-Intermediate Compartment." *Journal of virology*. **2000**.74 (8): 3842–51. [10.1128/jvi.74.8.3842-3851.2000](https://doi.org/10.1128/jvi.74.8.3842-3851.2000).

Saraiva N, Prole D, Carrara G, Johnson B, Taylor C, Parsons M, Smith G. "HGAAP Promotes Cell Adhesion and Migration via the Stimulation of Store-Operated Ca²⁺ Entry and Calpain 2." *Journal of Cell Biology*. **2013**.202 (4): 699–713. <https://doi.org/10.1083/jcb.201301016>.

Schwinn D, Price R. "Molecular Pharmacology of Human A1-Adrenergic Receptors:Unique Features of the A1a-Subtype." *European Urology*.**1999**.36 (Suppl. 1): 7–10. <https://doi.org/10.1159/000052311>.

Scott C, Griffin S. "Viroporins: Structure, Function and Potential as Antiviral Targets." *Journal of General Virology*. **2015**.96 (8): 2000–2027. <https://doi.org/10.1099/VIR.0.000201/CITE/REFWORKS>.

Seitz R. "Human Cytomegalovirus (HCMV)-Revised." *Transfusion Medicine and Hemotherapy*.

Karger Publishers. **2010**. 37(6).365-375.<https://doi.org/10.1159/000322141>.

Shamu E, Story C, Rapoport T, Ploegh H. "The Pathway of Us11-Dependent Degradation of Mhc Class I Heavy Chains Involves a Ubiquitin-Conjugated Intermediate." *Journal of Cell Biology*. **1999**.147 (1): 45–58. <https://doi.org/10.1083/JCB.147.1.45>.

Sharon F, Shenk T. "Human Cytomegalovirus PUL37x1-Induced Calcium Flux Activates PKC α , Inducing Altered Cell Shape and Accumulation of Cytoplasmic Vesicles." *Proceedings of the National Academy of Sciences of the United States of America*.**2014**.111 (12): E1140–48. <https://doi.org/10.1073/PNAS.1402515111/ASSET/4B605F4C-A505-41AA-970D-6472E3D181A7/ASSETS/GRAPHIC/PNAS.1402515111FIG10.JPEG>.

Shelbourn S, Sissons J, Sinclair J. "Expression of Oncogenic Ras in Human Teratocarcinoma Cells Induces Partial Differentiation and Permissiveness for Human Cytomegalovirus Infection." *Journal of General Virology*.**1989**.70 (2): 367–74. <https://doi.org/10.1099/0022-1317-70-2-367/CITE/REFWORKS>.

Sinzger C, Digel M, Jahn G. "Cytomegalovirus Cell Tropism." *Current Topics in Microbiology and Immunology*. **2008**.325: 63–83. https://doi.org/10.1007/978-3-540-77349-8_4.

Skaletskaya A, Bartle L, Chittenden T, McCormick A, Mocarski E, Goldmacher V. "A Cytomegalovirus-Encoded Inhibitor of Apoptosis That Suppresses Caspase-8 Activation." *Proceedings of the National Academy of Sciences of the United States of America* .**2001**.98(14).7829-34.[doi.10.1073pnas.141108798](https://doi.org/10.1073pnas.141108798).

Smith I, Tashintuna I, Rahhal F, Poweli H, Everett Ai, Mueller A, Spector S, Freeman W. "Clinical Failure of CMV Retinitis with Intravitreal Cidofovir Is Associated with Antiviral Resistance." *Archives of Ophthalmology*. **1998**. 116 (2): 178–85. <https://doi.org/10.1001/archophth.116.2.178>.

Somia N, Schmitt M, Vetter D, Van Antwerp D, Heinemann S, Verma I. "LFG: An Anti-Apoptotic Gene That Provides Protection from Fas-Mediated Cell Death." *Proceedings of the National Academy of Sciences of the United States of America*.**1999**.96 (22): 12667–72. <https://doi.org/10.1073/PNAS.96.22.12667/ASSET/12CFF1D8-0EB4-430D-A038-027147E64CB9/ASSETS/GRAPHIC/PQ2293795005.JPEG>.

Stasiak P, Mocarski E. "Transactivation of the Cytomegalovirus ICP36 Gene Promoter Requires the Alpha Gene Product TRS1 in Addition to IE1 and IE2." *Journal of Virology*. **1992**. 66 (2): 1050–58. <https://doi.org/10.1128/JVI.66.2.1050-1058.1992>.

Stern-Ginossar N, Weisburd B, Michalski A, Le V, Hein M, Huang S, Ma M. "Decoding Human Cytomegalovirus." *Science*.**2012**.338(6110):1088–93. https://doi.org/10.1126/SCIENCE.1227919/SUPPL_FILE/TABLES6.XLSX.

Story C, Furman M, Ploegh H. "The Cytosolic Tail of Class I MHC Heavy Chain Is Required for Its Dislocation by the Human Cytomegalovirus US2 and US11 Gene Products." *Proceedings of the National Academy of Sciences of the United States of America*.**1999**.96 (15): 8516–21. <https://doi.org/10.1073/PNAS.96.15.8516/ASSET/6CBC37B9-B264-4F8D-81FB->

F46C2C949221/ASSETS/GRAPHIC/PQ1591204006.JPEG.

Tanaka H, Shigenobu K. "Efonidipine Hydrochloride: A Dual Blocker of L-and T-Type Ca²⁺ Channels." *Cardiovascular Drug reviews*. **2002**. 20(1). 81-92. <https://doi.org/10.1111/j.1527-3466.2002.tb00084.x>.

Tandon R, Mocarski E. "Viral and Host Control of Cytomegalovirus Maturation." *Trends in Microbiology*. **2012**.20 (8): 392–401. <https://doi.org/10.1016/J.TIM.2012.04.008>.

Wang D, Shenk T. "Human Cytomegalovirus Virion Protein Complex Required for Epithelial and Endothelial Cell Tropism." *Proceedings of the National Academy of Sciences of the United States of America*. **2005**.102 (50): 18153–58. <https://doi.org/10.1073/PNAS.0509201102>.

Warming S. "GALK Recombineering." *Transform*. **2005**.1–6. [papers2://publication/uuid/AB25A639-A225-4CA8-8ABC-7A58558DD1FF](https://pubmed.ncbi.nlm.nih.gov/16254254/).

Wellington K, Scott L. "Azelnidipine." *Drugs*.**2003**.63 (23): 2613–21. <https://doi.org/10.2165/00003495-200363230-00004/FIGURES/1>.

Weston K. "An Enhancer Element in the Short Unique Region of Human Cytomegalovirus Regulates the Production of a Group of Abundant Immediate Early Transcripts." *Virology*. **1988**.162 (2): 406–16. [https://doi.org/10.1016/0042-6822\(88\)90481-3](https://doi.org/10.1016/0042-6822(88)90481-3).

Weston K, Barrell B. "Sequence of the Short Unique Region, Short Repeats, and Part of the Long Repeats of Human Cytomegalovirus." *Journal of Molecular Biology*. **1986**. 192 (2): 177–208. [https://doi.org/10.1016/0022-2836\(86\)90359-1](https://doi.org/10.1016/0022-2836(86)90359-1).

Wille P, Knoche A, Nelson J, Jarvis M, Johnson D. "A Human Cytomegalovirus GO-Null Mutant Fails to Incorporate GH/GL into the Virion Envelope and Is Unable to Enter Fibroblasts and Epithelial and Endothelial Cells." *Journal of Virology*. **2010**. 84 (5): 2585–96. <https://doi.org/10.1128/JVI.02249-09>.

Yu D, Silva M, Shenk T. "Functional Map of Human Cytomegalovirus AD169 Defined by Global Mutational Analysis". *Proceedings of the National Academy of Sciences of the United States of America*.**2003**.100(21).12396-401. <https://doi.org/https://www.pnas.org/doi/full/10.1073/pnas.1635160100>.

Zhou M, Lanchy J, Ryckman B. "Human Cytomegalovirus GH/GL/GO Promotes the Fusion Step of Entry into All Cell Types, Whereas GH/GL/UL128-131 Broadens Virus Tropism through a Distinct Mechanism." *Journal of Virology*. **2015**.89 (17): 8999–9009. <https://doi.org/10.1128/JVI.01325-15/ASSET/70DB707A-35EB-49CF-AB66-4AC6D32E2D5D/ASSETS/GRAPHIC/ZJV9990907050008.JPEG>.

Zhou Y, Frey T, Yang J. "Viral Calciomics: Interplays between Ca²⁺ and Virus." *Cell Calcium*. **2009**. 46 (1): 1–17. <https://doi.org/10.1016/J.CECA.2009.05.005>.

Acknowledgements

I first of all would like to express my gratitude to Prof. Giorgio Gribaudo for believing in me and providing me with this opportunity to work in this PhD project. It has been a wonderful experience working with you. Thank you for inspiring me, sharing your knowledge and guiding me.

My sincere thanks to Dr. Anna Luganini for being so kind and patient with me throughout and for your constant support. Thank you for teaching me everything and for helping me with all the work related stuff. You have indeed pushed me to do and be better.

My special thanks to Dr. Irene Stefanini for being so warm and kind. I will forever be grateful for your immense support and confidence in me. Thank you for the much needed positivity.

I would like to thank Prof. Alessandra Florio Pla and Prof. Giovanni Di Nardo and their team for helping me with the lab works.

Thank you, Giulia, for helping me around the lab from my first day here. Thank you for all the wonderful times. It was good to know you and work with you. I have learnt a lot from you. I wish you good luck for your future.

Also, I would like to thank Beatrice, for all the fun moments and talks in the lab. Though we spent a short duration, it has been a wonderful experience getting to know you. Thank you for sharing your wine making and food experiences with me.

My heartfelt thanks to Noemi, Francesca, Valentina, Marianna, Martina, Marta and Davide for your warm welcome, fun times, constant support and help. Thank you for all the Italian-English translations and giving me an insight on Italy. Thank you for making me a part of your celebrations, and for being with me in all the happy and sad moments. I will cherish all of them.

I will be grateful for all your help not just in the lab, but also outside. Thank you for sharing your work, culture, experiences and food. Thank you all for your words of encouragement, advice and good wishes. The three years here has been a wonderful journey and a good learning experience.

Finally, my utmost gratitude to my parents Sgt. Shivaram Bhat and Dr. Shailaja Y V. Your bravery and love for life and work has always driven me to do the best. Thank you for being my inspiration, my biggest support system and cheerleaders. Thank you for teaching me to dream big. Also, my biggest thanks to my friends and family members in India and Italy for all the wonderful memories.